Characterization of the sensory processings in the barrel cortex of the anaesthetized rat.

Luc Estebanez

Thèse de doctorat de l'École Normale Supérieure

École Doctorale n°474 Frontières du Vivant

Présentée par

Luc Estebanez[1,2]

Pour obtenir le grade de

Docteur de l'École Normale Supérieure

Caractérisation des traitements sensoriels dans le cortex à tonneaux du rat anesthésié.

Characterization of the sensory processings in the barrel cortex of the anaesthetized rat.

Thèse présentée et soutenue à Gif sur Yvette le _____2011 devant le jury composé de :

Dr. Laurent	Bourdieu	(École Normale Supérieure, Paris)	*directeur de thèse*
Dr. Sylvain	Crochet	(Centre de Recherche en Neurosciences, Lyon)	*examinateur*
Pr. Miguel	Maravall	(Instituto de Neurosciencias, Alicante)	*rapporteur*
Dr. James	Poulet	(Max Delbrück centrum, Berlin)	*examinateur*
Dr. Daniel	Pressnitzer	(École Normale Supérieure, Paris)	*président*
Dr. Daniel	Shulz	(Centre National de la Recherche Scientifique, Gif sur Yvette)	*directeur de thèse*
Pr. Garrett	Stanley	(Georgia Institute of Technology, Atlanta)	*rapporteur*

[1] Unité de Neurosciences, Information et Complexité, CNRS UPR-3293, 1 Avenue de la Terrasse, 91198 Gif-sur-Yvette, France.

[2] Ecole Normale Supérieure, Institut de Biologie de l'ENS, IBENS, Paris, F-75005 France

Résumé

Chez les rongeurs, le traitement par le cortex à tonneaux de l'information sensorielle en provenance des vibrisses est mal compris.

En effet, malgré l'aide fournie par l'organisation de ce cortex en une reproduction stricte de la topographie de l'appareil sensoriel, il a été difficile jusqu'à présent d'identifier de façon indiscutable le système de filtrage linéaire et non-linéaire qu'utilisent les neurones du cortex à tonneaux durant leur traitement des scènes tactiles auxquelles ils sont exposés.

Pour mieux identifier ces traitements corticaux, nous avons développé un système de stimulation vibrissale permettant d'appliquer des déflections sur un grand nombre de vibrisses indépendamment, dans toutes les directions possibles et ce à travers une vaste gamme fréquentielle.

En utilisant ce dispositif de stimulation multivibrissale durant des enregistrements extracellulaires de l'activité électrique des neurones du cortex à tonneaux de rats anesthésiés, nous avons pu identifier plus précisément le filtrage *linéaire* des stimulations vibrissales, qui s'avère similaire pour tous les neurones que nous avons pu enregistrer.

Par ailleurs, en explorant les aspects *non-linéaires* du traitement effectué par ces neurones, nous avons noté qu'ils se séparent en deux familles distinctes : d'un côté des neurones "locaux" qui se sont avérés sensibles à des contrastes locaux dans les déflections multivibrissales. De l'autre, des neurones "globaux" capables au contraire de détecter des situations où les déflections sont similaires pour de nombreuses vibrisses.

Enfin, en effectuant d'autres enregistrements dans la couche II/III du cortex à tonneaux, cette fois à l'aide d'un microscope deux-photons, nous avons pu noter que les neurones appartenant aux familles locales et globales étaient séparés en groupes spatialement distincts et que la position spatiale des neurones était plus généralement étroitement liée à l'ensemble de leurs propriétés de filtrage des déflections vibrissales.

Abstract

The processing of whisker deflections by rodents barrel cortex neurons is still poorly understood. Indeed, to date, the support provided by the strict mapping of the spatial arrangement of the peripheral sensory apparatus onto the cortical surface has not been sufficient to settle on a reasonable model of whisker processing. In particular, at the moment, the linear and non-linear filtering of whisker stimulations carried in this cortical area are unclear.

In order to tackle this problem, we developed a multiwhisker stimulator that allows the independent deflection of 24 whiskers, in any direction, over a wide frequency band.

By combining this whisker stimulation device with electrophysiological recordings carried in the barrel cortex of anaesthetized rats, we could identify a family of linear filters common to all recorded neurons.

In addition, we explored the non-linear responses of these neurons to spatio-temporal combinations of whisker deflections, and we observed two types of neuronal responses. In one side, "local" neurons responded to salient whisker deflections occurring on a single whisker and that contrasted with other whisker deflections. On the other side, "global" neurons were sensitive to the overall level of similarity between the deflections applied across stimulated whiskers.

Finally, we studied the functional response of the neurons found in the layer II/III of this cortex with the help of a two-photon microscope. Using this tool, we found that local and global neuron types were strongly spatially segregated. More generally, we observed a strict mapping of the functional tuning of barrel cortex neurons onto the surface of the rat barrel cortex.

Remerciements

Je tiens à remercier en tout premier lieu Daniel Shulz *et* Laurent Bourdieu*, mes deux directeurs de thèse. Pour des raisons que je ne m'explique toujours pas, ils ont bien voulu soutenir, accompagner, nourrir un projet un peu fou combinant deux laboratoires, deux méthodes d'enregistrement neuronal fondamentalement différentes, un projet requiérant le développement de dispositifs techniques lourds.*

Pour ce faire, ils ont mis en commun d'importants moyens financiers, et ils m'ont permis de soliciter le savoir faire des meilleurs artisans - terme empreint pour moi d'une grande noblesse - des deux laboratoires : Jean-Yves Tiercelin *et* Patrick Parra*, mécaniciens à l'INAF ont conçu avec moi puis entièrement réalisé l'ensemble des (très nombreuses) pièces mécaniques nécessaires à l'accomplissement de mes projets. Je veux ici leur exprimer mon admiration et ma très profonde gratitude.*

Gérard Paresys*, électronicien à l'ENS, a lui aussi été solicité pour prendre part dans cet improbable projet, et il a bien voulu qu'il prenne vie, même si pour cela il dût se lancer dans la conception de circuits électroniques à une échelle bien plus proche de la carte mère que du circuit RC...*

Enfin, Gérard Sadoc*, informaticien à l'UNIC, parlant le Delphy avec un accent parfait, a toujours résolu mes problèmes même les moins raisonnables (*.dat → .nex → .dat → .nex *?) avec une célérité et une élégance proprement déconcertantes.*

Sami El Boustani *voulait apprendre à "faire des expériences", on en a fait quelques unes ensemble... J'ai appris énormément en sa compagnie, de la modélisation des champs récepteurs à la rigueur la plus extrême dans l'interprétation des résultats. J'espère qu'on fera encore un bout de chemin ensemble !*

Julien Bertherat *a été mon compagnon durant les très très longues journées de microscopie deux-photon, où son endurence a fait merveille. Je resterai toujours ébloui par la perfection de ses craniotomies...*

Je n'oublie pas Jean-François Leger*, qui a conçu et réalisé avec Julien Bertherat, Laurent Bourdieu et* Yves Kremer *le microscope novateur que j'ai eu la chance d'utiliser.*

Je pense aussi à tous ceux qui ont été important pour moi au laboratoire de Gif-sur-Yvette : je pense à Yves Frégac *qui dirige le laboratoire et qui n'est pas avare en très bonnes idées,* Alain Destexhle, Valérie Ego-Stengel*, mais aussi* Yves Boubenec, Olivier Marre, Pierre Yger, Charlotte Deleuze, Pierre-Jean Arduin, Julie LeCam.

Guillaume Hucher *et* Aurélie Daret *on été les chevilles ouvrières de mes expériences, mais je pense aussi à tant d'autres personnes de l'UNIC avec qui j'ai partagé les JC des lundis ou qui, à des degrés divers, ont contribué au bon déroulement de ce travail de thèse.*

I still remember the excitement of starting my bachelor summer internship in Garrett Stanley *laboratory. This is the place where I found how mysterious and attractive the study of animal behaviour and the whisker system could be.*

I would also like to acknowledge here the deep impact of my one year stay in Carl Petersen laboratory, EPFL, prior to the onset of my PhD. There, I met some remarkable people, starting with Carl Petersen *himself, an ingenuous researcher who has this special gift for asking to right question using the right method.* Isabelle Ferezou, Sylvain Crochet *and* James Poulet *were post-doc in the lab at this time. Their respective research has deeply influenced my own work. I am thus honoured that both Sylvain Crochet and James Poulet agreed to take part in my examining committee, together with* Miguel Maravall*, Garrett Stanley and* Daniel Pressnitzer.

Finalement, comment ne pas avoir de gratitude pour Anouch, dont l'amour et le soutien m'ont porté tout au long de ces 4 années, ainsi que pour mes parents, mon frère et ma soeur, qui ont tous apporté leur pierre à ce fragile édifice...

Contents

Chapter 1

Introduction: identifying the whisker stimulations processed by the barrel cortex

1.1 A strategy for the study of cortical processing

What is the processing performed in the cortex? There seems to be little in common between the functions of primary sensory cortices [Mountcastle et al., 1957], [Hubel and Wiesel, 1959], the primary motor cortex ([Todorov, 2000] [Georgopoulos et al., 1986]) and higher area cortices such as the Broca area [Broca, 1861]. How could common processing principles be shared by such a diverse set of brain structures?

Still, to this large number of contrasted functions corresponds a very homogeneous columnar structure, classically described as a 6 layered stack ('the column') with a shared functional focus across layers - meaning in the case of the primary somatosensory cortex that contacts with the same area of the body triggered functional responses through layers [Mountcastle, 1957]. At first sight, the only notable structural heterogeneity across cortical areas is in the different thickness of specific layers of the cortex. This heterogeneity was used to tell apart cortical areas [Brodmann, 1909]: homotypic cortices show six layers of comparable thickness, while heterotypic cortices have uneven layer thicknesses. Among them, granular cortex shows a dense concentration of spiny stellate excitatory interneurons in layer IV (relaying information from the thalamus) while agranular cortex has a reduced layer IV and a much developed layer V containing large "Betz" pyramidal neurons that project directly to the spinal chord [Betz, 1874]. In accordance with these structural differences, agranular cortical areas have been linked to the planning and control of motor behaviours [Fritsch and Hitzig, 1870], while granular cortical areas have been found to be specialized in the processing of specific sensory inputs [Caton, 1875; Berger, 1929].

The specialization into sensory processing of granular areas makes them an attractive point of entry to study the microstructure and functional properties of the cortex. Indeed, in these cortical areas, a tight link exists between neuronal activity and sensory stimulation, as shown by the possibility to predict the neuronal activity of sensory cortices to a high degree with a linear/non-linear (LN) model of the sensory processing, a 'black-box' model that links the spiking activity of barrel cortex neurons with their functional input in two steps: stimuli are first projected into a sensory subspace for which the neuron encode

information (linear step), and second the firing rate of the neuron is estimated across this subspace (non-linear step). In the awake monkey primary visual cortex (V1), the variance of neurons activity that could be explained by such model ranged from 20% to 80% with a median at around 40% [Chen et al., 2007]. These high numbers were obtained despite the presence of patterns of spontaneous activity that may carry information unrelated to the immediate sensory stimulations [Kenet et al., 2003] and despite the potential impact of internally driven changes of state [Poulet and Petersen, 2008] that have been show (in barrel cortex) to affect cortical processing [Fanselow and Nicolelis, 1999; Ferezou et al., 2007].

This strong link between an external sensory input and neuronal activity is a useful leverage to study the cortical representations of information and the processing performed in these areas.

1.2 Barrel Cortex: beyond anatomical landmarks

1.2.1 A labelled line sensory system?

The study of many primary sensory cortices is made difficult by the lack of anatomical landmarks that would relate a given area of the brain with the processing of a well defined sensory input. For instance, in V1, very limited anatomical clues delineate the territory devoted to a specific part of the visual field such as the fovea (but see [Horton, 1984]).

In contrast with all other primary sensory cortices, barrel cortex is endowed with a sharp and visible anatomical representation of the corresponding peripheral sensory whiskers apparatus (fig. 1.1.a) in the form of "barrels" [Woolsey and der Loos, 1970] that can be revealed using cytochrome oxydase staining (fig. 1.1.b). Even better, the spatial extent of the whiskers that trigger functional responses to whisker deflections (barrel cortex spatial receptive fields [Axelrad et al., 1976]) seems to directly match this barrel organization [Welker, 1971; Welker and Woosley, 1974; Ito, 1981]. Indeed, multiunit recordings carried in a barrel show a dominant response to their corresponding whisker - the principal whisker (PW) - to the point of providing a barrel-precise localization of an electrode track within the cortex (fig. 1.1.c, *see the application of this method in Chapter 3*). The separation of this cortex in functionally distinct barrels is also clear in slices when studying the spread of electrical stimulations targeting layer IV barrels [Petersen and Sakmann, 2000, 2001]. Finally, this one to one link between whiskers and barrels is so strong that suppressing a whisker at birth results in the adult rodent cortex missing the corresponding barrel [der Loos and Woolsey, 1973].

Such a link between cortical structure and the spatial organization of the periphery has made barrel cortex a popular model for the study of the properties of the cortical column. This 'column' approach culminates in the systematic study of the C2 column from slices up to the awake behaving animal, for instance in the Petersen laboratory [Ferezou et al., 2006; Crochet and Petersen, 2006; Ferezou et al., 2007; Poulet and Petersen, 2008; Lefort et al., 2009; Gentet et al., 2010; Crochet et al., 2011].

1.2.2 Beyond the "principal whisker" model

Although the principal whisker paradigm holds well at the multiunit scale, single-unit recordings often display multiwhisker receptive fields [Simons, 1978; Ito, 1981; Simons, 1985; Chapin, 1986]. Following these initial works, barrel cortex receptive fields have been often described - and are still seen by some - as made of a strong response to the

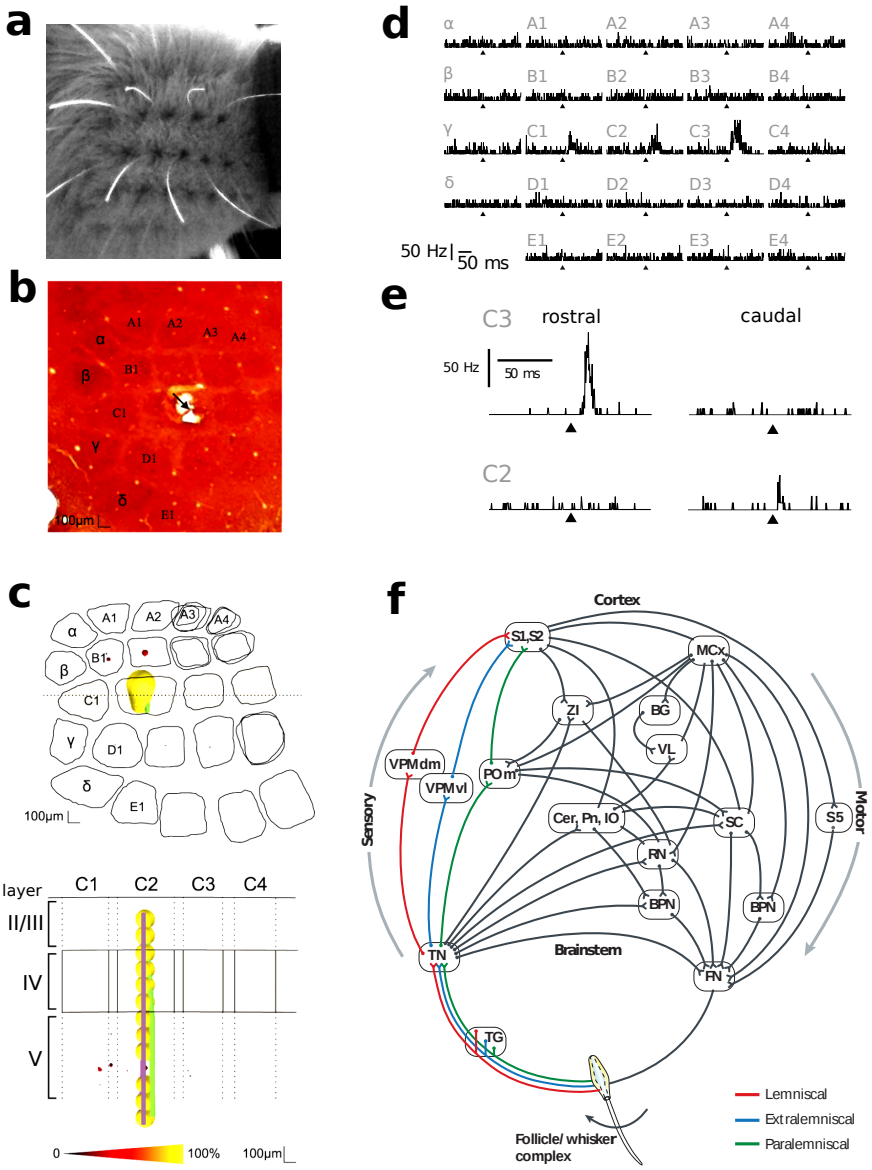

Figure 1.1 – The whisker sensory system. (a) Whiskers (white) inserted into the whiskerpad (black) on the left side of a rat snout. (b) 75 µm thick layer IV slice of a flattened and cytochrome oxydase processed rat barrel cortex. Arrow: electrical lesion produced by the electrode inserted in the C2 barrel following multiunit recordings. (c) Spheres: multiunit receptive fields recorded during the insertion of the electrode every 100 µm. Sphere size is proportional to the strength of the functional response to a given whisker. Purple: 3D linear regression of the multiunit recording. Green: actual electrode track derived from histological reconstruction of electric lesions. Notice the match between the multiunit regression and the anatomical electrode track (d) Single unit (RSU, layer IV) receptive field explored across 24 macrovibrissae. Notice the response to the stimulation of several adjacent whiskers. Triangles: stimulus onset (e) Single unit (RSU, layer IV) receptive field obtained for rostral deflections versus caudal deflections. Notice the displacement of the single whisker triggering functional responses from C3 to C2 between these two directions. (f) Network of nuclei and cortical areas taking part into the whisker system. In alphabetical order: BG:Basal Ganglia, BPN: Brainstem Premotor Nucleus, Cer: Cerebellum, FN: Facial Nucleus, IO: Inferior Olive, MCx: Motor Cortex, POm: POsterior nucleus median, Pn: Pontine nucleus, RN: Red nucleus, S1: primary Sensory cortex, S2: secondary Sensory cortex, TG: Trigeminal Ganglion, TN: Trigeminal Nucleus, VL: VentroLateral nucleus, ZI: Zona Inserta, VPMdm: dorsomedial section of the Ventral Posterior Medial nucleus, VPMvl: ventrolateral section of the Ventral Posterior Medial nucleus. Diagram modified from [Diamond et al. 2008]

principal whisker, surrounded by much weaker responses to the deflection of the adjacent whiskers [Wright and Fox, 2010]. However, even this rule of 'concentric circles' where increasingly remote whiskers trigger decreasingly strong functional response does not account for the properties of many receptive fields of barrel cortex neurons such as the layer IV regular spiking unit presented in Figure 1.1.d (these results regarding multiwhisker receptive fields are further discussed in Chapter 3).

Beyond this model, many functional properties of barrel cortex neurons are still not integrated into a broader picture: a large proportion of barrel cortex was found early on to be tuned to the direction of whisker deflections [Simons, 1985; Brecht and Sakmann, 2002; Wilent and Contreras, 2005] (fig. 1.1.e). Strongly non-linear summations of responses to the stimulation of adjacent whiskers were also observed in many studies [Simons, 1985; Simons and Carvell, 1989; Brumberg et al., 1996; Goldreich et al., 1998; Shimegi et al., 1999; Ego-Stengel et al., 2005]. These different selectivities and non-linearities all question the view of the barrel cortex as a straightforward mirror of the whiskerpad contacts with objects. They are however to this day not part of a clear functional picture of barrel cortex neurons.

1.2.3 A cortex embedded in a complex network of subcortical nuclei

The circuit that supports these functional properties also turned out to be far from a labelled line, in contrast with the "classical" picture of the system. In this classical view, the whisker system is made of a series of relays from the whiskers up to the barrel cortex. The first relay is the whisker follicle where the transduction is carried out. In this structure, whisker motion is highly reliably detected [Jones et al., 2004] by mechanoceptive neurons (their soma constitutes the trigeminal ganglion). These neurons project their axons to the trigeminal nucleus [Simons, 1985]. In turn, this nucleus relays its input to the thalamus where clearly delineated areas related to each whisker can be observed: the barreloids [Van Der Loos, 1976]. Finally, the afferent voley reaches layer IV of the barrel cortex where it is relayed separately within each of the different barrels, before being projected into layer V and II/III where convergence from multiple barrels give rise to multiwhisker receptive fields [Simons, 1985].

This simple picture of the whisker system has been attractive for researchers studying the barrel cortex since it depicts this cortical area as the only stage where multiwhisker integration of the sensory inputs is likely to occur, with a strong case being made for considering the rest of the system as a simple wiring that independently links each whiskers to its related barrel column. However, more recently, the circuit involved in the processing of whisker deflections has progressively turned into an increasingly complex network of recurrent subcortical nuclei.

Indeed, a renewed view of the whisker system has progressively emerged where multiwhisker responses are already found at the trigeminal nucleus level [Veinante and Deschênes, 1999] as well as in the thalamic nuclei that are projecting their axons to the cortex, including the VPM [Armstrong-James and Callahan, 1991]. In addition, no less than three different input pathways (lemniscal, paralemniscal and extraleminscal) have been found to project to the barrel cortex. Each have different temporal filtering and spatial integration properties. Each project to different parts of the barrel cortex [Bureau et al., 2006; Yu et al., 2006]. The lemniscal pathway originates from the VPMdm area of the thalamus and projects into the cortical layer 4 barrels. The extralemniscal pathway originates from the VPMvl and goes to the septum in layer 4 of the barrel cortex. Finally, POm projects into the septal area of layer Va (these different pathways are reviewed in [Diamond et al., 2008; Petersen, 2007], see also fig. 1.1.f).

Within the barrel cortex, these different pathways are integrated through many cortico-cortical projections, both internal to one given barrel column [Lefort et al., 2009] and also laterals, projecting from one column to the next (reviewed in [Schubert et al., 2007]).

Finally, active movements of the whiskerpad were found to be tightly coupled with perception. Active whisker movement were first seen as a direct homologue of passive whisker deflection, thus leading to the development of "passive" electrical whisking experiments where rostrocaudal "whisking" movements were mimicked by electrically stimulating in a rhythmic manner the facial nerve [Brown and Waite, 1974; Szwed et al., 2003]. In contrast, it has now been found that whisking is correlated with an internally driven change in the state of the barrel cortex [Poulet and Petersen, 2008] that affects directly the neuronal processing of whisker stimulations [Fanselow and Nicolelis, 1999; Ferezou et al., 2007]. Further, barrel cortex is involved into the motor control of whisker movements through a direct descending motor pathway [Matyas et al., 2010].

(1) Such complexity of the whisker system network as well as (2) the large number of tuning and non-linear responses that have been observed in the barrel cortex (see subsection 1.2.2 and Chapter 4) all suggest that barrel cortex is doing more than a simple mirroring of ongoing whisker deflections.

The elucidation of this potentially complex sensory processing rests largely on the study of the link between well chosen whisker stimulations and the resulting neuronal activity of barrel cortex neurons: to some extent, the identification of an optimal stimulus for the barrel cortex is a proxy for the identification of the processing carried out in this area. One illustration of such a direct link can be found in the study of the primary visual cortex. In this area, the identification of gabor filters as the optimal stimulus for V1 simple neurons [Hubel and Wiesel, 1962; Daugman, 1985] was quickly followed by their use in computer image analysis as one of the most efficient processing steps to identify object edges [Daugman, 1988]. This direct equivalence between optimal stimulations and sensory processing units has been formalized in the reverse correlation analysis of sensory systems [De Ruyter Van Steveninck and Bialek, 1988], a methodology that we thoroughly used in the work presented in Chapter 4.

In the following, we review the stimulations that best trigger functional responses in the barrel cortex, and we analyse the corresponding views of the processing going on in the barrel cortex. We argue that in contrast with the visual cortex, the actual processings carried in the barrel cortex have yet to be identified and that so far only the "envelop" of this processing has been identified.

1.3 Looking for the tuning of barrel cortex neurons

1.3.1 Studying a sensory system without the support of intuition

The whisker system has no human equivalent. The sensitivity of tactile hairs has been compared with the contact with fingers [Carvell and Simons, 1990] and a tentative replica of the whisker system for humans has been created to gain insight into the sensations mediated by this organ [Saig et al., 2010]. Still, no solid human intuition of the range or type of sensory stimulations available to the rat can be obtained on such grounds.

Comparing the study of the whisker system with the study of the visual system makes this shortcoming even more striking. The study of vision was supported by intuitions arising from human visual perception and its well developed psychophysics, including the knowledge that the visual system perceives spatial shape, that it is sensitive to binocular effects and even more basically that it is sensitive to a certain range of time and spatial

frequencies. In addition, the existence of a Human visual system ensured the availability of sensory stimulators tailored to match well the sensory range of mammalian visual systems (including cats and non-human primates): screens, that is, in their recent incarnations, television and computer screens.

In contrast, the lack of any intuition regarding even an estimate of the range of 'sensible' whisker stimulations adds up to a very limited set of anatomical indications regarding the "proper" use of whiskers as a sensory organ: Caudal whiskers are thick and seem strong, but are easily bent when strained [Carvell and Simons, 1990]. They can actually be exposed to a variety of stimuli including sand-papers [Guic-Robles et al., 1989] without showing clear signs of fatigue. In addition to this lack of clear mechanical boundaries regarding possible tactile stimulations, whiskers are inserted into the intricate muscular architecture of the whiskerpad [Dorfl, 1982; Simony et al., 2010] that allow fast and large scale changes in their position, and blood sinus surrounding each whisker follicle may modulate the damping and rigidity of the system over a wide range of values [Vincent, 1913; Fraser et al., 2006]. Overall, the general characteristics of relevant sensory stimulations appear hard to grasp on the basis of the mechanical structure of the whisker system.

In this condition, it may be useful to turn to the active functioning of the system and to find out the stimulations that are indeed taken into account and processed by the whisker system. This question can be addressed at several levels, that each correspond to widely different mindsets and experimental settings : in *freely behaving* animals, what are the spontaneous uses of whiskers by animals endowed with this sensory modality? During *trained behaviours*, what are the type of stimulations that the animal can efficiently discriminate? When recording neuronal activity in the barrel cortex of *non-behaving animals*, what range of whisker deflections makes the barrel cortex fire?

1.3.2 observing free animals use their whisker system

An ethological view on whisker systems across animal species

Whisker systems are found in virtually all mammals, regardless of their environment (sea, ground, air) with the exception of Humans (even monkeys have whiskers [Hayward, 1975]). Whisker systems are thought to share a common phylogenetic origin [Brecht et al., 1997]. As such, and despite the focus of this study specifically on the whisker system of the rat, it may be useful to go through the diversity of whisker uses across mammals since such a survey may unveil whisker functions that are also relevant to the rat albeit less prominent than in other, more specialized mammalian species.

Among the best described whisker systems, the harbor seal uses its whiskers for hunting by tracking the water turbulences produced by preys [Dehnhardt and Ducker, 1996; Dehnhardt et al., 1998, 2001].

Also using its whiskers to identify fluid turbulences, the bat makes use of sensory hairs implanted on its wings to measure the instantaneous air flow in which it flies, thus assessing the risk of a stall. By removing these hairs, the bat loses much of its ability to perform acrobatic flight [Sterbing-D'Angelo et al., 2011].

Fluid flow analysis thus appears across species as an unintuitive but major role of whisker systems. Although no direct study has shown this role to be well developed in rodents, we hypothesize that at least limited capabilities of this sort are present in this species since studies have been already carried describing functional response of the neurons of the rat barrel cortex to directed air blows on the whiskers [Welker, 1971; Sosnik et al., 2001; Ahissar et al., 2001]. Supporting this hypothesis is the behaviour of the Wa-

ter Shrew, a mammalian species that shares many homoplasies with rodents and that uses its whisker system for prey hunting both on the ground and underwater. Rodents - like the shrew - may well be capable of sensing both object contacts in the ground and fluid flow in water and in the air.

Another major difference between whisker systems is between 'whisking' and 'non-whisking' animals. Rodents as well as some other mammals such as shrews can perform so called whisking: active and rhythmic movement of their whiskers in the rostrocaudal axis at 5-15Hz (rat), 10-40Hz (mice) [Jin et al., 2004], and around 25Hz in shrews [Anjum et al., 2006]. Rats whisk during the tactile exploration of novel objects [Moreno et al., 2010] and are capable of efficient tactile discriminations while carrying out this active whisker displacement [Carvell and Simons, 1990] associated with a marked internally driven change in cortical state [Poulet and Petersen, 2008].

However, although cats have whiskers and perform nocturnal hunting (likely relying heavily on their whiskers in this condition) and are indeed endowed with cortical neurons capable of functional responses to whisker stimulations [Schultz et al., 1976], they cannot whisk, similar in this to many other mammals such as dogs. Such examples of non-whisking whisker systems add to the interest of studying the rat whisker system in a situation where whisking does not take place, such as in an anaesthetized preparation. The relevance of this non-whisking situation has also been recently fully established by the development of a non-whisking rat discrimination task [Adibi and Arabzadeh, 2011]. It is also being studied in Daniel Shulz laboratory through a novely discrimination task (Boubenec et al., *in preparation*).

The use of whiskers by behaving rodents

By performing behavioural experiments comparing rats with all whisker intact versus all whiskers cuts it was shown that rats depend strongly on their whiskers to solve mazes, and that whiskers are an important organ to help carry out tactile discrimination [Vincent, 1912]. However, it was not until the late twentieth century that a full demonstration was made of the ability of rats to perform tactile discrimination between different levels of texture roughness with their full whiskerpad [Guic-Robles et al., 1989; Carvell and Simons, 1990] and down to only two whiskers in the case of large scale features or even a single whisker in the case of smaller scale features that produce different whisker vibration frequencies [Carvell and Simons, 1995].

If whiskers are necessary and sufficient to tell apart two textures, it means that the whisker motion resulting from these two textures differs in critical "features" that are used as a discrimination criterion by the system.

One frequent strategy to identify such features has been to look at the most prominent aspects of the mechanics of individual whisker, starting with ex-vivo whiskers, plucked and glued on a stand, and filmed with high speed videography. In such studies, whiskers displayed a marked ringing when touching objet. Ringing was also found, to a lesser extend, in the awake animal [Neimark et al., 2003; Hartmann et al., 2003]. Following these initial studies, a ringing based model was proposed where each whisker, due to its different length, would vibrate to analyse the frequency spectrum of the contacted object, similar to the way a cochlea works [Moore, 2004].

Although it has been shown that some barrel cortex neurons are indeed capable of coding in a phase-precise manner high frequency sinusoidal deflections [Ewert et al., 2008], this property is unlikely to be used to code free-ringing at the natural frequency of the whisker for several reasons. First, in studies of the freely behaving animal, ringing per se does not seem to trigger neurons firing [Jadhav et al., 2009]. Second, the ringing fre-

quency of the whisker changes with the position of its contact with objects [Szwed and Shulz, 2007], thus making unlikely a code based on the intrinsic ringing frequency of whiskers.

More recently, the increased use of automated extraction of whisker movements from high speed cameras movies [Knutsen et al., 2005] has lead to a careful examination of whisker micromotions resulting from the rat contacting textures [Ritt et al., 2008; Wolfe et al., 2008]. The main observation extracted from this work is that "stick and slip" motion events are prominent. These events (taking place in the course of about 20ms) are two step processes where the whisker is first stopped in its sweeping by a contact with the texture, and after a few milliseconds is then suddenly released, thus leading to a dampened oscillation at the ringing frequency. Interestingly, these features not only are frequently found during free whisker contacts with objects, but also turn out to efficiently trigger functional response, both in the urethane anaesthetized trigeminal ganglion [Lottem and Azouz, 2009] and in the awake cortex [Jadhav et al., 2009].

It is interesting to note that comparable features have been found when looking for optimal filters across the whisker system by using the reverse correlation approach in the penthobarbital anaesthetized trigeminal ganglion [Jones et al., 2004] as well as in the urethane anaesthetized VPm [Petersen et al., 2008] and in the urethane anaesthetized cortex [Maravall et al., 2007] as well as in our own work on the isoflurane anaesthetized rat (see Chapter 3).

However - in contrast with the 'ringing cochlea' hypothesis, the stick and slip hypothesis does not propose any specific role for the spatial organization of the whiskerpad beyond the fact that multiple whiskers sample simultaneously a wider space than a single whisker. This lack of function does not seem to be a reasonable assumption in the view of the highly structured and reproducible geometry of the whiskerpad across individuals [Towal et al., 2011] and across mammalian species [Ahl, 1986]. Indeed, such a stable structure across species is necessarily strongly selected by evolutionary pressure and is thus likely to take part in a valuable biological function, beyond simple spatial pavement.

What could be this important function? One consequence of the row/column organization is that sequential deflection of whiskers when touching the edge of an object mainly differ in the dephasing between whisker rows [Sachdev et al., 2001]: such delayed correlation between consecutive whiskers may be used by the animal to compute kinetic properties of the touched object.

In addition to the analysis of object kinetics, we hypothesize that the analysis of the correlation between multiple whisker contacts results in different levels of cross-whisker correlation in function of the scale - granulometry - of the contacted objects. Tactile objects with a characteristic size smaller that the intervibrissal distance would lead to uncorrelated adjacent whisker deflections, while increasingly large-scale textures would drive adjacent whiskers in an increasingly correlated fashion. This hypothesis has been our working model to define multiple whisker stimulations in the study of their analysis by barrel cortex neurons (see Chapter 3).

In the view of the potential implication of interwhisker statistics in the coding of several parameters of the tactile scene, it is surprising to note that barely no study has investigated the characteristics of multiple-whisker stimulations taking place when animals touch textures and objets: tracking multiple whiskers in an awake behaving animal simultaneously makes experiments difficult. Still, the few studies that succeed in this feat [Von Heimendahl et al., 2007; Ritt et al., 2008; Wolfe et al., 2008] did not take that opportunity to describe the statistics of the multiple whisker contacts, instead limiting the multiwhisker analysis to the coherence between whisker movements when no physical contact occured [Wolfe et al., 2008].

1.3.3 Identifying whisker stimulations by the yardstick of neuronal activity

So far, we have seen that whisker-based behaviours reveal the type of whisker stimulations they favour. These stimulations provide a valuable estimate of the space of 'ethological' whisker stimulations that should be further considered. However, to identify within this ethological range the stimulations encoded by barrel cortex neurons, the activity of barrel cortex neurons should be recorded and directly related to whisker movements.

The 'simplest' strategy to build a link between whisker stimulations and neuronal activity is to let the animal freely behave and to relate post-hoc the stimulations sensed by the animal and neuronal activity. Such an approach is hindered by both practical and theoretical drawbacks. Indeed, it is difficult to track the precise movements of whiskers in freely behaving animals, and electrophysiological recordings in this setting also are demanding.

Still, beyond technical issues, the general lack of well defined unitary events in 'natural stimulations' hinders forward correlation (PSTH) approaches. Indeed, these analyses are based on the assumption that spikes code the functional response to a well defined stimulation event. Three noteworthy exceptions that have been studied using forward correlation approaches in the freely behaving animal are the onset of a single whisker contact with a piezoelectric sensor [Crochet and Petersen, 2006; Curtis and Kleinfeld, 2009], the whisking cycle as reported by electromyography or high speed videography [Fee et al., 1997; Crochet and Petersen, 2006; Curtis and Kleinfeld, 2009] and sick and slip whisker deflections occuring during the whiskers contacts with a texture [Jadhav et al., 2009]. For all three types of events, barrel cortex neurons of awake freely behaving animals were elegantly shown to produce a marked modulation of their firing rate. Still, due to the lack of experimental control on the type of stimulations applied by the animal on its whisker, it does not seem possible to characterize much further the animal neuronal selectivity, for instance to different shapes of stick and slips, or for different directions of whisker contact.

In contrast, reverse correlation approaches may appear at first sight better adapted to analyse the link between the discharge of a neuron and uncontrolled *self*-stimulations. Indeed reverse-correlation analysis is based on the statistical analysis of the ensemble of stimulations that occurred just before the onset of spikes. Spike triggered average (STA) is the analysis that results from averaging the spike triggered ensemble, while spike triggered covariance (STC) amounts to performing a PCA of the spike triggered ensemble. Noise sensory stimulations are used in these experiments to explore in an unbiased manner the widest possible stimulus ensemble.

However, although 'natural' stimulations look a lot like noise to the unexperienced eye, their statistical properties do not match the requirements of classical reverse correlation analysis methods such as STA or STC [Schwartz et al., 2006]. Indeed, such stimuli do not present equally all possible stimulus frequencies, and they also tend to be particularly rich in higher order statistics [Simoncelli and Olshausen, 2001]. Both characteristics can induce strongly bias in the output of reverse correlation algorithms. More complex and computationally intensive methods should be used in such situations [Sharpee et al., 2004] to alleviate this caveat. Anyhow, all reverse correlation methods require a very large number of spikes (more than 50 per stimulus dimension), meaning that one should often collect several thousand spikes from a neuron to attain an adequate characterization of its functional properties - such a requirements is unlikely to be attained in the awake behaving animal.

Controlled stimulations in the awake animal

Such limits to the examination of the stimulus selectivity of barrel cortex neurons in the freely behaving animal can only be an enticement to better control the stimulation applied to the animal whiskerpad. One of the slightest possible departure from the 'awake behaving' animal is to control whisker stimulation in the awake animal. We could successfully developed such a behavioural setting during a one year stay at Carl Pertersen laboratory (EPFL) just prior to the onset of my PhD.

Water scheduled head fixed mice were trained to associate a deflection of their remaining C2 whisker with the immediate and short term availability of water on a port next to their mouth ((fig. 1.2.a)). The buildup of this behavioural association was assessed by measuring licking patterns through the crossing of an optical gate by the mouse tongue ((fig. 1.2.b)). Mice maintained a clear focus on the task through the 10 minute daily training sessions (fig. 1.2.c).

The end product of this training was a low latency (240 ms) licking response of the animal to whisker stimulations (fig. 1.1.d), with latencies showing a progressive decrease through training sessions (fig. 1.1.e), while the ability of the animal to specifically condition its licking on stimulation, as measured by the ratio between whisker stimulation triggered and non-trigged licking (behavioural index) steadily increased (fig. 1.1.f).

Further development of this behaviour and the study of the corresponding activity of barrel cortex neurons are being currently carried out in Carl Petersen laboratory. Importantly, training sessions are being shortened so as to limit the 'overtraining' effects that is likely to have made the task barrel cortex independent (fig. 1.1.g)

To perform whisker stimulations on an awake behaving animal, we applied on the only untrimmed whisker, C2, a ferromagnetic paste made of iron powder mixed with high viscosity grease, and we applied brief magnetic pulses on this actuator through a strong electromagnet set below the mouse. This method was derived from a previoulsy designed whisker stimulation with a metal particle glued on the whisker [Melzer et al., 1985; Ferezou et al., 2006] with the added aim of being able to let the whisker of the mouse intact training days after training days. The choice of this technique made whisker stimulations independent of any whiskerpad movement performed by the mouse (thus opening the sensory-motor loop without the need for surgery or anaesthesia). However, only limited control could be exerted on the whisker: the stimulation past exerted a constant downward deflection on the whisker. In addition, the impulse stimulation resulted in a marked whisker ringing at an unnatural frequency dictated by the loading of the whisker with paste. The stimulation could only produce a dorso-ventral deflection. Finally, such magnetic stimulation could not be applied independently on more than a single whisker at a time. All these limitations make awake whisker stimulations of limited use for the in depth characterization of the sensitivity of the whisker system. We expect similar issues to affect most strategies that could be used to control whisker stimulations without fully controlling whisker movements.

Controlled stimulations in the anaesthetized animal

A radical departure from the freely behaving awake animal approach is to favour a high degree of control on whisker stimulations to the expense of the potentially active functioning of the whisker system. The use of anaesthetics has long been - and is still - the preferred method to set the animal in a passive and pain-free state where both surgical procedures and arbitrary whisker stimulations can be carried out. However, the infusion of such chemicals in the animal body affects many of the properties of the whisker system:

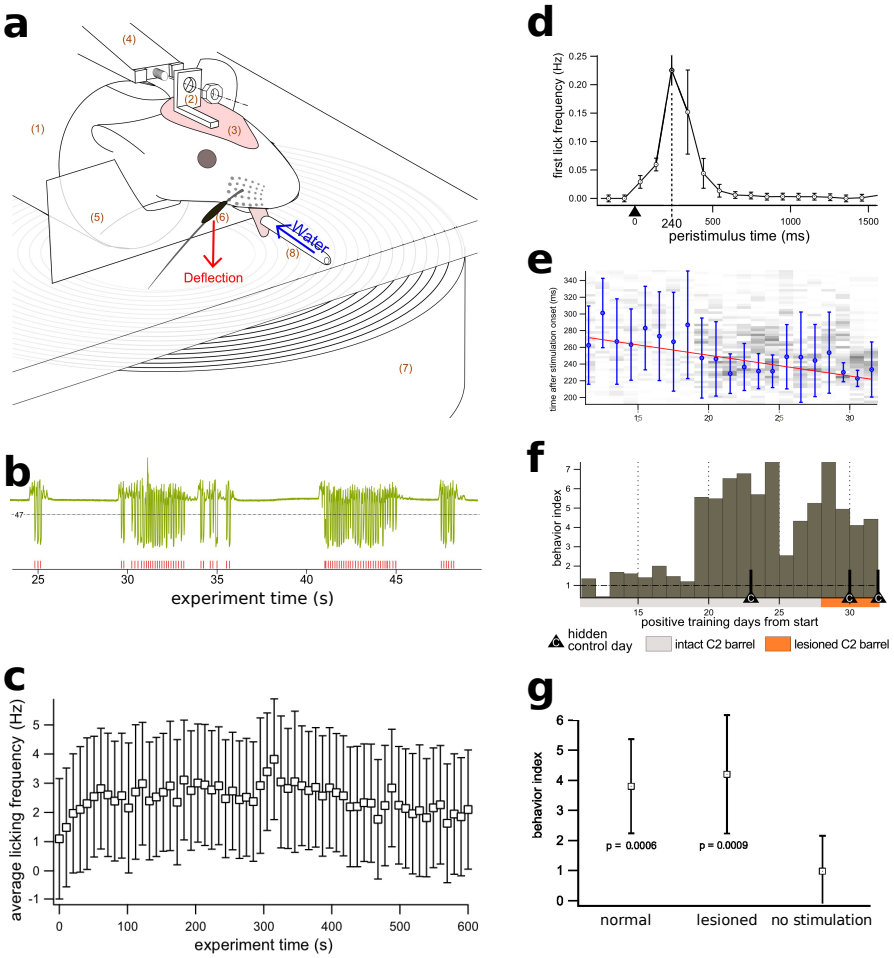

Figure 1.2 – The stimulus detection task carried in the head-fixed mouse. (a) General preparation. The mouse is sitting in a tube (1). The headpost (2) is secured with glue and dental cement (2) on the mouse skull and is screwed (3) on a head fixation system (4) during behaviour training sessions. A tube closure (5) prevents the mouse from removing the magnetic stimulation paste (6) from the whisker with its paws. Magnetic pulses generated by a coil (7) deflect the stimulated whisker that has been fitted with a magnetic past. Immediately following magnetic stimulations, water can be obtained during a fixed time by licking on a tube (8) lying next to the mouse mouth. Licks on the tube are are optically detected and used as the direct measurement of the task learning. (b) Example of optical monitoring of lick patterns (top) and their threshold based detection (bottom). (c) Steady licking across 10 min training sessions. (d) Peristimulus lick histogram obtained from a trained animal. Estimated licking latency is 240 ms. (e) Mean latency to lick progressively decreases across training sessions. (f) Ratio between licking trigged by a whisker stimulation and an untrigged licking (behaviour index) across training sessions. (g) Average behaviour index across all 4 trained animals with magnetic past on the whisker (left), following a lesion of the barrel cortex (right) and when no magnetic past was applied on the whisker.

- All active movements are removed, thus breaking the sensory-motor properties of the whisker system, including whisking but also motor feedback in response to passive whisker stimulations [Ferezou et al., 2007].

- The cortical state is deeply affected by anaesthesia. Isoflurane and halothane, two volatile anaesthetics, can induce a wide range of cortical states, from III-1 to IV, depending on their concentration in the breathing gaz [Friedberg et al., 1999]. In contrast, urethane is usually used to generate a deeper anaesthesia, around III-4, including slow oscillations between up and down states, as well as spindles (although lighter stages can also be attained by carefully adjusting the injection volume [Erchova et al., 2002]). In addition, urethane anesthesia affects the functional responses of barrel cortex neurons, leading to rebounds in the functional response [Simons et al., 1992]. Overall, anaesthetics induce similar pattern of increasingly correlated and decreased firing rate, including the now less common pentobarbital barbiturate [Simons, 1985]. Exceptions to this common pattern are non-general anaesthetics, such as (1) curares that induce a pure muscular paralysis [Simons, 1978], (2) morphinics such as fentanyl that induce a poweful analgesia [Brumberg et al., 1996] and (3) neuroleptics such as acepromazine that produce drowsiness [Brecht et al., 2004]. However, ethical use of anaesthetics includes the suppression both of painful sensation and of the general distress due to the experiment. To attain such a result, complex cocktails of non-general anesthetics must be used - a situation that may not be substantially better than a single-molecule general anaesthesia.

Still, general anaesthesia is capable of setting the studied animal in a remarkably stable brain state for hours, in particular if one uses a light and well controlled and well monitored anaesthesia (for instance using EEG and breathing measurements). This unique level of control on the animal state is invaluable for collecting the large spike counts that are needed to evaluate the functional properties of neurons. In addition, the lack of motor activity in the anaesthetized rodent is actually instrumental to the high degree of control on whisker stimulations that is required to explore neurons functional responses across the whole range of physiological whisker stimulations. We will review the whisker stimulation strategies made possible by the anaesthetize rodent preparation in Chapter 2.

The many tunings of barrel cortex neurons

In accordance with the range of stimulations identified by studying the whisker mechanics and whisker use in freely behaving animals, barrel cortex neurons of anaesthetized animals have been found to respond to a wide range of stimulus frequencies [Simons, 1978; Arabzadeh et al., 2003; Ewert et al., 2008]. Stick and slip patterns have also been found to trigger marked functional responses in the anaesthetized rat [Lottem and Azouz, 2009].

Adding to - and historically preceding - the findings obtained on awake animals, several additional tunings have been identified in barrel cortex neurons of anaesthetized rodents, by taking advantage of the precise control of the stimulation made possible by this preparation.

First, barrel cortex neurons receptive field have also been shown to often respond to more than a single whisker. This "multiwhisker" functional response property turns out to be dependent both on the type and level of anaesthetics used. Using only a paralysing agent, receptive fields turned out to be small and single whisker receptive fields dominated

layer IV barrels [Simons, 1978]. Such observations were not reproduced under deep general anaesthesia. In that condition, larger receptive fields were observed using pentobarbital [Simons, 1985; Ghazanfar and Nicolelis, 1999] or urethane [Ito, 1981; Brecht and Sakmann, 2002; Jacob et al., 2008] as we also report in Chapter 3. When using isoflurane and aiming at low levels of anaesthesia such as III-1/2, we found (Chapter 4) a high proportion of single-whisker neurons, comparable with observations previously made in curarized awake animals.

Barrel cortex neurons were also found to respond selectively across directions of whisker deflection in the awake curare paralysed rat [Simons, 1978] as well as in the urethane anaesthetized rat [Brecht and Sakmann, 2002]. Subthreshold mechanisms responsible for this tuning property have been described in the pentobarbital anaesthetized animal [Wilent and Contreras, 2005] and the spatial organization within the barrel of this direction tuning has been described as developing across late developmental stages: this tuning was not found in juvenile rats anaesthetized with urethane [Kerr et al., 2007] but it was observed in two studies using isoflurane anaesthetized adult rats grown in an enriched environment [Andermann and Moore, 2006; Kremer et al., 2011].

The selectivity of the barrel cortex neurons to different basic kinetic features of whisker deflections has also be explored in order to determine which one of amplitude, speed or acceleration of whisker deflections is the main property encoded by barrel cortex neurons [Simons, 1978; Ito, 1981; Pinto et al., 2000].

The observations that the firing rate of barrel cortex neuron may chiefly encode vibrational speed (Amplitude $\times$ Frequency, [Arabzadeh et al., 2004]) has been quickly followed by the discovery that the optimal patterns of whisker deflection indeed maximize this parameter. These patterns, comparable to 'stick and slips' [Ritt et al., 2008; Wolfe et al., 2008; Lottem and Azouz, 2009; Jadhav et al., 2009] have been isolated at several levels in the whisker system, from the trigeminal ganglion [Jones et al., 2004], up to the VPm [Petersen et al., 2008] and to the cortex [Maravall et al., 2007] by the mean of reverse correlation techniques [Petersen et al., 2008; Maravall et al., 2007] as well as a relate technique [Jones et al., 2004].

During our PhD, we have ourself carried a reverse correlation study in the barrel cortex, revealing that these 'stick and slip'-like optimal filters are actually part of a simple, 2D phase subspace in which different neurons can be tuned to different phases - similar to the way different neurons can be tuned to different directions of whisker deflection. Further description of this specific tuning can be found in Chapters 4 and 5.

1.4 Beyond tuning: processing and context dependence of processing

1.4.1 Interactions be multiple sensory dimensions can define powerful sensory processings

So far, we have made a recension of the wide parametric space of the whisker system and of the systematic tuning of barrel cortex neurons to the different dimensions of this space. How are these different tunings put together to perform sensory processing? For instance, in one hand, directional tuning tells us that neurons tend to respond more to one direction of deflection for a given whisker. In the other hand, barrel cortex neurons are known to be responsive to the deflection of several whiskers (multiwhisker receptive fields). How does these two tunings combine? Are adjacent whiskers within the receptive field tuned

to opposed directions, similar to V1 gabor filter "simple" cells [Hubel and Wiesel, 1962]? Or are all neurons tuned to the same direction of deflection [Kida et al., 2005]? These two opposite direction/space combinations would result in a totally different processing being performed. This is why we argue that to capture more than the "envelop" of the processing and to fully understand the processing operations carried by barrel cortex neurons, one should directly study the way barrel cortex neurons interconnect the tuning curves to the different dimensions of the barrel cortex sensory space.

A review of the effort to link variables across sensory dimensions can be found in Chapter 3. We carried experimental studies attempting to make the link between dimensions of the whisker sensory space both using classical forward analysis of "dirac"-like whisker stimulation (see Chapter 3) as well as using reverse correlation (see Chapter 4).

1.4.2 Are barrel cortex neurons processings also dependent on sensory context?

Ethological studies in rats and other whiskered mammals have shown that profoundly different sensory tasks may be carried out by the rat whisker sensory system, including object shape analysis, texture recognition and also probably air flow analysis (see section 1.3.2).

The corresponding diversity of sensory processing may be carried out in different cortical areas, similar to the large number of secondary sensory areas present in the visual cortex, each being involved in different visual processings [Felleman and Van Essen, 1991]. However, in the whisker system, only one primary and one secondary cortical areas have been identified. This diversity of whisker-associated processings may thus not be spread on spatially segregated areas. Instead, we propose that several of these disjoint processings are already carried out in the barrel cortex, and that the selection of the appropriate processing is made by the general statistics of the current sensory scene.

Such sensory context dependence of the processing in the barrel cortex is also supported by the previous observation of properties that can be compared to a context dependence, in both the visual and the auditory cortex.

Indeed, in V1 cortex, visually responsive neurons display a sparser coding [Vinje and Gallant, 2000], an increased spike precision [Haider et al., 2010] as well as a markedly strengthened antagonist surround when they are exposed to natural stimulations [Lesica et al., 2007] versus classical decorrelated "receptive field" stimulations.

Similarly, primary auditory cortex (A1) neurons have been shown to respond more strongly to the less frequent sounds, depending on the sounds present in the ongoing auditory context [Ulanovsky et al., 2003]. Another example of statistics-dependent processing in A1 is the observation that in situations where sounds in different frequency bands are correlated (co-modulated over time) A1 neurons responses are enhanced, including when a background noise is added [Nelken et al., 1998]: a clear example of processing being dependent on second-order statistical properties of the sensory stimulus.

Our work exploring the context-dependent processing that may take place in the barrel cortex is reported in Chapters 4 and 5.

1.5 Aims of the thesis

In the following chapters, we will present the work carried in the frame of this thesis. During this period, we attempted to identify (1) the type of multiwhisker stimulations that are sensed by barrel cortex neurons, (2) how this multiwhisker selectivity is affected by changes in the statistics of the sensory stimulus (the "sensory context") and (3) how

the identified context dependent multiwhisker selectivities are spatially distributed at the surface of the barrel cortex.

To carry such studies we developed a multiwhisker stimulator capable of deflecting independently 24 whiskers in one side of the whiskerpad, with arbitrary directions and over a wide range of stimulation frequencies. We will describe it in Chapter 2 (international patent and publication as co-first author in the Journal of Neuroscience Methods).

We will then describe (in Chapter 3) how a previously developed version of this multiple whisker stimulator was used to characterize with forward correlation techniques the connection between two classical properties of barrel cortex receptive fields: the tuning to the direction of stimulation and the shape of barrel cortex receptive fields (publication as co-first author in the Journal of Neurophysiology).

In Chapter 4, we will present work done to better identify the optimal stimulations that drive barrel cortex neurons, and what is the impact of sensory context on the sensitivity of barrel cortex neurons (publication as co-first author currently in revision at Nature Neuroscience).

In Chapter 5, we will present our exploration of the spatial organization of barrel cortex neurons as a function of their functional response. To this aim, we used two-photon calcium imaging coupled with the novel stimulation device presented in Chapter 1 of this thesis (Publication as co-first author in preparation).

Finally, in Chapter 6, we will discuss the motor aspect of the whisker system, one aspect of this system that we did not explore during this thesis but that we envision as an attractive follow up for this work.

Chapter 2

The craft of whisker stimulation

The anaesthetized preparation, despite its many drawbacks (see Introduction) permits a unique control on the sensory stimulation of the whisker system. The relaxation of the whiskerpad motor apparatus makes it possible to precisely move the whiskers with actuators without having either to mechanically force the whiskers to stay still [Stuttgen et al., 2006; Stuttgen and Schwarz, 2008; Gerdjikov et al., 2010] or to actively measure and compensate for the movements of the whiskerpad - a difficult problem that has found no practical answer beyond the limited control provided by magnetic deflections of single whiskers ([Melzer et al., 1985; Ferezou et al., 2006], see also Figure 1.2).

Even the static anaesthetized whisker system remains a complex and difficult structure to study. It holds a large number of whiskers forming a 3D fan, with for instance the most rostral whiskers pointing towards the front of the animal while the most caudal point on the opposite direction [Jacob et al., 2010; Towal et al., 2011]. Whiskers are heterogeneous in length and mechanical properties. Some 30 larger whiskers - the "Macrovibrissae" - are grouped on the caudal part of the whiskerpad and are involved in whisking in the awake animal. These whiskers (stradlers and arcs 1 to 4) are well chracterized. They have length ranging from 30 to 60 mm [Neimark et al., 2003], and ringing frequencies in the air ranging from 40 to 150 Hz (these values vary greatly with the length of the whisker and the way the whiskers are held, either into the whiskerpad, or ex-vivo, glued on a metal holder [Hartmann et al., 2003]).

In contrast, the many "Microvibrissae" that sit next to the animal mouth have not been precisely characterized [Brecht et al., 1997]. These tactile hairs are not much larger than fur hairs and cannot be whisked by the animal [Hartmann, 2001]. Still, these densely packed sensors (40 times the density of macrovibrissae) are thought to be involved in whisker dependent tasks [Hartmann, 2001].

Despite the potential interest of microvibrissae as a sensory system, these whiskers are hard to access due to their small size and they show a much less clear and regular pattern of insertion into the whiskerpad. These must be among the reasons that lead to the development of a large number of whisker stimulators aimed specifically at the macrovibrissae, while no stimulator has been developed to study the functional properties of microvibrissae.

2.1 Single macrovibrissa mechanical stimulation

Initial studies of the anaesthetized whisker system used hand deflections of the macrovibrissae to trigger functional responses [Welker, 1971]. However, the controlled mechanical deflection of identified whiskers has become quickly the basis of most studies of the whisker representations in the barrel cortex [Axelrad et al., 1976; Simons, 1978; Ito, 1981]. The lack of time precision of hand deflections, the uncertainty as to the type of stimulation generated by this method, and their low speed are all reasons that lead to this change.

Indeed, the study of the whisker system requires time precise and controlled whisker stimulations. In contrast with the visual cortex where reliable spiking responses can be triggered by the hand-directed lightening of an area of the visual field [Hubel and Wiesel, 1962], the barrel cortex shows only sparse activity in response to single whisker stimulations. As a consequence, even the first studies in the field found necessary to setup complex electronics to compute average electro-corticograms [Axelrad et al., 1976] or to build PSTHs [Simons, 1978] triggered by the precise timing of mechanical whisker deflections.

In addition, neurons in the barrel cortex are known to respond best to fast whisker deflections [Arabzadeh et al., 2004; Maravall et al., 2007]. In the awake behaving animal, whisker deflection speeds in the range of 1000°/s during stick and slip have been reported using high speed cameras [Ritt et al., 2008; Wolfe et al., 2008]. Extremely fast whisker stimulation - only attainable with mechanical whisker stimulations - are thus needed to meet such angular speeds.

2.1.1 Electromagnetic stimulators

The first technology capable of deflecting whiskers in the adequate range of angular speeds has been the galvanomagnetic actuator, a tool created to translate electrical current into mechanical movement [Simons, 1978; Ito, 1981; Nicolelis and Chapin, 1994; Shimegi et al., 1999]. This actuator technology is based on the repulsion of a couple of magnets. One is permanent and is held fixed on the actuator stand while the second, mounted on an axis, is an electromagnet. By adjusting the current flow going through the electromagnet, the strength of the repulsion between the two magnets fluctuates and is translated into a rotation of the actuator that holds the whisker. Such actuators are capable of large - millimetric - whisker deflections and they provide a good level of control on the characteristics whisker stimulus such as the direction of deflections. However, *accelerations* of standard galvanometric actuators are rather slow [Simons, 1978] - actuator excursions have an exponential time course with a 9ms time constant [Ito, 1981] - despite the high *speeds* attained by such devices (570°/s) [Simons, 1978; Ito, 1981].

One alternate design that can be related to the galvanomagnetic whisker stimulator is the solenoid actuator [Chapin, 1986; Ghazanfar and Nicolelis, 1999; Krupa et al., 2001; Rodgers et al., 2006; Hirata and Castro-Alamancos, 2008]. In this design, the electromagnet is not held on the axis and moves along it in a bistable way between two positions, one 'resting' and one 'energised' position, thus only allowing a single direction and a single amplitude of deflection. Still, solenoid based whisker actuators have been shown to produce ringing-free and extremely fast whisker deflections (around 6000°/s for a whisker moved at 10mm from its whiskerpad insertion) [Krupa et al., 2001], although such observations have not been consistent across laboratories. For instance, even by implementing closed-loop designs on top of this actuation technology, [Walker et al., 2010] could not avoid whisker movements to be contaminated by strong ringing.

2.1.2 Piezoelectric stimulators

In parallel to the use of galvanometers, piezoelectric 'benders' have been introduced [Simons, 1983] in the field of whisker stimulations. The principle of operation of these actuators is fundamentally different than that of the galvanometric actuator. There, the actuator arm is made of a sandwich of piezoelectric ceramic blades that responds to electric tension by shrinking or expanding. By gluing together two piezoelectric blades and by applying a different voltage to the two blades, mechanical tension bluilds into the assembly and results into a bending that moves laterally the tip of the actuator (and the attached whisker). In contrast with galvanometric actuators, piezoelectric benders cannot generate large movements (they classically move by hundreds of microns, not millimeters), but they are capable of accelerations/speeds comparable to those of solenoid actuators (up to 1500°/s [Simons and Carvell, 1989]) and they are capable of arbitrary movements with better than micron precision.

Finally, in contrast with electromagnetic actuators, piezoelectric actuators have been developed that can explore all directions of deflections, both following the rostrocaudal and the dorsoventral axis. Such omnidirection whisker deflections have been first implemented by gluing together two monodirectional piezoelectric actuators [Simons, 1983]. However, more recently, applications of piezoelectric benders to the field of imaging have lead to the development of compact monobloc 2D actuators that are particularly well suited for the omnidirectional deflection of multiple whiskers in the whiskerpad. They have been used in several studies [Andermann and Moore, 2006; Petersen et al., 2008], including in our team [Jacob et al., 2008]. We used these actuators as the basis of our own technical developments (see patent). This omnidirectional whisker actuator is also a very compact solution (actually more compact than classical 1D benders), in contrast with other 2D stimulators that take up a vast amount a lateral space, including solenoid based [Tsytsarev et al., 2010] and linear motor based [Kremer et al., 2011] 2D actuators.

The main drawback of piezoelectric actuators is their limited range. Indeed, if the range of classical 1D benders reaches up to 2 mm [Simons, 1983], the range of 2D benders was in our hands limited to 360 µm. Such limits in whisker deflection range can be compensated by stimulating the whiskers nearer to their insertion into the whiskerpad - with the effect of bending more strongly the stimulated whiskers, an aspect of the whisker stimulation that may be sensed by the rat transduction apparatus.

2.1.3 Electrical whisking

An alternate strategy to the deflection of the static anaesthetized whiskers with and actuator is to make the whiskerpad move by electrically driving periodically the facial nerve, a nerve that projects to the whiskerpad muscles [Brown and Waite, 1974]. The resulting whisker oscillations can be made to mimic the whisking movements observed in the behaving animal: so called 'electrical whisking'. By setting objects in the trajectory of the whisking movement, it is possible to generate whisker stimulations that trigger sensory responses in barrel cortex neurons [Szwed et al., 2003, 2006].

However, to define properly the onset of these whisker stimulations, high speed filming is required to define the precise onset of whisker contacts with the stimulating object, making such experiments not much different in their difficulties than more physiological awake experiments [Crochet and Petersen, 2006; Ferezou et al., 2007]. Beyond these technical considerations, artificial whisking should not be mistaken for actual whisking. Indeed, in contrast with active whisking, it is not correlated with an internally driven change of state [Poulet and Petersen, 2008] and changes in the processing of whisker

stimulations [Fanselow and Nicolelis, 1999; Ferezou et al., 2007] in the barrel cortex. More critically, such whisker movements have not been produced by the activation of the motor neurons that normally drive voluntary whisker movements in the sensory loop, including motor barrel cortex neurons [Matyas et al., 2010]. This situation may lead to a potential mismatch between the sensory input, the sensory processing and the motor command taking place in the barrel cortex.

2.2 Towards the faithful reproduction of arbitrary whisker stimulations

2.2.1 Controled impulse stimulations with mechanical stimulators

Forward correlation - the most frequently used functional characterization strategy in the barrel cortex - is based on the repeated application of a common, standardized whisker deflection across all explored dimensions of the sensory ensemble.

To select an adequate time course for the command used to generate the whisker stimulation, the resulting actuator movement should be measured and searched for artefactual ringing: uncontrolled actuator movement at its natural frequency that may trigger unwanted sensory responses. Such verifications of the actuator movement have been performed in previous studies by using photodiods [Simons, 1983; Ito, 1985; Neimark et al., 2003; Andermann et al., 2004; Lee and Simons, 2004; Stuttgen et al., 2006; Stuttgen and Schwarz, 2008; Gerdjikov et al., 2010; Boloori and Stanley, 2006], piezoelectric sensors [Krupa et al., 2001], and more recently laser telemeters [Kida et al., 2005; Wilent and Contreras, 2005; Drew and Feldman, 2007; Jacob et al., 2008; Kremer et al., 2011] and high speed cameras [Andermann and Moore, 2006]. However, it should be noted that overall, only a limited proportion of the studies using whisker stimulators do report having performed such validation of their whisker stimulation protocols, thus casting doubt on the functional properties reported elsewhere.

2.2.2 Linear models of whisker stimulators for mechanical and software corrections

The faithful reproduction of elaborate whisker stimulations - such as the contacts of whiskers on a textured surface - requires more elaborate strategies than the reproduction of a simple unitary whisker deflection. In this section, we will keep our focus on piezoelectric actuators since they are currently the dominant whisker deflection technology and are capable of highly precise and reproducible stimulation - an important prerequisite to produce arbitrary movement with an actuator.

A classical engineering method to predict and potentially correct the movement of a actuator in front of an arbitrary input is to build a linear model of the device by comparing known inputs with the corresponding output generated by the device. Such linear models are generally limited to the amplitude/phase subspace - so called 'transfert functions'. To compute the transfert function of an actuator, it should be submitted to sinusoidal driving commands with constant amplitude and gain, and with a systematic sampling of the frequencies across the studied range. For each sampled frequency, the phase and gain of the resulting actuator movement should be measured. The resulting gain and phase curves across frequencies provide a good model of piezoelectric actuators, only *in their linear range*. Indeed, they can account neither for the properties of the actuator around

its natural frequency (ringing frequency) nor for hysteresis, that is a non-linear drift of the piezoelectric actuator that depends on its past movements.

Still, such a simple Gain/Phase model provides a good estimate of the range of frequencies for which the actuator maintains a constant gain and dephasing and can generate faithful reproductions of arbitrary waveforms. It has been used to assess the proper transduction of stimulations [Sheth et al., 1998; Petersen et al., 2008; Boloori et al., 2010] and to validate improvements in the mechanical properties of whisker stimulators (for instance by shortening the piezoelectric actuator to increase the actuator natural frequency [Andermann et al., 2004]).

Better, the characterization of the actuator transfer function can be directly used *in the linear regime* of the actuator to cancel out deviations from a 'perfect' transfer function, in order to obtain an actuator with equal gain and dephasing over a wide range of frequencies [Maravall et al., 2007]. This 'equalizing' is obtained by filtering the stimulus waveforms by the inverse of the transfer function. However, this method entirely depends on the proper characterization of the current actuator transfer function: as soon as the actuator transfer function changes, this cancelling method is disrupted. Causes for such changes in the transfer function include any adjustment in the mechanical assembly that holds the actuator in order to change its positioning.

In our own development of a high performance whisker stimulator, we specifically tuned the mechanics of the actuator to increase its natural frequency to very high values (> 1000 kHz) so as to widen the frequency range that can be corrected by the mean of the inverse transfert function method. In addition, to be able to apply in a routine manner the same inverse transfer function correction without constantly re-evaluating the transfer function, we designed position adjustment mechanisms (a ball joint and a translation) that do not affects the transfer function of the actuator - meaning that the positioning of the actuator onto the whisker can be carried out without changing its transfer function. A patent on this technological developments has be registered and can be found starting at page 34.

2.3 Multiple whisker stimulations

Time-controled single whisker deflections have been increasingly possible in the awake behaving head-fixed rodent [Crochet and Petersen, 2006; Ferezou et al., 2006; Stuttgen et al., 2006; Stuttgen and Schwarz, 2008; Gerdjikov et al., 2010], albeit with limited control on the shape of the applied stimulation. On the other end of the spectrum, a few studies have focused on the functional response to fully correlated multi-whisker stimulations and could thus rely on a single whisker stimulator to deflect bundles of whiskers [Mirabella et al., 2001; Maravall et al., 2007; Petersen et al., 2008; Galvez et al., 2009]. Such studies could probably to some extent also be carried in the awake animal using magnetic stimulations of the whole whiskerpad.

However, a larger proportion of the studies on multiwhisker stimulations have rather focused on the strongly non-linear functional responses to delays between stimulations occuring on adjacent whiskers [Simons, 1985; Shimegi et al., 1999; Ego-Stengel et al., 2005] as well as on the tunings to the onset [Drew and Feldman, 2007] and direction [Jacob et al., 2008] of propagating waves of deflections across the whiskerpad. To this day, these different functional properties can only be studied using independent stimulation of multiple whiskers in the anaesthetized preparation.

The development of the required multiwhisker stimulators has been a demanding task because of the complex geometry of the whiskerpad [Towal et al., 2011; Brecht et al.,

1997] and also because of the need to assemble a set of independent whisker stimulators converging into the approximative 1 cm^2 of the rat whiskerpad. Multiwhisker have been progressively developed that allow the independent stimulation of 2 whiskers [Simons and Carvell, 1989; Goldreich et al., 1998; Kida et al., 2005; Ego-Stengel et al., 2005], 3 whiskers [Shimegi et al., 1999, 2000; Rodgers et al., 2006], 5 whiskers [Simons, 1985; Brumberg et al., 1996], 9 whiskers [Drew and Feldman, 2007; Andermann and Moore, 2006] and finally 24 whiskers (meaning that most of the macrovibrissae are stimulated) [Ghazanfar and Nicolelis, 1999; Krupa et al., 2001; Jacob et al., 2008].

Larger arrays, holding 9 to 24 whisker stimulators, can actually "display" whole tactile scenes. They have been used to represent simplified versions of what might happen when an object edge gets in contact with the rat whiskerpad [Drew and Feldman, 2007; Jacob et al., 2008]. However, such very large multiwhisker stimulators have been limited by the type of actuators they used: bistable solenoids [Krupa et al., 2001] or single axis piezoelectric actuators [Jacob et al., 2008]. These actuators offer only access to a limited subset of the full whiskerpad sensory space, lacking in one case all directional aspects, and in the other case one directional dimension and all high frequency components of the stimulations.

However, this unattainable sensory space is certainly explored by the awake animal when it touches textured objects. To gain the widest possible access to the sensory space potentially encoded by barrel cortex neurons, we have adapted the anatomical holding frame that had been previously developed in the laboratory [Jacob et al., 2008] and we set on this frame 24 of the omnidirectional/wide frequency range stimulator that we had developed to this aim (see section 2.2.2). We then setup this stimulator under a two photon microscope and used it to characterize the functional responses of layer 2/3 barrel cortex neurons (see Chapter 4). These technical developments are presented together with a description of the previous multiwhisker actuator developed in the laboratory in our first publication (see page 51).

Patent

Micrometric Movement device and method for implementing it

Luc Estebanez, Jean Yves Tiercelin, Vincent Jacob, Daniel Shulz

Patent PCT/FR2010/000541 ; WO 2011/015722. International submission: 2010

Abstract: We developed an actuator device based on piezo-electric technology. It is aimed at deflecting the whiskers of anaesthetized rodents. This device has the following properties. (1) it is capable of deflecting whiskers in arbitrary orientations (2) it is capable of fast deflections (in the order of 1000°/s) and (3) it has a flat transfer function up to 1 kHz, meaning that it does not distort the shape of the stimuli that it reproduces, up to that 1 kHz frequency.

These three properties make this whisker actuator well suited to reproduce arbitrary, multidirectional stimulations such as the whisker deflections that occur during the free behavior of rodents.

Finally, this single whisker actuator has been designed to be sufficiently compact to be combined with others into a multiwhisker stimulator, comparable in its geometry and mechanic frame to a previous multiwhisker actuator that had been assembled in the laboratory of Daniel Shulz [Jacob2008].

(12) DEMANDE INTERNATIONALE PUBLIÉE EN VERTU DU TRAITÉ DE COOPÉRATION EN MATIÈRE DE BREVETS (PCT)

(19) Organisation Mondiale de la Propriété Intellectuelle
Bureau international

(43) Date de la publication internationale
10 février 2011 (10.02.2011)

PCT

(10) Numéro de publication internationale
WO 2011/015722 A1

(51) Classification internationale des brevets :
H01L 41/09 (2006.01) *B25J 7/00* (2006.01)

(21) Numéro de la demande internationale :
PCT/FR2010/000541

(22) Date de dépôt international :
27 juillet 2010 (27.07.2010)

(25) Langue de dépôt : français

(26) Langue de publication : français

(30) Données relatives à la priorité :
09/03752 30 juillet 2009 (30.07.2009) FR

(71) Déposants *(pour tous les États désignés sauf US)* : **CENTRE NATIONAL DE LA RECHERCHE SCIENTIFIQUE** [FR/FR]; 3, rue Michel Ange, F-75016 Paris (FR). **ECOLE NORMALE SUPERIEURE** [FR/FR]; 45, rue d'Ulm, F-75005 Paris (FR).

(72) Inventeurs; et

(75) Inventeurs/Déposants *(pour US seulement)* : **TIERCELIN, Jean-Yves** [FR/FR]; 69, rue de Gergovie, F-75014 Paris (FR). **ESTEBANEZ, Luc** [FR/FR]; 154, rue Gambetta, F-45120 Chalette Sur Loing (FR). **SHULZ, Daniel** [FR/FR]; 20, Bannière de Maupertuis, F-91198 Gif Sur Yvette (FR). **JACOB, Vincent** [FR/GB]; 127 Richmond road, Flat B, Cardiff South Glamorgan LF 233 B5 (GB).

(74) Mandataires : **CABINET ORES** et al.; 36, rue de St Pétersbourg, F-75008 Paris (FR).

(81) États désignés *(sauf indication contraire, pour tout titre de protection nationale disponible)* : AE, AG, AL, AM, AO, AT, AU, AZ, BA, BB, BG, BH, BR, BW, BY, BZ, CA, CH, CL, CN, CO, CR, CU, CZ, DE, DK, DM, DO, DZ, EC, EE, EG, ES, FI, GB, GD, GE, GH, GM, GT, HN, HR, HU, ID, IL, IN, IS, JP, KE, KG, KM, KN, KP, KR, KZ, LA, LC, LK, LR, LS, LT, LU, LY, MA, MD, ME, MG, MK, MN, MW, MX, MY, MZ, NA, NG, NI, NO, NZ, OM, PE, PG, PH, PL, PT, RO, RS, RU, SC, SD, SE, SG, SK, SL, SM, ST, SV, SY, TH, TJ, TM, TN, TR, TT, TZ, UA, UG, US, UZ, VC, VN, ZA, ZM, ZW.

(84) États désignés *(sauf indication contraire, pour tout titre de protection régionale disponible)* : ARIPO (BW, GH, GM, KE, LR, LS, MW, MZ, NA, SD, SL, SZ, TZ, UG, ZM, ZW), eurasien (AM, AZ, BY, KG, KZ, MD, RU, TJ, TM), européen (AL, AT, BE, BG, CH, CY, CZ, DE, DK, EE, ES, FI, FR, GB, GR, HR, HU, IE, IS, IT, LT, LU, LV, MC, MK, MT, NL, NO, PL, PT, RO, SE, SI, SK, SM, TR), OAPI (BF, BJ, CF, CG, CI, CM, GA, GN, GQ, GW, ML, MR, NE, SN, TD, TG).

Publiée :
— *avec rapport de recherche internationale (Art. 21(3))*

WO 2011/015722 A1

(54) Title : MICROMETRIC MOVEMENT DEVICE AND METHOD FOR IMPLEMENTING SAME

(54) Titre : DISPOSITIF DE DEPLACEMENT MICROMETRIQUE ET PROCEDE DE MISE EN OEUVRE.

Fig. 1

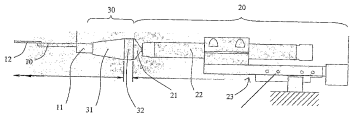

(57) Abstract : The invention relates to a micrometric movement device, comprising a bending piezoelectric actuator (10) connected to a supporting and adjusting structure (20) via a decoupling means (30) including an inertial body (31), a portion of which is attached to the piezoelectric actuator, another portion being attached to a layer (32) secured to the supporting and adjusting structure, said layer being made of a material having a high capacity for absorbing vibrations, and having an energy dissipation factor tan (δ) of between 0.5 and 0.7 in a frequency range of 5 to 1000 Hz.

(57) Abrégé : L'invention propose un dispositif de déplacement micrométrique comportant un actionneur piézoélectrique (10) de type fléchisseur, lié à une structure de support et de réglage (20), par l'intermédiaire d'un moyen de découplage (30) comprenant une masse inertielle (31) dont une partie est fixée à l'actionneur piézoélectrique, une autre partie étant fixée à une couche (32) solidaire de la structure de support et de réglage, cette couche étant en matériau à forte capacité d'absorption des vibrations, présentant un facteur de dissipation de l'énergie tan (δ) compris entre 0,5 et 0,7 dans une gamme de fréquence de 5 à 1000Hz.

DISPOSITIF DE DEPLACEMENT MICROMETRIQUE ET PROCEDE DE MISE EN ŒUVRE.

L'invention se rapporte à un dispositif de déplacement micrométrique et à un procédé de mise en œuvre.

Les actionneurs piézoélectriques sont utilisés dans de nombreux domaines techniques. Notamment, on utilise des actionneurs piézoélectriques pour la réalisation de mouvements précis, de l'ordre du micromètre à la centaine de micromètres, d'un objet de faible inertie.

La recherche en physique, en optique et en biologie nécessite des actionneurs piézoélectriques de type fléchisseurs permettant d'atteindre de grandes fréquences de battement (fléchissement).

Par exemple, chez le rongeur, l'étude du système des vibrisses requiert des fréquences de stimulation allant jusqu'à 1000 Hertz (soit 1000 battements par seconde).

Par ailleurs, dans les microscopes à balayage, une grande vitesse de balayage optique permettrait d'accélérer la cadence d'acquisition des images et l'observation de phénomènes à des échelles temporelles plus courtes. Ainsi, une grande vitesse de déplacement rendrait possible des méthodologies de balayage optique dites « intelligentes ». Dans ces méthodologies, seuls les points d'intérêt de l'échantillon sont pointés par le dispositif de balayage, ce qui requiert de pouvoir passer très vite d'un point d'intérêt au suivant.

Or, actuellement, le déplacement d'actionneurs électroniques de type fléchisseurs (en anglais, de type « bender ») ne peut se faire que pour des gammes de fréquence allant de 0 à 100 Hertz (soit 100 battements par seconde). Au-delà de 100 Hertz, les actionneurs fléchisseurs de l'état de la technique entrent en résonnance et ne sont plus utilisables car leur mouvement n'est pas maîtrisé et les commandes de l'actionneur ne sont pas reproductibles. On observe, en effet, une amplification, ou une atténuation selon les cas, de certaines fréquences.

Une solution envisagée consiste à filtrer la commande de l'actionneur par sa fonction de transfert inverse.

Une fonction de transfert est une représentation mathématique de la relation entre le signal d'entrée (ou commande) et le signal de sortie (le mouvement de l'actionneur) du dispositif de déplacement micrométrique.

Cette technique de correction fréquentielle est classique pour les systèmes linéaires invariants (c'est-à-dire sans élément mobile). Le principe de cette technique est d'acquérir la fonction de transfert de l'actionneur (gain et déphasage jusqu'à la première fréquence de résonnance) afin de pré-filtrer le signal par l'inverse de cette fonction de transfert.

Cette solution n'a jamais été envisagée pour les actionneurs fléchisseurs à positionnement réglable (selon un, deux ou trois axes) car la présence d'éléments mobiles dans la structure de l'actionneur (rotule de réglage, moyens de translation de l'actionneur) conduit à des changements dans la fonction de transfert de l'actionneur, en fonction du positionnement spatial des différents éléments mobiles et en fonction du degré de serrage des éléments de fixation dans cette position. Ainsi, au-delà de 100 Hertz, la correction par inversion de la fonction de transfert est instable.

Or, dans le cadre d'une utilisation courante, le dispositif de déplacement micrométrique doit pouvoir être réglable en position selon les axes X, Y et Z (voir la figure 3a). L'actionneur piézoélectrique doit donc être solidaire d'éléments mécaniques mobiles.

Ainsi, pour que la méthode de filtrage par la fonction de transfert inverse soit efficace, et que l'actionneur puisse être activé à une fréquence supérieure à 100 Hertz, il faudrait mettre à jour la mesure de la fonction de transfert de l'actionneur après chaque réglage du positionnement. Cette contrainte est très lourde car cela implique d'installer un appareil de mesure du mouvement de l'actionneur (par exemple un télémètre laser), et de soumettre l'actionneur à une mesure longue de la fonction de transfert

(environ deux minutes pour l'ensemble du processus), ce qui a conduit à l'abandon de cette méthode.

Il n'est donc actuellement pas possible d'obtenir des actionneurs de type fléchisseurs, réglables en position, pouvant être activés à une fréquence supérieure à 100 Hertz.

Un premier objectif de la présente invention est de fournir un actionneur de type fléchisseur à positionnement réglable, présentant une fréquence de résonnance supérieure à 1000 Hertz. Un deuxième objectif de la présente invention est de proposer un tel actionneur dont le gain est constant.

A cette fin, l'invention a pour objet un dispositif de déplacement micrométrique comprenant :

- un actionneur piézoélectrique de type fléchisseur,
- lié à une structure de support et de réglage,
- par l'intermédiaire d'un moyen de découplage comprenant :
  - une masse inertielle
  - dont une partie est fixée à l'actionneur piézoélectrique,
  - une autre partie étant fixée à une couche solidaire de la structure de support et de réglage, cette couche étant en matériau à forte capacité d'absorption des vibrations, présentant un facteur de dissipation de l'énergie tan (δ) compris entre 0,4 et 0,7, de préférence entre 0,53 et 0,6, dans une gamme de fréquence de 5 à 1000Hz.

Ce dispositif de déplacement micrométrique présente une fréquence de résonnance supérieure à 1000 Hertz.

Selon d'autres modes de réalisation :

- le matériau à forte capacité d'absorption des vibrations peut être un polymère viscoélastique d'uréthane tel que du sorbothane ;
- la masse inertielle peut être en un matériau choisi parmi le plomb, le cuivre, l'acier, et un alliage de masse volumique supérieure à 5000 ;
- la structure de support et de réglage peut comprendre :
  - une rotule de fixation du moyen de découplage, et

- un stylet tubulaire comprenant
  - une chambre de réception de la rotule,
  - un tampon de blocage en rotation de la rotule dans sa chambre de réception, et
  - un moyen réglable de compression du tampon contre la rotule ;

- le moyen réglable de compression du tampon contre la rotule peut comprendre un ressort dont une extrémité, destinée à être en contact avec le tampon lors du blocage de la rotule, est fixée à un axe fileté en prise avec un pas de vis porté par une molette de réglage, de telle sorte que lorsque la position de la rotule doit être modifiée, le serrage de la molette bande le ressort afin qu'il cesse d'exercer sa pression sur le tampon de caoutchouc, et lorsque la rotule doit être bloquée, le desserrage complet de la molette de réglage relâche pleinement le ressort qui compresse le tampon de caoutchouc contre la rotule avec une force sensiblement égale à la constante de raideur du ressort. Ce dispositif de déplacement micrométrique présente une fréquence de résonnance supérieure à 1000 Hertz et un gain constant ;
- la structure de support et de réglage peut comprendre un micromanipulateur en translation monoaxiale ; et /ou
- le micromanipulateur en translation monoaxiale peut comprendre un roulement à billes muni d'au moins deux billes blocables en rotation par serrage au moyen de vis de serrage.

L'invention se rapporte également à un procédé de mise en œuvre du dispositif de déplacement micrométrique précédent, ledit procédé comprenant une phase d'activation de l'actionneur piezoélectrique comprenant la transmission à l'actionneur d'un signal de commande à une fréquence comprise entre 5 et 1000 Hertz, de préférence, comprise entre 100 et 1000 Hertz.

Selon d'autres modes de réalisation :

- le procédé peut comprendre une phase d'initialisation comprenant les étapes suivantes :
  a) activer l'actionneur piezoélectrique à une fréquence d'activation initiale ;
  b) acquérir le gain et le déphasage de l'actionneur à cette fréquence ;
  c) incrémenter ou décrémenter la fréquence d'activation de l'activateur ;
  d) répéter les étapes b) et c) jusqu'à ce que la fréquence d'activation soit égale à une première fréquence de résonnance de l'actionneur ;
  e) établir la fonction de transfert de l'activateur à l'aide des gains et déphasages acquis à l'étape b) ;

  la phase d'initialisation étant suivie d'une phase d'activation de l'actionneur piezoélectrique comprenant la transmission à l'actionneur d'un signal de commande pré-filtré par l'inverse de la fonction de transfert ;
- le procédé peut comprendre une étape de réglage de la pression exercée sur chaque bille du roulement à billes par une vis, afin d'égaliser la position d'un rebond de la fonction de transfert pour toutes les positions de translation ;
- le procédé peut comprendre les étapes suivantes :
  - envoyer en continu à l'actionneur (10) une commande sinusoïdale de fréquence constante et proche de la fréquence moyenne du rebond de la fonction de transfert ;
  - mesurer de manière continue la position de l'actionneur ;
  - ajuster la pression effectuée par chaque vis, afin de fixer l'amplitude du mouvement de l'actionneur pour l'ensemble des positions de la translation ;
- l'étape de mesure de la position de l'actionneur peut être réalisée à l'aide d'un télémètre laser branché sur un oscilloscope.

Ce procédé permet de conserver le gain homogène et le déphasage nul dans toute la gamme d'utilisation de l'actionneur.

Il permet également de fixer la position du rebond sur l'ensemble de la trajectoire. La fonction de transfert de l'ensemble actionneur/support est ainsi fixée à travers tout son espace de réglage, à savoir la translation et la rotation.

D'autres caractéristiques de l'invention seront énoncées dans la description détaillée ci-après, faite en référence aux figures annexées qui représentent, respectivement :

- la figure 1, une vue schématique de profil du dispositif de déplacement micrométrique selon l'invention ;
- la figure 2, une vue schématique en coupe longitudinale d'une partie de la structure de support du dispositif de déplacement micrométrique selon l'invention ;
- la figure 3a, une vue schématique en perspective de l'actionneur piézoélectrique du dispositif de déplacement micrométrique selon l'invention ;
- la figure 3b, trois courbes illustrant le filtrage de la commande par la fonction de transfert inverse du dispositif de déplacement micrométrique selon l'invention ;
- la figure 4, six courbes montrant le déphasage et le gain du dispositif de déplacement micrométrique selon l'invention, avec ou sans filtrage de la commande par la fonction de transfert inverse ;
- la figure 5a, un histogramme illustrant l'indice de corrélation de Pearson entre la commande et le mouvement du dispositif de déplacement micrométrique selon l'invention, en fonction du nombre de réglages en position ;
- la figure 5b, une courbe illustrant les mouvements superposés de l'actionneur piézoélectrique pour quinze positions différentes de la rotule et de translation avec une commande identique ;

- la figure 6a, une courbe illustrant la linéarité du gain commande/mouvement pour une fourchette d'amplitude comprise entre 10 et 90% de l'amplitude maximale de commande ;
- la figure 6b, une courbe illustrant la reproductibilité de la commande avec plusieurs gains ; et/ou
- la figure 7, un diagramme illustrant l'indépendance de mouvement entre l'axe X et l'axe Y.

La présente description se rapporte à un actionneur piézoélectrique de type fléchisseur tel que le CMB-2D fabriqué par la société NOLIAC A/S (Hejreskovvej 18C, DK-3490 Kvistgaard, Danemark). Bien entendu, l'invention n'est pas restreinte à cet exemple d'actionneur piézoélectrique.

L'actionneur CMB-2D possède une amplitude de mouvements de 400 micromètres et une fréquence de résonnance, sans couplage, de plusieurs milliers de Hertz. Le couplage de l'actionneur piézoélectrique CMB-2D induit une chute de sa fréquence de résonnance à 200 Hertz. En conséquence, aucun mouvement plus rapide que 100 Hertz ne peut être effectué par l'actionneur sans générer d'artéfact de résonnance.

Conformément au montage selon l'invention, illustré en figure 1, l'actionneur 10 est couplé à une structure de support et de réglage 20 par un moyen de découplage 30. Ce moyen de découplage 30 comprend une masse inertielle 31, sur laquelle est couplé l'actionneur 10, et une couche 32 en matériau à forte capacité d'absorption de vibrations.

Plus particulièrement, l'actionneur piézoélectrique 10 est relié à la masse inertielle 31 par l'intermédiaire d'une pièce 11 en plexiglas (PMMA). La pièce 11 en plexiglas a pour but de fournir un montage rigide de l'actionneur piézoélectrique 10 sur la masse inertielle 31. Le choix du plexiglas est lié au fait que cette pièce 11 est relativement complexe, et qu'elle doit pouvoir être usinée à moindre coût. En effet, à chaque fois que l'actionneur piézoélectrique 10 est usagé, il est remplacé avec la pièce 11 en plexiglas.

Dans le contexte de l'invention, d'autres montages rigides sont également possibles (autre matériau, autre configuration spatiale).

D'autre part, l'actionneur piézoélectrique 10 comprend une pièce 12 en acier fixée à son extrémité libre. Cette pièce 12 permet d'atteindre une amplitude du mouvement, à la pointe, de 400 µm.

Pour des applications spécifiques, cette pièce 12 pourrait être modifiée (ou même remplacée) pour accueillir un outil ou un capteur particulier. La pièce 12 doit présenter, de préférence, une grande rigidité pour transmettre les mouvements de l'actionneur piézoélectrique 10 même à haute fréquence (module de Young - 200000 Mpa) tout en étant très légère, de telle sorte à représenter une masse négligeable devant celle de la masse inertielle (voir ci-après). Cette légèreté relative est aussi utile pour limiter la charge de l'actionneur piézoélectrique 10, et donc son vieillissement prématuré. Ce sont ces différentes raisons qui justifient l'utilisation d'un tube en acier, à la fois léger et très rigide. D'autres matériaux comme le tungsten ou la céramique (tubes d'alumine pure) sont de bons substituts, mais ils sont plus couteux et plus fragiles (pour ce qui est de la céramique).

La couche 32 de matériau à forte capacité d'absorption de vibrations est, de préférence, en polymère viscoélastique d'uréthane : le sorbothane.

Le Sorbothane est un élastomère viscoélastique. Chaque élastomère de ce type présente un spectre d'absorption des vibrations différent. Dans l'article de Shipkowitz, Chen & Lakes « *Characterization of high-loss viscoelastic elastomers* », (Journal of material science, 23 (1988) 3660-3665), une méthodologie de description quantitative de différents élastomères est proposée.

En mesurant sur un intervalle de fréquence de 0 à 10000Hz le module de cisaillement (mesure de la déformation induite par les mouvements) ainsi que tan (δ) (le facteur de dissipation de l'énergie) des différents élastomères, cet article offre une description assez complète du

comportement des viscoélastiques (tenue mécanique à l'effort et dissipation d'énergie vibratoire).

Pour la mise en œuvre de l'invention, seul tan (δ) est un paramètre important, car l'inertie de la masse en plomb garantie une faible amplitude de cisaillement à sa base : le module de cisaillement n'est donc pas un paramètre critique.

Le Sorbothane présente un duromètre Shore OO 70 (une certaine rigidité est nécessaire afin que le Sorbothane ne ploie pas sous la charge, donc le Shore OO 30 est exclu, et le Shore OO 50 est acceptable dans le cadre du dispositif présenté).

Un matériau à forte capacité d'absorption de vibrations pouvant être substitué au Sorbothane (de duromètre supérieur ou égal) peut être envisagé, par exemple pour améliorer la tenue mécanique du support de l'actuateur. Ce matériau de substitution doit présenter facteur de dissipation d'énergie tan(δ) suffisant.

Les valeurs correspondant au Sorbothane Shore OO 70 sont les suivantes (source : Sorbothane inc.) :

Frequence (Hz)	5	15	30	50	100
tan(δ)	0.56	0.6	0.59	0.55	0.53

Le matériau de substitution devrait présenter des valeurs de tan (δ) pour les fréquences supérieures à 100Hz, semblables à celles du Sorbothane Shore OO 50 ou Shore OO 70.

De préférence, le matériau à forte capacité d'absorption de vibrations présente un tan(δ) compris entre environ 0,4 et 0,7, de préférence entre 0,53 et 0,6, pour toute fréquence dans la gamme de fréquence 5-1000Hz.

La masse inertielle située à la base de l'actuateur a pour fonction de fournir, par son inertie, un point fixe pour le mouvement de l'actuateur malgré le fait que l'ensemble soit fixé sur un matériau viscoélastique. À cet effet, cette masse inertielle doit posséder une masse « très grande » devant la masse 12 fixée à l'extrémité mobile de l'actuateur.

En effet, à des fréquences d'oscillation élevées (supérieures à 5Hz), l'amplitude de déplacement de l'extrémité mobile résultant de la torsion de l'actionneur est principalement défini par le rapport entre les masses fixées aux deux extrémités de l'actuateur (l'élastomère n'est pas rigide à ces fréquences).

De préférence, on choisi la masse inertielle pour que sa masse soit au moins dix fois supérieure à la masse 12 fixée à l'extrémité l'actionneur piézoélectrique mobile.

Plus le rapport entre la masse de la masse inertielle et la masse de l'actionneur piézoélectrique est important, plus l'effet technique de point fixe est obtenu.

Cependant, ce rapport est limité par le fait que l'ensemble masse inertielle/actionneur piézoélectrique est en suspension sur le moyen de découplage en sorbothane.

De préférence, la masse inertielle est en plomb. Le choix du plomb comme matériau de la masse inertielle est dû à sa forte densité, qui permet de réduire l'encombrement du dispositif. Ceci offre deux avantages substantielles : (1) une réduction du bras de levier exercé sur le moyen de découplage en élastomère par la masse du fait de sa faible longueur, et (2) une réduction de l'encombrement général du dispositif. Il serait parfaitement envisageable de remplacer le plomb par le cuivre ou l'acier (qui sont seulement un peu moins denses) ou un alliage de masse volumique supérieure à 5000 $kg.m^{-3}$.

Les valeurs des différents paramètres indiqués (masse, duromètre, tan (δ)) sont valables pour des actionneurs de type fléchisseur de 37 mm de long environs. Par exemple, si l'actionneur est plus long, sa fréquence de résonance est abaissée ; si l'actionneur est plus court, sa fréquence de résonance est plus élevée et il faut modifier le dispositif pour obtenir le même effet technique en ajustant les paramètres précités.

Essentiellement, pour des actionneurs de 27 à 47 mm de long, il est envisageable de simplement ajuster la longueur de la masse

inertielle de telle sorte que le système actionneur/masse inertielle présente une fréquence de résonance égale à celle du système décrit en détail ci-après. Pour des actionneurs qui s'écartent de ces longueurs, les ajustements des différentes caractéristiques du dispositif devront être plus nombreux.

La couche de matériau 32 est fixée à la structure de support et de réglage 20.

Le moyen de découplage 30 permet une activation de l'actionneur fléchisseur à une fréquence supérieure à 100 Hertz et jusqu'à 1000 Hertz sans phénomène de résonnance.

La structure de support et de réglage 20 comprend une rotule 21 bloquée en rotation sur un stylet 22. Ce dernier est fixé sur un micromanipulateur 23 permettant une translation monoaxiale du stylet 22.

Un exemple de micromanipulateur particulièrement intéressant pour la mise en œuvre de l'invention est le micromanipulateur UL-1C-P fabriqué par la société NARISHIGE (27-9, Minamikarasuyama 4-chomen Setagaya-ku, Tokyo 157-0062, Japan). Ce micromanipulateur permet une translation monoaxiale avec un débattement de 15 millimètres. Cette translation repose sur un roulement à billes dont le serrage peut être réglé par une série de vis qui ajuste la pression s'exerçant sur les billes du roulement dans leur cavité.

La structure de support et de réglage 20 est illustrée, en coupe, à la figure 2.

Selon l'invention, le stylet 22 comprend un corps tubulaire 22a logeant un moyen de compression réglable tel qu'un ressort 22b, pour la compression d'un tampon 22c en matériau élastique contre la bille de la rotule 21. Le tampon 22c est, de préférence, en caoutchouc.

L'extrémité du ressort 22b en contact avec le tampon 22c est fixée à un axe fileté 22d en prise avec un pas de vis porté par une molette de réglage 22e.

Lorsque l'on souhaite modifier la position de l'actionneur 10 selon les axes X et Y (figure 3a), la bille de la rotule 21 doit être mise en libre

rotation. Pour se faire, l'utilisateur serre la molette de réglage 22e qui est en prise avec l'axe fileté 22d. Le serrage de la molette bande le ressort afin qu'il cesse d'exercer sa pression sur le tampon de caoutchouc 22c. Une fois que la position de la rotule est réglée selon les axes X et Y, l'utilisateur desserre totalement la molette de serrage de telle sorte que le ressort 22b exerce, à nouveau, précisément la même pression sur la bille de la rotule que celle qu'il exerçait avant le réglage. Cette pression est constante puisqu'elle dépend uniquement de la constante de raideur du ressort.

De cette manière, la pression exercée sur la bille est indépendante du serrage de la molette de réglage : il suffit que celle-ci soit totalement desserrée pour que le ressort exerce la même force contre la rotule. La pression sur la bille de la rotule est donc reproductible et n'engendre pas de modification de la fonction de transfert.

Autrement dit, grâce à la structure selon l'invention, la fonction de transfert de cette rotule est ainsi préservée au cours des cycles de serrage/desserrage liés aux ajustements d'angles.

Afin de s'assurer que la pièce 22c en caoutchouc n'est pas entraînée en rotation par l'axe fileté (ce qui induirait une rotation de la bille et donc de l'actionneur), un dispositif de blocage en rotation (non représenté) de l'axe fileté est, de préférence, prévu dans le stylet.

Grâce à cette structure, la position de l'actionneur peut être réglée selon deux axes X et Y.

La position de l'actionneur selon l'axe Z est réglable grâce au micromanipulateur 23.

La structure de support et de réglage 20 de l'exemple précédent comprend deux éléments : un micromanipulateur permettant une translation monoaxiale (déplacement selon l'axe Z) et une rotule (rotation en deux dimensions selon les deux axes X et Y). Ces deux éléments ont la propriété d'être stables pour leur fonction de transfert dans toute leur étendue de positionnement. Leur combinaison dans le montage illustré aux figures 1 et 2 est donnée à titre d'exemple. Cependant, l'invention couvre également les

supports permettant une translation triaxiale, c'est-à-dire un réglage de la position de l'actionneur piézoélectrique selon les trois axes X, Y et Z.

Grâce à la structure de support et de réglage selon l'invention, il devient possible d'appliquer, avec une grande souplesse d'utilisation, la technique de préfiltrage par fonction de transfert inverse, alors même que la structure comprend des éléments mobiles.

La figure 4 illustre le déphasage et le gain du dispositif de déplacement micrométrique selon l'invention, avec ou sans filtrage de la commande par la fonction de transfert inverse. Cette figure montre que le filtrage systématique de la commande par la fonction de transfert inverse permet de parvenir à un gain constant et un déphasage nul sur toute la gamme de fréquences de l'actionneur (5 à 1000 Hertz).

Cette souplesse d'utilisation vient du fait que la fonction de transfert des éléments mobiles selon l'invention est conservée aux cours des cycles de serrage/desserrage liés aux ajustements d'angles de l'actionneur piézoélectrique et à l'ajustement de position du micromanipulateur 23.

Ceci est illustré en figure 5. La figure 5a représente un histogramme de la corrélation entre une commande et un mouvement de l'actionneur pour différentes positions du support. Les barres d'histogramme en hachures représentent l'indice de corrélation de Pearson pour dix réglages en angles différents de la rotule. Les barres d'histogramme en grisé représentent l'indice de corrélation de Pearson pour neuf réglages en translation différents du micromanipulateur.

La figure 5b illustre les mouvements superposés de l'actionneur piézoélectrique pour quinze positions différentes de la rotule et de translation avec une commande identique.

Ces deux figures 5a et 5b montrent donc que le dispositif de déplacement micrométrique selon l'invention présente une excellente reproductibilité de mouvement : le coefficient de corrélation de Pearson moyenne entre la commande employée pour les tests et le mouvement

mesuré est de 0,998. En outre, la correction par la fonction de transfert est stable : la corrélation minimale observée est de 0,995.

D'une manière générale, la technique de préfiltrage par fonction de transfert inverse comprend, dans un premier temps, une étape d'acquisition de la fonction de transfert de l'actionneur (gain et déphasage jusqu'à la première fréquence de résonnance). Cette étape est réalisée, de préférence, à l'aide d'un télémètre laser, tel que le télémètre Micro-Epsilon LD1605 Type 0.5.

Le dispositif de déplacement micrométrique selon l'invention comprend, de préférence, un logiciel de contrôle qui pilote l'acquisition de la position de l'actionneur à l'aide du télémètre laser pendant que des commandes sinusoïdales balayant le spectre de fréquence sont transmises à l'actionneur. Cette étape permet de calculer la fonction de transfert de l'actionneur. Dans une deuxième étape, le logiciel de contrôle filtre les commandes envoyées à l'actionneur à l'aide de la fonction de transfert inverse (voir la figure 3b).

Plus particulièrement, le procédé selon l'invention comprend une phase d'initialisation comprenant les étapes suivantes :

a) activer l'actionneur piezoélectrique à une fréquence d'activation initiale ;
b) acquérir le gain et le déphasage de l'actionneur à cette fréquence ;
c) incrémenter ou décrémenter la fréquence d'activation de l'activateur ;
d) répéter les étapes b) et c) jusqu'à ce que la fréquence d'activation soit égale à une première fréquence de résonnance de l'actionneur ;
e) établir la fonction de transfert de l'activateur à l'aide des gains et déphasages acquis à l'étape b).

La phase d'initialisation est alors suivie d'une phase d'activation de l'actionneur piézoélectrique comprenant la transmission à l'actionneur d'un signal de commande pré-filtré par l'inverse de la fonction de transfert.

Lors de l'étape a), la fréquence initiale peut être arbitraire. Elle peut donc être située à l'intérieure de la gamme de fonctionnement de l'actionneur. Ainsi, il peut être nécessaire, lors de l'étape c) d'incrémenter ou de décrémenter la fréquence d'activation de l'activateur pour aboutir à la première fréquence de résonnance de l'actionneur puis établir la fonction de transfert.

Le préfiltrage par la fonction de transfert inverse annule les effets de la fonction de transfert de l'actionneur (figure 3b), ce qui permet de parvenir à un gain égal et un déphasage nul sur l'ensemble de la gamme d'utilisation de l'actionneur.

La structure de l'actionneur décrite en relation avec les figures 1 et 2 permet des réglages mécaniques de position et de rotation de l'actionneur 10, tout en assurant la stabilité de la fonction de transfert. Puisqu'il n'est plus nécessaire de recommencer l'initialisation précédemment décrite à chaque réglage mécanique, l'utilisation de la technique de filtrage par la fonction de transfert inverse peut être utilisée et l'actionneur selon l'invention présente un gain homogène et un déphasage nul sur l'ensemble de sa gamme d'utilisation, contrairement aux actionneurs de l'État de la Technique.

Les courbes illustrées en figures 4 et 6 montrent que ce filtrage permet d'obtenir un gain constant et un déphasage nul entre la commande effective et le déplacement de l'actionneur.

Lorsqu'un micromanipulateur 23 est utilisé pour la translation monoaxiale du stylet 22, on s'aperçoit que la translation du stylet déforme la fonction de transfert de l'actionneur de façon différente suivant son réglage en position. En effet, on observe un rebond en amplitude dans la fonction de transfert. Selon le réglage, ce rebond est présent à des fréquences différentes.

Les inventeurs se sont aperçus qu'un réglage de la pression exercée par les vis de réglage sur le roulement à billes du micromanipulateur

permet de moduler la position en fréquence du rebond présent dans la fonction de transfert de l'actionneur.

De nombreuses translations à un axe présentent un chariot monté mobile dans une coulisse grâce à roulement à bille. Un mécanisme de réglage permet de réguler la pression qui s'exerce sur les billes en plusieurs points le long de l'axe de translation.

Ceci permet de pouvoir moduler la friction subie par le chariot lorsqu'il se déplace le long de l'axe de translation, dans le but de moduler la facilité de translation et d'assurer la stabilité du positionnement statique du chariot.

L'invention détourne ce dispositif de son but initial et l'utilise pour obtenir une même fonction de transfert de l'actuateur piezoélectrique pour les différentes positions de la translation grâce à la modulation de la pression exercée par les vis disposées le long de l'axe.

Le procédé selon l'invention peut être appliqué à tout dispositif à roulement à bille présentant un dispositif permettant d'exercer une pression réglable en des points multiples le long du roulement à bille.

Le procédé de mise en œuvre du dispositif de déplacement micrométrique selon l'invention, comprenant un micromanipulateur monoaxial, comprend une étape de réglage de la pression exercée par chaque vis sur les billes du roulement à billes afin d'égaliser la position du rebond de la fonction de transfert pour toutes les positions de translation. Pour cela, une commande sinusoïdale de fréquence constante et proche de la fréquence moyenne du rebond est envoyée en continu à l'actionneur. Une mesure continue de la position de l'actionneur est effectuée, par exemple à l'aide du télémètre laser branché sur un oscilloscope. En ajustant la pression effectuée par chaque vis, il est possible de fixer l'amplitude du mouvement de l'actionneur pour l'ensemble des positions de la translation, ce qui revient à fixer la position du rebond sur l'ensemble de la trajectoire. La fonction de transfert de l'ensemble actionneur/support est ainsi fixée à travers tout son espace de réglage, à savoir la translation et la rotation.

Grâce à ce procédé selon l'invention, la stabilité de la reproduction de mouvements pour des positions en translation différentes est assurée.

Comme le montre la figure 6, la relation commande/mouvement du dispositif de déplacement micrométrique selon l'invention est linéaire y compris pour une commande présentant des fréquences très élevées (figure 6b).

Par ailleurs, la figure 7 montre que l'utilisation spécifique de l'actionneur CMB-2D (qui possède deux axes de liberté), dans le dispositif selon l'invention, n'influence pas l'indépendance du mouvement des deux axes de l'actionneur 10. Autrement dit, un mouvement effectué sur un axe ne vient pas interférer avec un mouvement effectué sur l'autre axe.

Plus particulièrement, le mouvement résultant d'une commande sur un seul axe a été comparé à la sommation du mouvement résultant de la même commande sur le même axe ajouté à une commande en phase puis en antiphase sur l'autre axe. Ce mouvement résultant, qui devrait être influencé par une interaction entre les mouvements sur l'un et l'autre des axes, est très proche du mouvement issu de la commande sur un seul axe.

Ainsi, la figure 7 illustre l'absence d'effet d'un mouvement sur l'axe Y sur le mouvement enregistré sur l'axe X. Les deux axes de déplacement du dispositif de déplacement micrométrique selon l'invention sont donc indépendants.

On obtient ainsi un actionneur piézoélectrique de type fléchisseur réglable selon les trois axes X, Y et Z dans une bande de fréquence large, allant jusqu'à 1000 Hertz et possédant des caractéristiques stables pour des ajustements.

Le dispositif de déplacement micrométrique selon l'invention permet une utilisation pour le positionnement de précision : réalisation de mouvements précis de l'ordre du micromètre à la centaine de micromètres d'un objet de faible inertie.

En outre, le mode de réalisation illustré est économique à fabriquer et présente un faible encombrement car il ne nécessite aucun capteur de position monté de façon permanente sur l'actionneur (contrairement à l'État de la Technique). Seule, l'étape de calibration initiale nécessite un capteur de position (télémètre laser).

REVENDICATIONS

1. Dispositif de déplacement micrométrique caractérisé en ce qu'il comprend :
   - un actionneur piézoélectrique de type fléchisseur,
   - lié à une structure de support et de réglage,
   - par l'intermédiaire d'un moyen de découplage comprenant :
     - une masse inertielle
     - dont une partie est fixée à l'actionneur piézoélectrique,
     - une autre partie étant fixée à une couche solidaire de la structure de support et de réglage, cette couche étant en matériau à forte capacité d'absorption des vibrations, présentant un facteur de dissipation de l'énergie tan (δ) compris entre 0,4 et 0,7, de préférence entre 0,53 et 0,6, dans une gamme de fréquence de 5 à 1000Hz.

2. Dispositif de déplacement micrométrique selon la revendication 1, dans lequel le matériau à forte capacité d'absorption des vibrations est un polymère viscoélastique d'uréthane (sorbothane).

3. Dispositif de déplacement micrométrique selon l'une quelconque des revendications 1 ou 2, dans lequel la masse inertielle est en un matériau choisi parmi le plomb, le cuivre, l'acier, et un alliage de masse volumique supérieure à 5000 $kg.\cdot m^{-3}$.

4. Dispositif de déplacement micrométrique selon l'une quelconque des revendications 1 à 3, dans lequel la structure de support et de réglage comprend :
   - une rotule de fixation du moyen de découplage, et
   - une translation monoaxiale formée par un stylet tubulaire comprenant :
     - une chambre de réception de la rotule,
     - un tampon de blocage en rotation de la rotule dans sa chambre de réception,

- un moyen réglable de compression du tampon contre la rotule.

5. Dispositif de déplacement micrométrique selon la revendication 4, dans lequel le moyen réglable de compression du tampon contre la rotule comprend un ressort (22b) dont une extrémité, destinée à être en contact avec le tampon lors du blocage de la rotule, est fixée à un axe fileté (22d) en prise avec un pas de vis porté par une molette de réglage (22e), de telle sorte que lorsque la position de la rotule doit être modifiée, le serrage de la molette bande le ressort afin qu'il cesse d'exercer sa pression sur le tampon de caoutchouc (22c), et lorsque la rotule doit être bloquée, le desserrage complet de la molette de réglage relâche pleinement le ressort (22b) qui compresse le tampon de caoutchouc (22c) contre la rotule avec une force sensiblement égale à la constante de raideur du ressort.

6. Dispositif de déplacement micrométrique selon l'une quelconque des revendications 1 à 5, dans lequel la structure de support et de réglage comprend un micromanipulateur en translation monoaxiale.

7. Dispositif de déplacement micrométrique selon la revendication 6, dans lequel le micromanipulateur en translation monoaxiale comprend un roulement à billes muni d'au moins deux billes blocables en rotation par serrage au moyen de vis de serrage.

8. Procédé de mise en œuvre du dispositif de déplacement micrométrique selon l'une quelconque des revendications 1 à 7, caractérisé en ce qu'il comprend une phase d'activation de l'actionneur piezoélectrique comprenant la transmission à l'actionneur d'un signal de commande à une fréquence comprise entre 5 et 1000 Hertz, de préférence, comprise entre 100 et 1000 Hertz ;

9. Procédé selon la revendication précédente pour la mise en œuvre du dispositif de déplacement micrométrique selon la revendication 4, caractérisé en ce qu'il comprend une phase d'initialisation comprenant les étapes suivantes :

a) activer l'actionneur piezoélectrique à une fréquence d'activation initiale ;
b) acquérir le gain et le déphasage de l'actionneur à cette fréquence ;
c) incrémenter ou décrémenter la fréquence d'activation de l'activateur ;
d) répéter les étapes b) et c) jusqu'à ce que la fréquence d'activation soit égale à une première fréquence de résonnance de l'actionneur ;
e) établir la fonction de transfert de l'activateur à l'aide des gains et déphasages acquis à l'étape b) ;

la phase d'initialisation étant suivie d'une phase d'activation de l'actionneur piezoélectrique comprenant la transmission à l'actionneur d'un signal de commande pré-filtré par l'inverse de la fonction de transfert.

10. Procédé selon la revendication précédente, pour la mise en œuvre du dispositif de déplacement micrométrique selon la revendication 7, caractérisé en ce qu'il comprend une étape de réglage de la pression exercée sur chaque bille du roulement à billes par une vis, afin d'égaliser la position d'un rebond de la fonction de transfert pour toutes les positions de translation.

11. Procédé selon la revendication précédente, comprenant les étapes suivantes :

- envoyer en continu à l'actionneur (10) une commande sinusoïdale de fréquence constante et proche de la fréquence moyenne du rebond de la fonction de transfert ;
- mesurer de manière continue la position de l'actionneur ;
- ajuster la pression effectuée par chaque vis, afin de fixer l'amplitude du mouvement de l'actionneur pour l'ensemble des positions de la translation.

12. Procédé selon la revendication précédente, dans lequel l'étape de mesure de la position de l'actionneur est réalisée à l'aide d'un télémètre laser branché sur un oscilloscope.

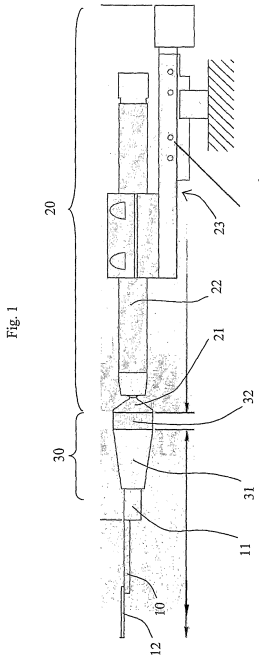

Fig. 1

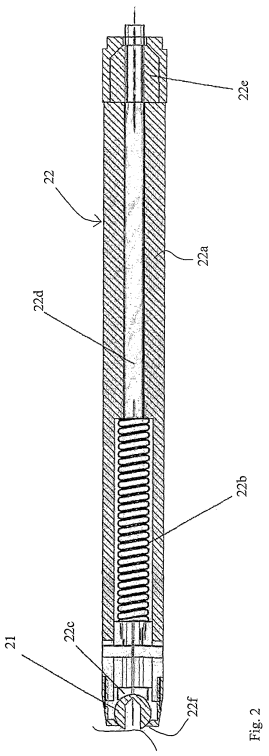

Fig. 2

Fig. 3 **(a)**

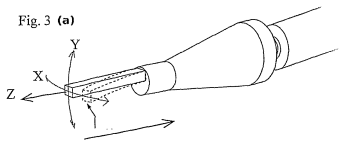

Fig. 3 **(b)**

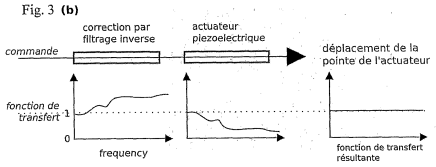

Fig. 4

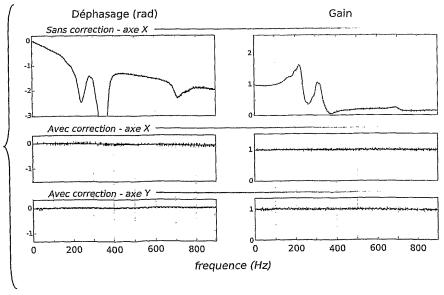

Fig. 5 **(a)**

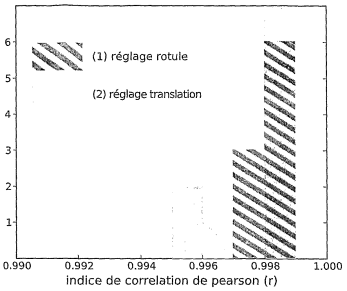

Fig. 5 **(b)**

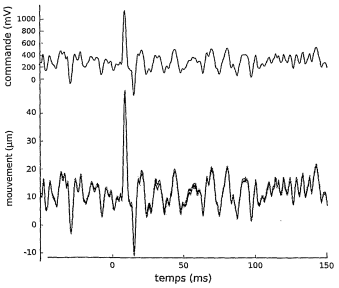

Fig. 6 **(a)**

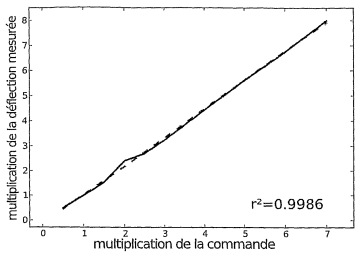

Fig. 6 **(b)**

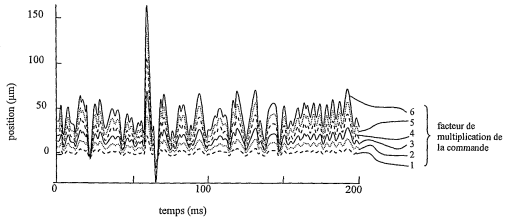

Fig. 7 **(a)**

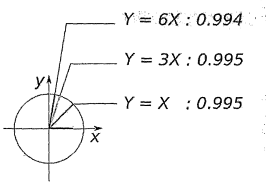

Fig. 7 **(b)**

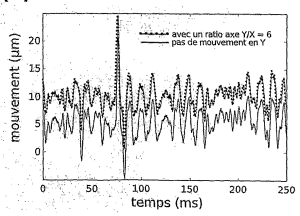

INTERNATIONAL SEARCH REPORT

International application No
PCT/FR2010/000541

A. CLASSIFICATION OF SUBJECT MATTER
INV. H01L41/09 B25J7/00
ADD.

According to International Patent Classification (IPC) or to both national classification and IPC

B. FIELDS SEARCHED

Minimum documentation searched (classification system followed by classification symbols)
H01L B25J

Documentation searched other than minimum documentation to the extent that such documents are included in the fields searched

Electronic data base consulted during the international search (name of data base and, where practical, search terms used)
EPO-Internal, WPI Data, INSPEC, COMPENDEX

C. DOCUMENTS CONSIDERED TO BE RELEVANT

Category*	Citation of document, with indication, where appropriate, of the relevant passages	Relevant to claim No.
A	WO 03/049908 A1 (KALLIO PASI ET AL) 19 June 2003 (2003-06-19) page 11, line 35 - page 13, line 19; figures 6,7	1,6,8
A	JP 9 267278 A (DENSO CORP) 14 October 1997 (1997-10-14) paragraphs [0036] - [0049]; figures 1-4	1,8
A	US 5 170 089 A (FULTON LANGDON H) 8 December 1992 (1992-12-08) column 4, line 24 - column 5, line 28; figures 5,6	1,8

☐ Further documents are listed in the continuation of Box C. ☒ See patent family annex.

* Special categories of cited documents :

"A" document defining the general state of the art which is not considered to be of particular relevance
"E" earlier document but published on or after the international filing date
"L" document which may throw doubts on priority claim(s) or which is cited to establish the publication date of another citation or other special reason (as specified)
"O" document referring to an oral disclosure, use, exhibition or other means
"P" document published prior to the international filing date but later than the priority date claimed
"T" later document published after the international filing date or priority date and not in conflict with the application but cited to understand the principle or theory underlying the invention
"X" document of particular relevance; the claimed invention cannot be considered novel or cannot be considered to involve an inventive step when the document is taken alone
"Y" document of particular relevance; the claimed invention cannot be considered to involve an inventive step when the document is combined with one or more other such documents, such combination being obvious to a person skilled in the art.
"&" document member of the same patent family

Date of the actual completion of the international search	Date of mailing of the international search report
2 November 2010	18/11/2010

Name and mailing address of the ISA/	Authorized officer
European Patent Office, P.B. 5818 Patentlaan 2 NL - 2280 HV Rijswijk Tel. (+31-70) 340-2040, Fax: (+31-70) 340-3016	Köpf, Christian

INTERNATIONAL SEARCH REPORT

Information on patent family members

International application No
PCT/FR2010/000541

Patent document cited in search report	Publication date	Patent family member(s)	Publication date
WO 03049908 A1	19-06-2003	AT 414593 T	15-12-2008
		AU 2002349073 A1	23-06-2003
		CA 2469041 A1	19-06-2003
		EP 1455990 A1	15-09-2004
		JP 2005511333 T	28-04-2005
		US 2005006986 A1	13-01-2005
JP 9267278 A	14-10-1997	NONE	
US 5170089 A	08-12-1992	NONE	

RAPPORT DE RECHERCHE INTERNATIONALE

Demande internationale n°
PCT/FR2010/000541

A. CLASSEMENT DE L'OBJET DE LA DEMANDE
INV. H01L41/09 B25J7/00
ADD.

Selon la classification internationale des brevets (CIB) ou à la fois selon la classification nationale et la CIB

B. DOMAINES SUR LESQUELS LA RECHERCHE A PORTE

Documentation minimale consultée (système de classification suivi des symboles de classement)
H01L B25J

Documentation consultée autre que la documentation minimale dans la mesure où ces documents relèvent des domaines sur lesquels a porté la recherche

Base de données électronique consultée au cours de la recherche internationale (nom de la base de données, et si cela est réalisable, termes de recherche utilisés)
EPO-Internal, WPI Data, INSPEC, COMPENDEX

C. DOCUMENTS CONSIDERES COMME PERTINENTS

Catégorie*	Identification des documents cités, avec, le cas échéant, l'indication des passages pertinents	no. des revendications visées
A	WO 03/049908 A1 (KALLIO PASI ET AL) 19 juin 2003 (2003-06-19) page 11, ligne 35 - page 13, ligne 19; figures 6,7	1,6,8
A	JP 9 267278 A (DENSO CORP) 14 octobre 1997 (1997-10-14) alinéas [0036] - [0049]; figures 1-4	1,8
A	US 5 170 089 A (FULTON LANGDON H) 8 décembre 1992 (1992-12-08) colonne 4, ligne 24 - colonne 5, ligne 28; figures 5,6	1,8

☐ Voir la suite du cadre C pour la fin de la liste des documents

☒ Les documents de familles de brevets sont indiqués en annexe

* Catégories spéciales de documents cités:

"A" document définissant l'état général de la technique, non considéré comme particulièrement pertinent

"E" document antérieur, mais publié à la date de dépôt international ou après cette date

"L" document pouvant jeter un doute sur une revendication de priorité ou cité pour déterminer la date de publication d'une autre citation ou pour une raison spéciale (telle qu'indiquée)

"O" document se référant à une divulgation orale, à un usage, à une exposition ou tous autres moyens

"P" document publié avant la date de dépôt international, mais postérieurement à la date de priorité revendiquée

"T" document ultérieur publié après la date de dépôt international ou la date de priorité et n'appartenenant pas à l'état de la technique pertinent, mais cité pour comprendre le principe ou la théorie constituant la base de l'invention

"X" document particulièrement pertinent; l'invention revendiquée ne peut être considérée comme nouvelle ou comme impliquant une activité inventive par rapport au document considéré isolément

"Y" document particulièrement pertinent; l'invention revendiquée ne peut être considérée comme impliquant une activité inventive lorsque le document est associé à un ou plusieurs autres documents de même nature, cette combinaison étant évidente pour une personne du métier

"&" document qui fait partie de la même famille de brevets

Date à laquelle la recherche internationale a été effectivement achevée	Date d'expédition du présent rapport de recherche internationale
2 novembre 2010	18/11/2010

Nom et adresse postale de l'administration chargée de la recherche internationale	Fonctionnaire autorisé
Office Européen des Brevets, P.B. 5818 Patentlaan 2 NL - 2280 HV Rijswijk Tel. (+31-70) 340-2040, Fax: (+31-70) 340-3016	Köpf, Christian

RAPPORT DE RECHERCHE INTERNATIONALE

Renseignements relatifs aux membres de familles de brevets

Demande internationale n°
PCT/FR2010/000541

Document brevet cité au rapport de recherche	Date de publication	Membre(s) de la famille de brevet(s)	Date de publication
WO 03049908 A1	19-06-2003	AT 414593 T	15-12-2008
		AU 2002349073 A1	23-06-2003
		CA 2469041 A1	19-06-2003
		EP 1455990 A1	15-09-2004
		JP 2005511333 T	28-04-2005
		US 2005006986 A1	13-01-2005
JP 9267278 A	14-10-1997	AUCUN	
US 5170089 A	08-12-1992	AUCUN	

Article 1

The Matrix: A new tool for probing the whisker-to-barrel system with natural stimuli.

Vincent Jacob*, Luc Estebanez*, Julie Le Cam*, Jean-Yves Tiercelin, Patrick Parra, Gérard Parésys, Daniel E. Shulz

Journal of Neuroscience Methods 189 (2010) 65–74

* *equally contributed to the work*

Abstract: Over the years, the laboratory of Daniel Shulz has developed two multiwhisker stimulation devices based on two different piezoelectric technologies (1D deflection PI benders versus 2D deflection noliac prisms). These devices also use different methods to keep a good level of control on the actuator motion. For the first generation of multiwhisker actuators, the piezoelectric actualtors were used in their low frequency, *linear* regime (up to 90 Hz). while in the newer generation that we developed, the actuator transfer function was corrected beyond its linear regime by a combination of mechanical and software based approaches.

In this work, we explore in detail both approaches to whisker stimulation, and we present different experimental protocoles that can be achieved by either the first or only by the newer design that we developed. In particular, we show that we are capable to reproduce natural whisker deflections with a high degree of precision using this novel design.

We also show that this faithful reproduction is robust face to the actuator position adjustments that are typically necessary to fit the actuators to the precise whiskerpad morphology of a given animal.

Journal of Neuroscience Methods 189 (2010) 65–74

Contents lists available at ScienceDirect

Journal of Neuroscience Methods

journal homepage: www.elsevier.com/locate/jneumeth

The Matrix: A new tool for probing the whisker-to-barrel system with natural stimuli

Vincent Jacob[a,1,2], Luc Estebanez[a,c,1], Julie Le Cam[a,1], Jean-Yves Tiercelin[b], Patrick Parra[b], Gérard Parésys[c], Daniel E. Shulz[a,*]

[a] CNRS, Unité de Neurosciences, Information et Complexité (UNIC), 1 avenue de la Terrasse, 91190 Gif sur Yvette, France
[b] CNRS, Institut de Neurobiologie Alfred Fessard, 91190 Gif sur Yvette, France
[c] Laboratoire de Neurobiologie, Ecole Normale Supérieure, 75005 Paris, France

ARTICLE INFO

Article history:
Received 15 January 2010
Received in revised form 10 March 2010
Accepted 16 March 2010

Keywords:
Multi-whisker stimulation
Natural stimuli
Sensory processing
Barrel cortex
Stimulator
Tactile
Somatosensory

ABSTRACT

The whisker to barrel system in rodents has become one of the major models for the study of sensory processing. Several tens of whiskers (or vibrissae) are distributed in a regular manner on both sides of the snout. Many tactile discrimination tasks using this system need multiple contacts with more than one whisker to be solved. With the aim of mimicking those multi-whisker stimuli during electrophysiological recordings, we developed a novel mechanical stimulator composed of 24 independent multi-directional piezoelectric benders adapted to the five rows and the five caudal arcs of the rat whisker pad. The most widely used technology for producing mechanical deflections of the whiskers is based on piezoelectric benders that display a non-linear behavior when driven with high frequency input commands and, if not compensated, show high unwanted ringing at particular resonance frequencies. If not corrected, this non-linear behavior precludes the application of high frequency deflections and the study of cortical responses to behaviorally relevant stimuli. To cope with the ringing problem, a mechanical and a software based solutions have been developed. With these corrections, the upper bound of the linear range of the bender is increased to 1 kHz. This new device allows the controlled delivery of large scale natural patterns of whisker deflections characterized by rapid high frequency vibrations of multiple whiskers.

1. Introduction

Since the pioneering work of Woolsey and Van der Loos (Woolsey and Van der Loos, 1970), the whisker to barrel system in rodents has become one of the major models for the study of sensory information processing. Its success is due to an outstandingly high degree of anatomical organization of the neuronal pathway linking the whiskers on the snout of the animal to the postero-medial barrel sub-field (also known as the barrel cortex), the area of the primary somatosensory cortex that receives information from the whiskers. Rodents acquire tactile information on textures and objects through repetitive contacts with multiple whiskers (Carvell and Simons, 1990; Harvey et al., 2001; Sachdev et al., 2001). In certain tactile tasks the performance level was shown to depend on the number of macrovibrissae available on the snout (Krupa et al., 2001; Celikel and Sakmann, 2007). Contact of multiple whiskers with an object as it sweeps across the whisker pad appears in those cases as an important factor for accurate discrimination. Thus, to accurately mimic this observation in the laboratory a whisker stimulator that deflects independently most of the large macrovibrissae is required. Several previous attempts to produce such a device have been successful for small number of whiskers: five whiskers in a row (Brumberg et al., 1996; Rodgers et al., 2006), nine whiskers in a 3 by 3 grid (Drew and Feldman, 2007) and even 16 whiskers in a 4 by 4 array of 16 miniature-solenoid driven actuators (Krupa et al., 2001). Here we present a new device for large scale whisker stimulation that allows isotropic and symmetrical stimulation of 24 whiskers centered on whisker C2.

Although the classical description of a whisk cycle is a protraction on the caudo-rostral plane, followed by a hold period and then a retraction back to the rest position, the contacts of the whiskers on a surface generate unique kinetic signatures of whisker vibrations (Arabzadeh et al., 2005). Moreover, during texture discrimination tasks, particular events occur where the whisker sticks on the surface and then is suddenly released (stick-and-slip events) resulting in a period of high frequency vibrations (Hipp et al., 2006; Ritt et al., 2008; Wolfe et al., 2008). Thus, the trapezoid or ramp-and-hold stimulation does not cover the full range of rele-

* Corresponding author. Tel.: +33 1 69823400; fax: +33 1 69823427.
E-mail address: shulz@unic.cnrs-gif.fr (D.E. Shulz).
[1] Contributed equally to the work.
[2] Present address: School of Biosciences, Cardiff University, Cardiff CF10 3US, UK.

0165-0270/$ – see front matter © 2010 Elsevier B.V. All rights reserved.
doi:10.1016/j.jneumeth.2010.03.020

vant parameters for whisker deflections in a natural context. The generation of natural high frequency whisker deflections is limited by the mechanical properties of the piezoelectric benders, a technology used in most of the laboratories working on the barrel system. Indeed, when driven with high frequency commands, the benders display a non-linear behavior with a high gain for particular resonance frequencies, usually around 100 Hz. This non-linear behavior precludes the application of high frequency deflections. To overcome these problems, there is a need for a device that can reproducibly and faithfully replicate behaviorally relevant stimuli while recording the system functional responses.

Here we present a new device for large scale whisker stimulation with a linear behavior up to 1 kHz. The stimulation device consists of 24 piezoelectric benders each of them being hold by an independent arm lever and allowing the controlled delivery of spatio-temporal patterns of whisker deflections. We performed a detailed analysis of the mechanical properties of the device and validated it using *in vivo* electrophysiological recordings. The biological relevance of the stimulations is guaranteed by two characteristics of the device: first, the high degrees of freedom of its mechanical structure makes it possible to align each stimulator at the resting position of the whiskers, and second, the use of a method to cope with the ringing problem increased the upper bound of the linear range of the bender from 100 to 1000 Hz. A first generation stimulator that permitted deflections only in the rostro-caudal axis at lower frequencies has been used recently to apply a coherent pattern of multi-whisker stimulations while recording unitary activity in the barrel cortex (Jacob et al., 2008). In a more recent phase of this project, we have developed a second generation stimulator including multi-directional piezoelectric benders allowing the deflection of anyone of the 24 whiskers in any direction up to 1 kHz. Both stimulators are described here.

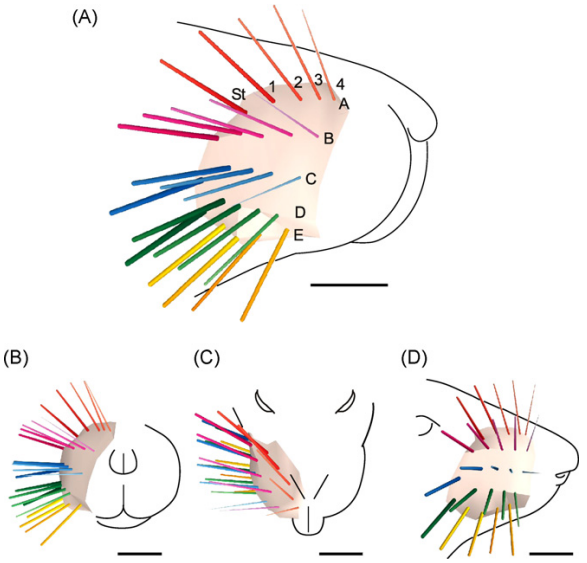

Fig. 1. 3D reconstruction of the 24 right macrovibrissae of a 300 g Wistar rat. Only the first 7 mm of each whisker are shown. Whisker positions, vertical and horizontal angles and widths at skin level and at 7 mm from the skin were measured in an anesthetized animal and depicted here (see also Supplementary Table 1). The surface delimited by the whiskers is an open convex polyhedron with the follicle positions as vertex. Whisker rows A, B, C, D and E are figured with colors red, purple, blue, green and yellow, respectively. St. Straddlers. (*A*) 3D projection. (*B*) Front view. (*C*) Top view. (*D*) Lateral view. (For interpretation of the references to color in this figure legend, the reader is referred to the web version of the article.)

2. Materials and methods

2.1. General overview of the whisker deflection device

The whiskers on the snout of the animal are organized in a grid of rows (A to E) and arcs (1–9 and a caudal row of four whiskers called straddlers, see Fig. 1). For rats of 250–350 g, the surface of the snout where the facial whiskers are inserted is on average 73.5 mm^2 (±3.6 mm^2, SD, $n = 13$). Each whisker, having at its base a mean diameter of 126 μm (±24 μm, SD), is on average 2.1 mm (±0.3 mm, SD, $n = 24$) away from its neighbors along a row and 1.8 mm (±0.4 mm, SD) across arcs (see Supplementary Table 1 for a complete quantification of whisker positions, length and angles and Supplementary Figure 1 for a 3D diagram of the follicle positions from two animals). These measures impose spatial constraints to the stimulator since the 24 piezoelectric benders have to converge into a very small area without touching each other. Moreover, because of the spherical shape of the pad, the angle of the whiskers and of their follicles with respect to a vertical plane depends on the identity of the whisker. For example, while whiskers in row C have an horizontal rest position, the whiskers of row A are almost vertical (see Fig. 1 and Supplementary Table 1).

Our stimulator (Fig. 2) was designed to position 24 piezoelectric benders in contact with 24 macrovibrissae (the four straddlers and 20 caudal whiskers) of the five rows and the most caudal five arcs. The lever arms holding the benders (described below, see Fig. 3) had several degrees of freedom to adjust the angle of the benders to the natural position of the whiskers as measured on the anesthetized rat (see Supplementary Table 1).

The lever arms were attached to five rods running parallel to the snout and corresponding each to one row of whiskers (from A to E, see Fig. 2*A* and *D*). The attachment of the five rods to the main frame gave them three degrees of freedom allowing to adjust their horizontal, vertical and angular position (Fig. 2*C*). In particular, each rod could be rotated so as to adjust the angle of the five lever arms attached to it to the global resting angles of each row of whiskers. The vertical position of each rod could be precisely adjusted by sliding their point of attachment on a rack rail (Fig. 2). This allowed positioning the five rods in turn in front of the corresponding rows of whiskers. To ensure a good stability of the entire apparatus, the rack rail was mounted on a heavy base plate screwed to the experiment table (Fig. 2*A* and *D*). We have also recently adapted this base plate to position the stimulator in a two-photon microscope set-up. The final setting of the angle was made for each bender individually by rotating and translating the lever arm using the connecting bolt to the rod and using a ball joint on which the bender was glued (Fig. 3).

The lever arms were mounted on a precision translation stage (a one-axis micromanipulator, UL-AC-P, Narishige, Japan) with a 15 mm movement range (Fig. 3). This mechanism allows the movement of the lever arm and of the bender towards the whisker pad. Whiskers were trimmed to 10 mm length and inserted 3 mm into short polypropylene or metal tubes (see Section 3) of adjusted diameter glued on the tip of the bender. The whiskers were inserted into the tubes by first, adjusting the angle of the lever arm to the resting angle of each whisker and second, by approaching the whisker towards the tubes with the one-axis micromanipulator. In this way, the whiskers were not bended to insert them into the tubes ensuring a stable unconstrained position of the whisker once it was inserted. This was visually verified at the end of the experiment when the Matrix was disconnected from the whiskers. Whiskers were inserted row after row and we never experienced loss of positioning of the inserted whiskers while manipulating the other whiskers.

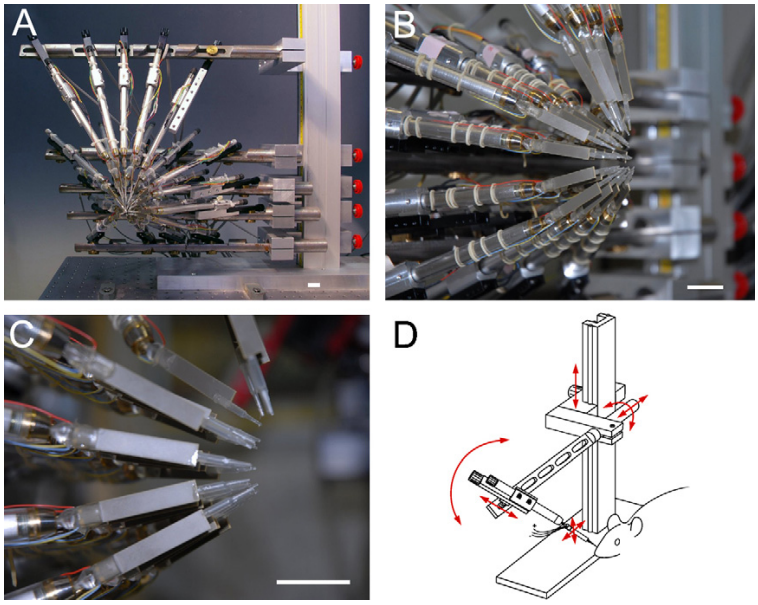

Fig. 2. (*A*) Front view of the stimulator. (*B*) Zoom in of the stimulator from a diagonal angle. (*C*) Side view of the tip of the lever arms (from top to bottom, rows A to E) with the piezoelectric benders and the attached plastic tubes where whiskers are inserted. Scale bars = 2 cm. (*D*) Schematic drawing of the stimulator with only one rod and one lever arm. All degrees of freedom are indicated with red arrows.

2.2. Two solutions for holding piezoelectric benders

The whiskers were deflected by attaching them to piezoelectric benders that allow precise and fast displacement of low inertial objects. However, the precision of this displacement is compromised at higher frequencies by the occurrence of dephasing and amplitude variation in the translation of electrical commands into motion. We applied two different strategies to cope with this problem: In a first version of the stimulator (see Jacob et al., 2008), one-directional piezoelectric benders (Polytec-PI, Germany) were used and a certain number of tests, described below, were performed to ensure that indeed the benders were functioning within their linear functioning range at frequencies below the resonance frequency. In a second, more recent version of the stimulator, we applied mechanical and software solutions to multi-directional piezoelectric benders in order to linearize their behavior above the initial resonance frequency. Both solutions are described below.

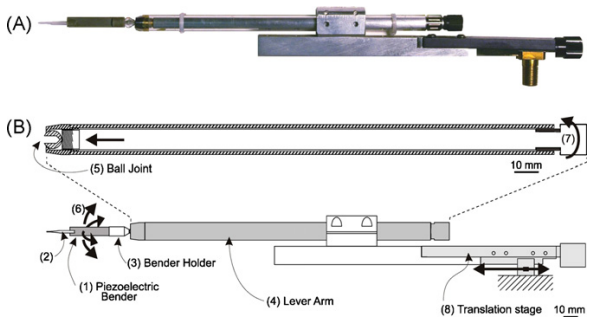

Fig. 3. (*A*) Photograph of a piezoelectric bender attached to a lever arm and a translation stage. (*B*) Schematic drawing of the lever arm and of the translation stage. The piezoelectric bender (1) with a polypropylene tube (2) glued on it extremity is hold by a plastic piece (3). This piece is attached to the lever arm (4) through a ball joint (5) that allows 2D angular motion (6). The ball joint can be clamped and unclamped remotely through a screw (7). The lever arm is hold on a 1D translation stage (8) that provides position adjustments parallel to its main axis (black arrow).

2.3. First generation stimulator: spatial linearity and normalization of the movement of the bender

In the first version of the stimulator we used long voltage pulses (500 ms) at different amplitudes to study the spatial linear behavior of the benders. The deflections of the benders were recorded with a PSD/laser displacement sensor (LD1607-0.5, Micro-Epsilon, France, Fig. 4*A*) at a resolution of one micrometer. The movement was measured at the tip of the polypropylene tube where the vibrissa was inserted. We computed a linear regression between the input voltage and the resulting amplitude of the deflection of the bender measured after the ringing period induced by the front edge of the stimulus (Fig. 4*B*). For all benders the amplitude of the deflection depended linearly (r^2 larger than 0.997) on the amplitude of the voltage input (Fig. 4*C*). Nevertheless different benders showed different amplitudes of deflections in response to the same voltage input. To uniform the amplitude of deflection of the 24 benders, we used the input/output regression function to adjust the voltage input of each bender so as to obtain equal amplitudes of deflection. To control for temporal drifts in the behavior of the benders, the measure of the input/output function was repeated several times at intervals of three to six months. The maximal deviation observed was less than 5% of the initial linear relationship.

Impulse-like stimulations are widely applied to study the linear receptive field of sensory neurons. Square pulses or ramp-and-hold deflections with sufficient initial velocity to optimally drive cortical neurons are usually applied to whiskers. However high-speed deflections of the bender induces unwanted ringing at the resonance frequency (see Fig. 4*B*). To find the trade-off between speed of deflection and ringing amplitude we studied how different ramp durations from 1 to 50 ms affect the behavior of the bender. The benders were driven with RC-filtered (time constant = 2 ms) voltage inputs that introduced a 1 ms delay that should be subtracted from the response delay. As expected, longer ramp durations resulted in less ringing (Fig. 5*A*, only ramps of 2, 4, 10 and 30 ms durations are shown). We choose then 10 ms long ramps that in our

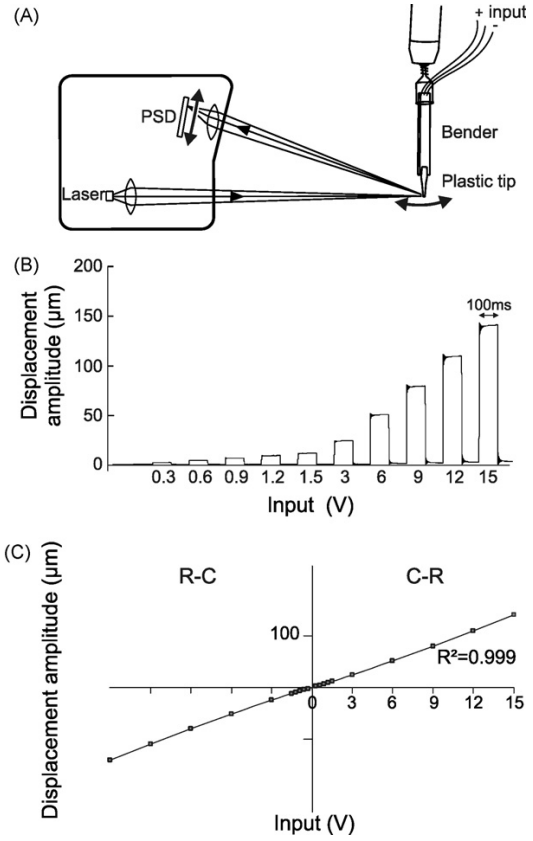

Fig. 4. Study of the linear behavior of a piezoelectric bender. (*A*) Measurement of the displacement of the bender (arrow) with a PSD/laser sensor. (*B*) Bender displacement to a gradually increasing input voltage of 100 ms duration. (*C*) Displacement amplitude as a function of the input voltage for rostro-caudal (R-C) and caudo-rostral (C-R) directions. A linear regression line was computed between the input voltage and the resulting amplitude of the deflection measured after the initial ringing period.

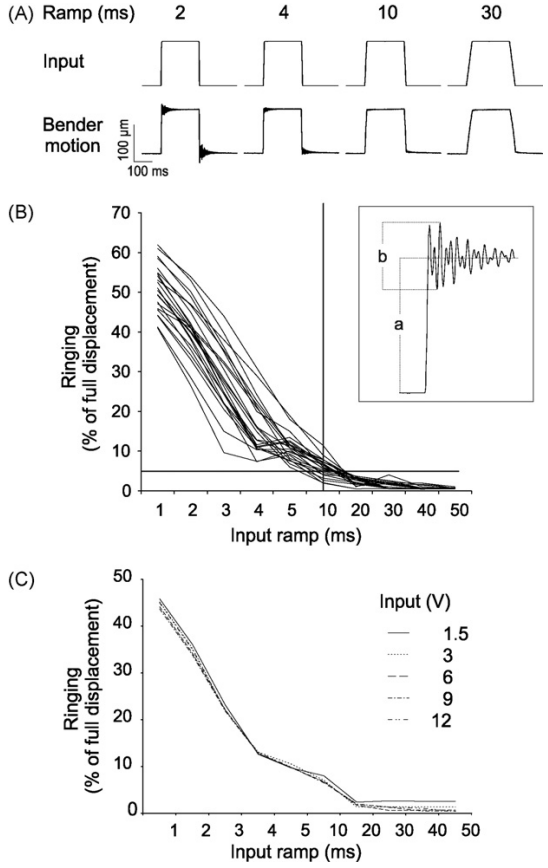

Fig. 5. Quantification of the ringing behavior of the benders as function of the duration of the input ramp. (*A*) Bender displacement for input voltages of 6 V and different ramp durations (2, 4, 10 and 30 ms). (*B*) Ringing amplitude as a function of the ramp duration for a 6 V input. Measures for all 24 benders are superimposed. The ringing is calculated as a percentage of the full displacement of the bender (see Inset where a is the full deflection amplitude and b is the ringing amplitude). (*C*) Ringing amplitude as a function of the ramp duration for different input intensities (from 1.2 to 12 V) measured on one bender. Note that ringing depends on the ramp duration but is independent of the input voltage.

hands induced ringing with amplitude of less than 5% of total deflection amplitude (Fig. 5*B*) independently of input amplitude (Fig. 5*C*).

2.4. Second generation stimulator: hardware and software solutions for a linear behavior.

In a more recent development of the stimulator (Fig. 6*A*), the problem of dephasing and ringing evoked above was corrected using a mechanical and a software approach (Patent application N° FR 09 03752). The transfer function of the bender can be measured over the range of frequencies of interest and the inverse transfer function can be applied to all inputs. However, this correction can only be applied to a piezoelectric bender under two conditions: First, the bender should not display any ringing peak in the frequency range of interest and second, the bender should maintain its transfer function constant during the adjustment of its position within the experimental set-up. Here we describe the solutions we developed to ensure that both aforementioned conditions are verified in the mechanical design of the second generation stimulator. We then present a software solution that builds on top of the mechanical device to provide a fully adjustable 2D whisker displacer with a flat transfer function up to 1 kHz.

The stimulator uses multi-directional piezoelectric benders (CMB-2D, Noliac, Denmark). The displacement achieved by these benders, when they work against no external load is in the range of 250 µm, and show a resonance frequency above 2 kHz. However, the benders are classically fixed rigidly by one of their ends. This causes a strong coupling between the bender and the holding device, hence causing a lowering of the ringing frequency down to near 300 Hz, a frequency lying within the physiological range of the rat whiskers motion. In order to displace the ringing frequency well above that range, we devised a method to uncouple the bender from the structure that holds it (Fig. 6*C*): We separated the bender from the holder by a layer of elastomer (Sorbothane, 5 mm thick), a material that efficiently transforms high frequency mechanical vibrations into heat. The static stiffness of this material allows the bender to be held in place, and the mechanical energy absorption allows efficient uncoupling of both parts of the device at higher motion frequencies. In addition, an inertia body (a 20 g piece of lead) was also placed between the bender and the elastomer layer in order to ensure rigid holding of the bender at higher frequencies. The uncoupling of the bender from the holder pushed back the ringing frequency on the edge of the kHz range (see Section 3).

The compound bender/elastomer/lead piece was connected to the lever arm through a ball joint and the lever arm was mounted on a one-axis translation stage (Figs. 3 and 6B). These two elements

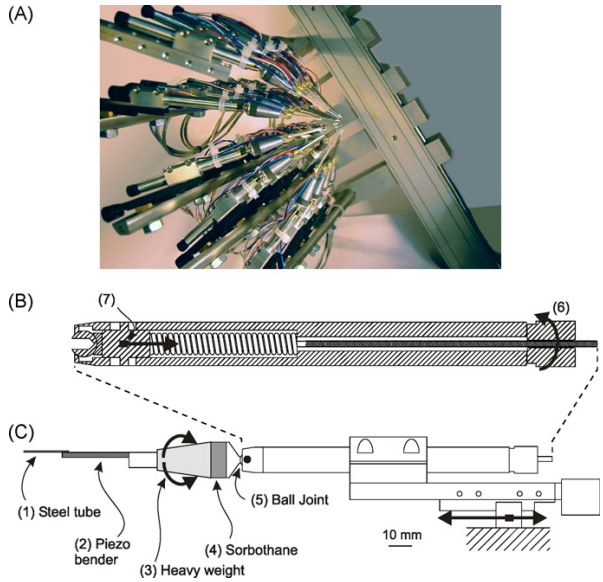

Fig. 6. Second generation stimulator. (*A*) Global lateral view of the device. The tilted rack is an adaptation to fit the stimulator under a two-photon microscope. (*B*) Schematic drawing of a lever arm. A small steel tube (1) is glued on a 2D piezoelectric bender (2) which is held on a heavy weight (3). A sorbothane layer (4) separates this structure from a ball joint (5). The joint can be unclamped by remotely removing (6) the pressure exerted by a spring on the ball (7). Other mechanical structures are similar to the first generation stimulator.

help respectively to obtain the correct angle of the bender and to approach the bender to the whisker. To apply a correction to the voltage input based on the inverse of the transfer function of the stimulator (see e.g. Maravall et al., 2007; the software is described below) the transfer function of each part should be stable, and this in spite of the adjustments that are necessary to connect the stimulator to each of the 24 whiskers. We designed a particular ball joint and we fine tuned the translation stage so that both display a stable transfer function over their whole range of adjustment. The bead of the ball joint that allows the rotation of the bender is locked by the pressure exerted on it by a spring independently of its angle (Fig. 6*B*). In addition, changes in the axial position of the one-axis translation stage induced changes in the transfer function of the bender. We corrected this by carefully equalizing the pressure exerted on the stage over the whole translation range. The mechanical structure of the bender we presented so far showed a stable and ringing free transfer function on the kHz range. An additional correction was made though to linearize its behavior by using a software that performs a filtering of the input commands of the bender by the inverse of its transfer function (see Maravall et al., 2007 for an example of this procedure in the range of 0–200 Hz) (Fig. 7*A*). The software was implemented using Elphy (in-house development, Gerard Sadoc) and the Python programming language. The program code and implementation procedure are given as supplementary material (code.py and Supplementary Figure 2). To compute the transfer function of the piezoelectric bender, a pure sinus-based approach was used. A sweep made of a series of sinus of increasing frequency was applied to the piezoelectric bender and the resulting motion was measured using a

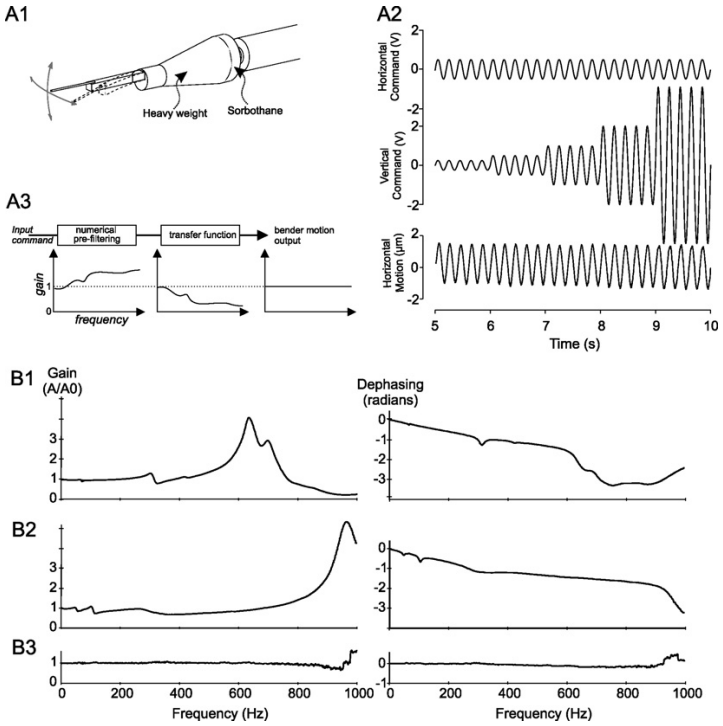

Fig. 7. Characterization of the second generation stimulator. (*A1*) Schematic drawing of the two deflection axes of the piezoelectric bender. (*A2*) Test of independence of the two axes. Input command applied to the horizontal (top) and to the vertical axis (middle). Bottom trace: difference between the motion of the bender in the horizontal plane in response to the vertical axis input command only and to both inputs together. (*A3*) Scheme of the principle of the software correction performed on the bender. For each axis, the transfer function of the bender is computed and its inverse is applied to the input commands. (*B*) Gain (left) and dephasing (right) transfer functions for the horizontal axis of the bender under three conditions. (*B1*) The sorbothane uncoupling is bypassed by a set of metallic bridges that connect together the heavy weight with the ball joint. No software correction is applied. (*B2*) The sorbothane uncoupling is in place but no software correction is applied. (*B3*) Both software and hardware corrections are applied.

PSD/laser displacement sensor over the range 0–1000 Hz. The gain and the dephasing between the command and the motion were computed over this range. To obtain the corrected version of a given bender input command from the computed gain and dephasing values, the input command, previously converted into the Fourier domain, was pre-compensated at each frequency by subtracting the computed dephasing from the phase of the input command, and by dividing its amplitude by the computed gain (see Fig. 7*A3*). This procedure was computed twice, for the *x* and the *y* axes of movement of the multi-directional bender. Fig. 7*A2* shows that a movement made along one axis does not interfere with the movement on the other axis. Both, the mechanical uncoupling and the software correction were necessary to linearize the behavior of the bender as shown by the following tests. The gain (left) and dephasing (right) transfer functions were calculated when the sorbothane uncoupling was bypassed by a set of metallic bridges that connected together the heavy weight with the ball joint and no software correction was applied (Fig. 7*B1*), with the sorbothane uncoupling but without software correction (Fig. 7*B2*), and with both software and hardware corrections applied (Fig. 7*B3*).

2.5. Driving electronics for the multiple-whisker stimulator

Piezoelectric benders require electrical power/current for dynamic applications. Each bender was driven by a fixed voltage and a variable voltage for each of the two axes. The command signals aimed at each of the 24×2 axes were delivered by two 32 channels DAC cards (PD2-AO-32/16, UEI, MA) driven by custom made software (Elphy, G. Sadoc, UNIC-CNRS) running on a PC. A detailed diagram of the electronics can be found in Supplementary Figure 3. An amplification stage was designed to condition properly the voltage commands issued by the DAC. This stage translated the DAC output ($\pm$10 V) into a high amperage (maximum 100 mA), $\pm$30 V driving signal that was fed into the piezoelectric bender. We made sure during the design of this amplification stage that it did not significantly low pass filter the command up to 1 kHz. To verify the adequate deflection of the benders during operation we added two signal assessment systems at the amplification stage.

First, each of the 24 amplification line outputs was branched into a secondary amplification stage driving a LED proportionally to the measured voltage. This allowed the detection of hardware failures in the primary amplification stage. It also helped to visually verify the appropriateness between the expected pattern of stimulation and the actual command being fed into the benders. Second, we added to each amplification line a current measurement module, so we could measure the current that was actually flowing through the capacitive benders when applying a voltage command. By this mean, we could ensure that the current flow caused by a voltage command followed closely the 'perfect capacitor' electric characteristic expected from well working piezoelectric benders (higher current or no current would mean a broken bender). To implement this current measurement module, we connected serially a resistor downstream the primary amplification stage. We measured the resistor voltage with the ADC circuit of a low cost Arduino board (Arduino Diecimila) after appropriate signal conditioning. By multiplexing the ADC input, we could perform all current flow measurements with a single command fed into a single Arduino board.

2.6. Animal preparation

Male Wistar albino rats were used. Experiments were performed in conformity with French (JO 87-848) and European legislation (86/609/CEE) on animal experimentation. Rats were anesthetized with urethane (1.5 g/kg, i.p.). Atropine methyl nitrate (0.3 mg/kg, i.m.) was injected to reduce respiratory secretions. The heart rate and the electrocorticogram (ECoG) were monitored throughout the experiment. Anesthesia was maintained at stage III-3 through online analysis of the frequency content of the ECoG, of the heart and breathing rates, and the control of reflexive movements (Friedberg et al., 1999). Supplementary doses of urethane (0.15 g/kg, i.p.) were administrated when necessary. Body temperature was maintained at 37 °C. The animal was placed in a stereotaxic frame, and the snout was held by a modified head holder (Haidarliu, 1996) allowing free access to the right vibrissae. The whisker stimulator was then connected to the 24 more caudal whiskers. The left postero-medial barrel sub-field (P0-4, L4-8 from Bregma) was exposed. Once the electrode had been positioned on the cortex, the craniotomy was covered with a silicon elastomer (Kwik-Cast, WPI).

2.7. Electrophysiological recordings

Neural activity was recorded extracellularly with tungsten electrodes (FHC, 2–10 MΩ at 1 kHz) vertically lowered in the barrel cortex. Signals were amplified (gain 5000) and filtered (0.3–3 kHz) for spike activity. For each recording site, up to three single units were isolated using a template-matching spike sorter (MSD, Alpha-Omega, Israel). For the control of electrical artifacts that could be elicited by the piezoelectric benders (see Fig. 9), the multi-unit activity was discriminated with a threshold at three standard deviations above noise.

3. Results

3.1. Input/output functions of whisker loaded piezoelectric benders

Trapezoidal deflections of the vibrissae with 10 ms rising and falling ramps were used to quantify the response characteristics of the deflection system once it was connected to the whiskers. The input voltage waveforms and the resulting movement waveform measured with the CDD/laser displacement sensor were compared. The movements of the whisker were measured as close as possible to the plastic tip in which the whisker is inserted. Fig. 8 shows the fidelity with which the voltage command injected into the bender is reproduced by the stimulator and by the connected whisker. We found that a small time lag occurred between the onset of the command and the beginning of the motion of the stimulator. This time lag was 1 ms long for the first generation, and 0.4 ms for the second generation stimulator. We hypothesize that these two different lags are due to the different capacitor characteristics of the two piezoelectric benders used in the two bender generations, combined with the capacitor that was added to the first generation electronic driver.

Since the plastic tubes where the whiskers were inserted are slightly larger than the diameter of the whiskers, one could expect a delay to occur between the motion of the piezoelectric bender and the motion of the whisker because of the separation between the tube and the whisker inside it. However, because of the natural curvature of the whiskers, they were always in contact with the internal wall of the tips and thus they were entrained immediately by the bender. To confirm this, we have recorded (10 kHz sampling rate) the motion of the bender and of the whisker (C2 whisker was used for this measurement) in identical conditions, and we have found that the highest correlation between these two recordings was obtained for a zero delay between the bender and the whisker recordings. If desired, the whisker could have been sealed within the plastic tip with wax. However, following this experiment, we choose not to do so since the input signal and the measured resulting movement presented no visible time delay. In the second, more recent version of the stimulator, the plastic tip was replaced

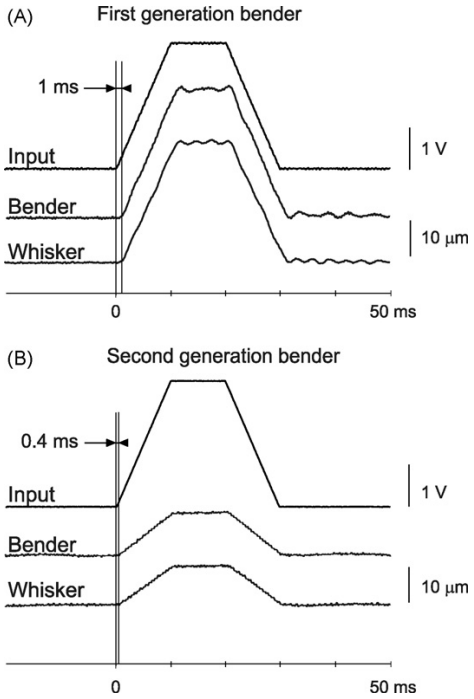

Fig. 8. Delay between the onset of the input command, the motion of the bender and the deflection of the whisker measured with a CDD/laser displacement sensor. (*A*) Ramp-hold-back profile of the input command (top), deflection of the first generation piezoelectric bender (middle) and deflection of a C2 whisker inserted in it (bottom). A 1 ms delay was measured between the onset of the command and the beginning of the bender deflection. (*B*) Same as A for the second generation piezoelectric bender. A 0.4 ms delay was measured between the onset of the command and the beginning of the bender motion. Notice the 0 ms delay between the bender motion and the whisker deflection.

by a metallic tube and the same quantitative observations were made.

3.2. Absence of electrical interference with electrophysiological recordings

Single barrel cortex neurons were recorded using extracellular electrodes in urethane-anesthetized adult rats while whiskers were stimulated. For each animal less than 30 min were required to adjust the device to the whisker pad and to connect all 24 whiskers to the piezoelectric benders. Once connected to the whiskers, the 24 benders were relatively close to the site of electrophysiological recordings and their activation could result in an inductive electromagnetic interference. Experiments to control for the absence of electrical artifacts were conducted and the results are presented in Fig. 9. The recording electrodes were not shielded and the stimulator was grounded to the general ground of the preparation. Electrophysiological data were collected from a multi-unit recording in infragranular layers of the barrel cortex while sparse noise stimulation was applied (Fig. 9*A*). The peri-stimulus time histograms (PSTHs) in Fig. 9 were constructed from events detected by a threshold discriminator at 3 SD above the noise. Identical stimuli were repeated a second time after the stimulator had been removed and the benders, disconnected from the whiskers, were placed in the air just behind them (Fig. 9*B*). Neuronal responses were recorded exclusively when the stimulator was connected to the whiskers and no induced voltage peaks (i.e. electrical artifacts) occurred during deflections of the benders in the air.

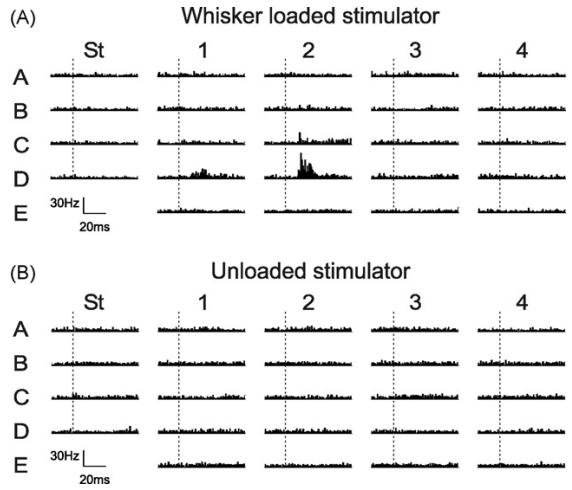

Fig. 9. (*A*) Peri-stimulus time histograms (PSTHs) of multi-unit responses to a sparse noise stimulation of 24 whiskers loaded to the stimulator. Vertical dashed lines indicate the onset of deflection. (*B*) The same protocol was applied with the whiskers disconnected from the stimulator. Notice the absence of electrical interference with the electrophysiological recordings.

3.3. Wide range of stimulation protocols can be produced by the new stimulator

The purpose of this section is to demonstrate the flexibility and power of the new whisker stimulation device. The new stimulator allows the application of complex spatio-temporal sequences of whisker deflections with great reproducibility and with a very wide range of parameters. In particular, precisely controlled deflections of the whiskers that mimic natural stimuli can be applied.

3.3.1. Linear receptive field obtained with sparse noise stimulation

Benders were driven with voltage pulses of 30 ms duration (with 10 ms plateau) to produce oscillation-free rostro-caudal deflections of 114 μm at 7 mm from the follicle, with an initial velocity of 93°/s. Sparse noise stimulation consisted in stimulating consecutively every whisker in a random order with a 50 ms delay both in the rostro-caudal and caudo-rostral direction. At least 120 random sequences were applied for a total duration of 5–10 min. We built the spatio-temporal receptive fields (STRFs) online using forward correlation methods (Bringuier et al., 1999). The STRF makes a good approximation of the linear receptive field of the neuron. The magnitude of the STRF was calculated by integrating the response to whisker stimulations between 10 and 60 ms after the stimulation onset and plotted it in a color map (Fig. 10).

3.3.2. Reproducing natural time series of whisker deflections

One of the major advantages of the second generation new stimulator is that, in addition to the performances described previously, it allows the faithful reproduction of natural whisker deflections with low variability between trials and with spectral content over a wide range including high frequencies.

Fig. 11 shows the reproduction of a natural stimulus having a spectral content that could have not been reproduced by the first version of the stimulator. To record natural time series of whisker deflections, we used a high-speed camera (2500 Hz, Fastcam APX RS, Photron CA, USA) with a spatial resolution of 13 μm per pixel. The camera was placed above the animal's head and a backlight system made of white light LEDs (Phlox, France) illuminated the

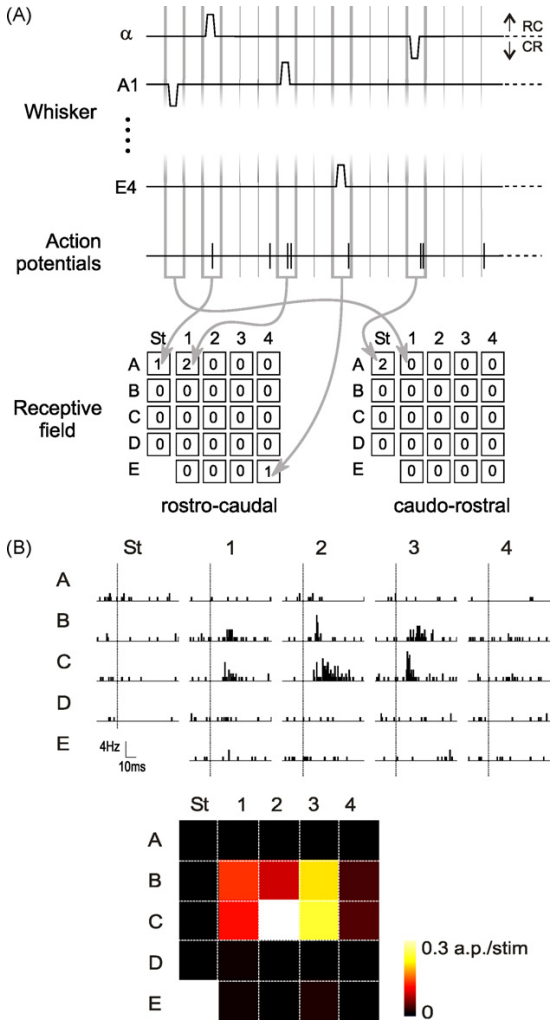

Fig. 10. Forward correlation analysis with sparse noise. (*A*) The 24 whiskers were independently stimulated (10 ms ramp, 10 ms plateau, 10 ms backward ramp) at 20 Hz in a random sequence of rostro-caudal (RC) and caudo-rostral (CR) deflections repeated 120 times. Action potentials were simultaneously recorded. Action potentials generated by a stimulus within a time window of 0 to +60 ms are used to increment the counting of the corresponding pixel of a rostro-caudal or a caudo-rostral spatial receptive field. (*B*: top) Peri-stimulus time histograms of response to the deflection (dashed lines) of the 24 whiskers in the rostro-caudal direction. (*B*: bottom) Response intensity map built by integrating the number of spikes within a time window of 10–60 ms after stimulation and subtracting the spontaneous activity.

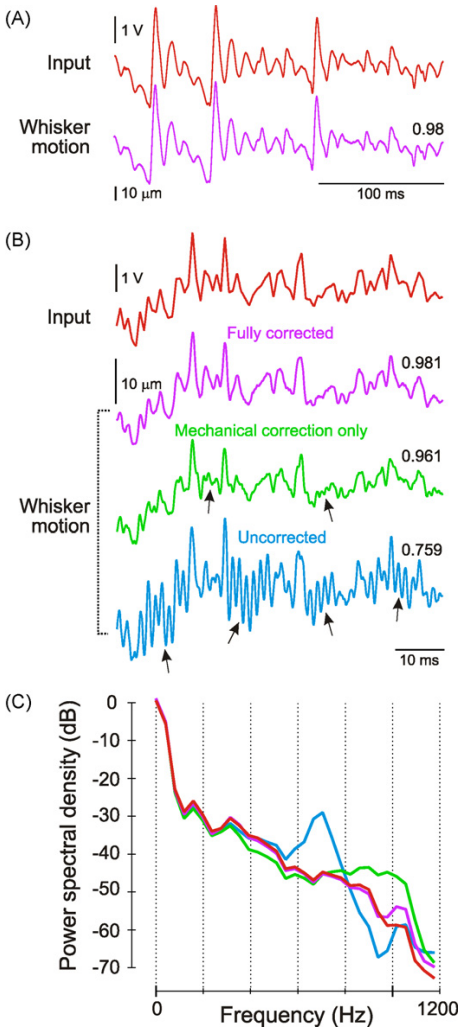

Fig. 11. Replaying natural whisker motions. (See main text for details on the whisker motion recordings.) (*A*) Stick-slip events are well reproduced by the second generation stimulator. The input command (in red) is well correlated ($r = 0.98$) to the resulting C2 whisker motion (in purple). (*B*) High frequency input command (red line) and the resulting deflection of a C2 whisker with the fully corrected second generation stimulator (purple); with mechanical but not software correction (green) and with no software nor mechanical correction (blue). Arrows are indicating ringing artifacts. Correlation values between each recording and the input command are indicated above each trace. (*C*) Normalized power spectral density of the four traces shown in B. Notice the similarity of the input command and of the fully corrected PSD up to 1 kHz (same colors as in B).

whiskers from below. The camera was pointed to whisker C2 of an anaesthetized animal while a motorized rail (Linear motor MLL302, Systro GmbH, Germany) moved a texture (a bar code pattern with a period of 1 mm) across the whisker tip at a constant speed of 60 mm/s and fixed radial distance (90% of total whisker length). We tracked whisker C2 at 2 mm from the follicle by computing the center of mass of squared intensities (pixel value) frame by frame (final spatial resolution of 5 μm). As shown in Fig. 11, under these conditions the whisker at its base showed resonance behavior as well as stick-and-slip events (see e.g. Ritt et al., 2008; Lottem and Azouz, 2009). We then reproduced these movements with the new stimulator by translating them into a voltage waveform input to the bender. When the bender was not corrected, a condition produced by short circuiting the Sorbothane with three metal bridges, the output showed clear periods of resonance vibrations (see arrows in Fig. 11*B*). We computed the power spectral density (PSD) of the command and of the motion recordings in all three conditions, and we found that the fully corrected stimulator displayed a very similar PSD as the original signal up to 1 kHz, while the uncorrected version departed from the original PSD mainly at the high frequencies. The 'bridged' version of the stimulator displayed a major ringing peak starting at 600 Hz. Finally, we observed that the closer the bender to the pad skin, the better the replaying and reproducibility of the movement, probably due to stronger constraint on the whiskers (data not shown).

In conclusion, the combined software and mechanical corrections (see Section 2 for details) provides optimal replaying of natural stimuli, that is waveforms that are particularly demand-

ing for the stimulator. With these corrections a wide avenue of empirical possibilities is opened up by the Matrix.

4. Discussion

The whisker to barrel cortex system became in the last decades an important model for the study of sensory processing. However, one of the inherent difficulties in stimulating a tactile system is that contrary to audition or vision, the sensory organ has to be physically contacted by the stimulating device. Several methods have been used to deflect whiskers. Manual deflections are easy to produce even on awake animals, but are not subject to any control and then cannot be used in a reproducible manner (Brecht and Sakmann, 2002). Using a computer-controlled device allows to stimulate the whiskers with a time-accurate onset. Individual whiskers have been traditionally stimulated using a galvanometer (Stephen, 1969; Nicolelis and Fanselow, 2002) and eventually moving magnet motors (Rajan et al., 2006), although with those methods whiskers are stimulated once at a time. More recent systems have been developed and applied to awake animals. Air puffs have been used for stimulating whiskers in head-restrained preparations (Hutson and Masterton, 1986; Nunez et al., 1994) but they unavoidably deflect several whiskers at a time. More recently a method for whisker deflection on freely moving rats was developed by attaching a small iron particle to one whisker and by delivering a brief magnetic pulse (1–5 ms) through an electromagnetic coil (Melzer et al., 1985; Ferezou et al., 2006). In both cases however the trajectory of whisker deflections is not controlled and not precisely known. In addition, the magnetic field affects simultaneously all the whiskers having a metallic attachment and thus is not suitable for studies where spatio-temporal multi-whisker stimulations are needed.

It is generally accepted that the cortical responses are strongly modulated when two or more whiskers are deflected simultaneously or slightly out of phase (Brumberg et al., 1996; Carvell and Simons, 1988; Drew and Feldman, 2007; Ego-Stengel et al., 2005; Erchova et al., 2003; Ghazanfar and Nicolelis, 1997; Ghazanfar et al., 2000; Higley and Contreras, 2003; Kleinfeld and Delaney, 1996; Mirabella et al., 2001; Shimegi et al., 1999; Simons, 1985). Similarly, many vibrissae are used for solving certain tactile tasks (Carvell and Simons, 1990; Sachdev et al., 2001; Krupa et al., 2001). In the past, a 16 whisker stimulator based on miniature solenoids has been used by Krupa et al. (2001). This system has the advantage that the spatial dimension of each solenoid is small and the whiskers can be held at their resting position. Although the kinetic properties of the movement are reasonably good, complex high frequency kinetics like natural whisker movements have not been tested yet and since only one single direction of stimulation can be applied, it is unlikely that this device can be upgraded to a version providing deflections with multiple directions.

One of the major advantages of our device is that it allows the deflection of 24 whiskers in any spatio-temporal configuration within a large parametric space. Piezoelectric benders have been used in number of studies. Their main advantage is that the amplitude and direction of the movement can continuously vary in a controlled manner. A few other laboratories used them for stimulating up to nine whiskers although the resting position of the whiskers was not maintained (Drew and Feldman, 2007). We showed here that the spatial dimensions of piezoelectric bimorphs can be compatible with the stimulation of a large number of whiskers while holding their natural position at rest. We also present a solution to cope with the ringing problem which was until now precluding the application of the high temporal frequencies (200–1000 Hz) encountered in natural scenes (but see Andermann and Moore, 2008 for modified piezoelectric benders able to apply small movements up to 800 Hz). We applied complex patterns of stimulation defined both at single and at multiple whisker levels. The stimulation varied spatially by changing the whisker identity and/or the amplitude and the direction of whisker deflection. It varied also temporally by controlling the interval of time between the whisker stimulation and/or by defining the kinetics of the deflection of the stimulated whiskers.

It is commonly accepted that the temporal profile of the angular velocity of deflection constitutes a relevant property of the stimulation to elicit cortical responses (Arabzadeh et al., 2005). Protraction velocities during free whisking are around 500–900°/s whereas retraction velocities reach 1500°/s (Gao et al., 2001; Grant et al., 2009). During texture discrimination, whisker deflection can reach a few thousands of degrees per second (Carvell and Simons, 1990; Ritt et al., 2008). While non-compensated piezoelectric benders show a limitation to reach those high velocities because of the ringing behavior, our corrected device can be used to deflect whiskers at those velocities relevant for natural tactile exploration by rats. For example, when the stimulator is used at 5 mm from the follicle it can produce a rapid deflection of 180 μm at 800 Hz corresponding to a velocity of 1650°/s.

4.1. Limitation of the stimulation device in studying responses in the awake animal

As we have shown here, the new stimulation device can be used in an anesthetized preparation. The connection of all 24 whiskers to the benders takes less than half an hour which is a reasonable period of time for an acute electrophysiological experiment. It is conceivable to use this stimulator in head-posted awake animals. However this probably would need to condition the animal to stay calm and not to whisk. One disadvantage of the system described here is that it is out of its possibilities to be used in head-posted animals solving a tactile task that needs whisking. Although this must be recognized as a limitation in the utility of this system, there are a number of observations that show that passive and active whisker deflections induce similar responses in the barrel cortex, making it pertinent to study the response of the system to passive whisker deflections. First, the exploratory strategies used by rats to discriminate objects are still not fully known. While texture discrimination tasks depend on whisking (see e.g. Guic-Robles et al., 1989; Carvell and Simons, 1990) some tactile tasks do not seem to depend on active whisking to be solved. For example, aperture or distance discrimination can be performed at very high levels of success with whisker contacts induced by head movements without whisking (Krupa et al., 2001). Hence, cortical processing of sensory information can be studied in conditions in which the whiskers are deflected passively like when using whisker stimulators in anesthetized animals. Second, voltage-sensitive dyes imaging of active sensory processing in awake, freely moving animals show that sensory responses to active touch are similar to those evoked by a passive stimulus in anesthetized and in quiescent awake animals (Ferezou et al., 2006). Finally, recent experimental data (Lottem and Azouz, 2009) showed that whisker contacts produced by a passive exposure to a texture or by active whisking produce similar responses in the trigeminal ganglia.

In conclusion, we have presented a novel stimulator for deflecting macrovibrissae individually or conjointly, in a controlled manner and with high fidelity. With this device we have shown that it is possible to probe the whisker somatosensory system with a range of spatio-temporal patterns of deflections having temporal frequencies encompassing those produced naturally by the exploring animal. Our stimulation device can be used to evaluate in a rapid manner the properties of spatio-temporal receptive fields of somatosensory neurons using sparse noise stimulation. It can also consistently reproduce high dimension tactile scenes inspired

from natural multi-whisker stimulations and therefore enlarge the possibilities for studying the complex interactions acting between sensory neurons receiving inputs from distinct whiskers.

Acknowledgements

We thank Yves Boubenec for providing the high-speed camera data. This work was supported by ANR (07-NEURO-025-01, NATACS) and FACETS (EC FP6-015879).

Appendix A. Supplementary data

Supplementary data associated with this article can be found, in the online version, at doi:10.1016/j.jneumeth.2010.03.020.

References

Andermann ML, Moore CI. Mechanical resonance enhances the sensitivity of the vibrissa sensory system to near-threshold stimuli. Brain Res 2008;1235:74–81.
Arabzadeh E, Zorzin E, Diamond ME. Neuronal encoding of texture in the whisker sensory pathway. PLoS Biol 2005;3:e17.
Brecht M, Sakmann B. Dynamic representation of whisker deflection by synaptic potentials in spiny stellate and pyramidal cells in the barrels and septa of layer 4 rat somatosensory cortex. J Physiol 2002;543:49–70.
Bringuier V, Chavane F, Glaeser L, Frégnac Y. Horizontal propagation of visual activity in the synaptic integration field of area 17 neurons. Science 1999;283:695–9.
Brumberg JC, Pinto DJ, Simons DJ. Spatial gradients and inhibitory summation in the rat whisker barrel system. J Neurophysiol 1996;76:130–40.
Carvell GE, Simons DJ. Membrane potential changes in rat SmI cortical neurons evoked by controlled stimulation of mystacial vibrissae. Brain Res 1988;448:186–91.
Carvell GE, Simons DJ. Biometric analyses of vibrissal tactile discrimination in the rat. J Neurosci 1990;10:2638–48.
Celikel T, Sakmann B. Sensory integration across space and in time for decision making in the somatosensory system of rodents. Proc Natl Acad Sci U S A 2007;104:1395–400.
Drew PJ, Feldman DE. Representation of moving wavefronts of whisker deflection in rat somatosensory cortex. J Neurophysiol 2007;98:1566–80.
Ego-Stengel V, Mello e Souza T, Jacob V, Shulz DE. Spatiotemporal characteristics of neuronal sensory integration in the barrel cortex of the rat. J Neurophysiol 2005;93:1450–67.
Erchova IA, Petersen RS, Diamond ME. Effect of developmental sensory and motor deprivation on the functional organization of adult rat somatosensory cortex. Brain Res Bull 2003;60:373–86.
Ferezou I, Bolea S, Petersen CC. Visualizing the cortical representation of whisker touch: voltage-sensitive dye imaging in freely moving mice. Neuron 2006;50:617–29.
Friedberg MH, Lee SM, Ebner FF. Modulation of receptive field properties of thalamic somatosensory neurons by the depth of anesthesia. J Neurophysiol 1999;81:2243–52.
Gao P, Bermejo R, Zeigler HP. Whisker deafferentation and rodent whisking patterns: behavioral evidence for a central pattern generator. J Neurosci 2001;21:5374–80.
Ghazanfar AA, Nicolelis MA. Nonlinear processing of tactile information in the thalamocortical loop. J Neurophysiol 1997;78:506–10.
Ghazanfar AA, Stambaugh CR, Nicolelis MA. Encoding of tactile stimulus location by somatosensory thalamocortical ensembles. J Neurosci 2000;20:3761–75.
Grant RA, Mitchinson B, Fox CW, Prescott TJ. Active touch sensing in the rat: anticipatory and regulatory control of whisker movements during surface exploration. J Neurophysiol 2009;101:862–74.
Guic-Robles E, Valdivieso C, Guajardo G. Rats can learn a roughness discrimination using only their vibrissal system. Behav Brain Res 1989;31:285–9.
Haidarliu S. An anatomically adapted, injury-free head-holder for guinea pigs. Physiol Behav 1996;60:111–4.
Harvey MA, Sachdev RN, Zeigler HP. Cortical barrel field ablation and unconditioned whisking kinematics. Somatosens Mot Res 2001;18:223–7.
Higley MJ, Contreras D. Nonlinear integration of sensory responses in the rat barrel cortex: an intracellular study in vivo. J Neurosci 2003;23:10190–200.
Hipp J, Arabzadeh E, Zorzin E, Conradt J, Kayser C, Diamond ME, et al. Texture signals in whisker vibrations. J Neurophysiol 2006;95:1792–9.
Hutson KA, Masterton RB. The sensory contribution of a single vibrissa's cortical barrel. J Neurophysiol 1986;56:1196–223.
Jacob V, Le Cam J, Ego-Stengel V, Shulz DE. Emergent properties of tactile scenes selectively activate barrel cortex neurons. Neuron 2008;60:1112–25.
Kleinfeld D, Delaney KR. Distributed representation of vibrissa movement in the upper layers of somatosensory cortex revealed with voltage-sensitive dyes. J Comp Neurol 1996;375:89–108.
Krupa DJ, Matell MS, Brisben AJ, Oliveira LM, Nicolelis MA. Behavioral properties of the trigeminal somatosensory system in rats performing whisker-dependent tactile discriminations. J Neurosci 2001;21:5752–63.
Lottem E, Azouz R. Mechanisms of tactile information transmission through whisker vibrations. J Neurosci 2009;29:11686–97.
Maravall M, Petersen RS, Fairhall AL, Arabzadeh E, Diamond ME. Shifts in coding properties and maintenance of information transmission during adaptation in barrel cortex. PLoS Biol 2007;5:e19.
Melzer P, van der Loos H, Dörfl J, Welker E, Robert P, Emery D, et al. A magnetic device to stimulate selected whiskers of freely moving or restrained small rodents: its application in a deoxyglucose study. Brain Res 1985;348:229–40.
Mirabella G, Battiston S, Diamond ME. Integration of multiple-whisker inputs in rat somatosensory cortex. Cereb Cortex 2001;11:164–70.
Nicolelis MA, Fanselow EE. Thalamocortical [correction of Thalamcortical] optimization of tactile processing according to behavioral state. Nat Neurosci 2002;5:517–23.
Nunez A, Barrenechea C, Avendano C. Spontaneous activity and responses to sensory stimulation in ventrobasal thalamic neurons in the rat: an in vivo intracellular recording and staining study. Somatosens Mot Res 1994;11:89–98.
Rajan R, Bourke J, Cassell J. A novel stimulus system for applying tactile stimuli to the macrovibrissae in electrophysiological experiments. J Neurosci Methods 2006;157:103–17.
Ritt JT, Andermann ML, Moore CI. Embodied information processing: vibrissa mechanics and texture features shape micromotions in actively sensing rats. Neuron 2008;57:599–613.
Rodgers KM, Benison AM, Barth DS. Two-dimensional coincidence detection in the vibrissa/barrel field. J Neurophysiol 2006;96:1981–90.
Sachdev RN, Sellien H, Ebner F. Temporal organization of multi-whisker contact in rats. Somatosens Mot Res 2001;18:91–100.
Shimegi S, Ichikawa T, Akasaki T, Sato H. Temporal characteristics of response integration evoked by multiple whisker stimulations in the barrel cortex of rats. J Neurosci 1999;19:10164–75.
Simons DJ. Temporal and spatial integration in the rat SI vibrissa cortex. J Neurophysiol 1985;54:615–35.
Stephen RO. Electro-mechanical harmonic stimulator. J Physiol 1969;202:71P–2P.
Wolfe J, Hill DN, Pahlavan S, Drew PJ, Kleinfeld D, Feldman DE. Texture coding in the rat whisker system: slip-stick versus differential resonance. PLoS Biol 2008;6:e215.
Woolsey TA, Van der Loos H. The structural organization of layer IV in the somatosensory region (S1) of mouse cerebral cortex. The description of a cortical field composed of discrete cytoarchitectural units. Brain Res 1970;17:205–42.

Chapter 3

An exploration of barrel cortex neurons linear filters

3.1 Barrel cortex neurons linear filters lack a well defined structure as well as consistency across experimental conditions

The most striking functional property of barrel cortex neurons is the non-linearity of their response to combinations of whisker stimulations. Suppressive [Simons, 1985] as well facilitative effects [Shimegi et al., 1999; Ego-Stengel et al., 2005] have been observed, including in response to the stimulation of whiskers that are not part of the neuron linear receptive field [Shimegi et al., 1999; Ego-Stengel et al., 2005]. These non-linearities structure spatiotemporally the functional response to multiwhisker responses, and they are likely to be involved in the emergence of multiwhisker selectivities [Drew and Feldman, 2007; Jacob et al., 2008] (although second order interactions were not sufficient to account for the directional selectivity observed in [Jacob et al., 2008]).

In contrast with these marked and structuring non-linearities, the study of barrel cortex neurons linear receptive fields has settled on a less notable picture.

The initial studies of barrel cortex functional responses described receptive fields as limited to the principal whisker, that is the whisker homologue to the recorded barrel [Welker, 1971]. However, further exploration of the system has shown that receptive field extend with weaker responses beyond this principal whisker [Simons, 1978, 1985] and can cover up almost the whole whiskerpad, both subthreshold [Moore and Nelson, 1998; Brecht and Sakmann, 2002] and suprathreshold [Chapin, 1986; Ghazanfar and Nicolelis, 1999; Jacob et al., 2008]. The spatial organization of these receptive fields has been described as a strong response to the principal whisker and weaker responses to surrounding whiskers [Moore and Nelson, 1998; Zhu and Connors, 1999]. Beyond summation of the stimulations arising from multiple whiskers, it is hard to relate this receptive field organization to a well defined processing ; one that could be compared for instance with the edge detectors described in the primary visual cortex [Daugman, 1985].

3.1.1 Linear receptive fields are affected by anaesthetics

Still, even such deceptively simple receptive fields do not seem robust face to changes in the type and depth of anaesthesia. For instance, urethane and pentobarbital anaesthesia have lead to recordings with large receptive field sizes : around 4 whiskers in layer IV and 5 in layer V from 5 whiskers [Ito, 1985; Jacob et al., 2008] up to 8 whiskers [Ghazanfar and Nicolelis, 1999], and from 1 to 16 whiskers subthreshold [Moore and Nelson, 1998]. Pentobarbital has lead to recordings with 6-15 significant whiskers subthreshold [Zhu and Connors, 1999].

In contrast, unanaesthetized/paralysed or lightly sedated preparations using fentanil have resulted in much smaller receptive fields across layers, with a vast majority (85%) of layer IV neurons displaying responses only to the principal whisker [Simons, 1978]. Although in this study layer II/III and layer V neurons displayed larger proportions of multiwhisker receptive fields (respectively 39% and 65%), these receptive field size were still smaller than what was observed under deep urethane anaesthesia, as confirmed by a study specifically comparing receptive field sizes in these two conditions [Simons et al., 1992].

3.1.2 Linear receptive fields are affected by the density of the multiwhisker stimulation

Not only anaesthetics, but also the statistics of the stimulus affect the measurement of barrel cortex linear receptive fields. Indeed, the complex non-linearities found in the rat barrel cortex make the measurement of the multiwhisker receptive field highly dependent on the density of whisker stimulations: barrel cortex neurons respond differently to independent deflections of whiskers and to simultaneous (air puff) whisker deflections, with some neurons responding more strongly while others show weaker responses to simultaneous whisker deflections, as seen in layers II/III [Brecht et al., 2003], in layer IV [Brecht and Sakmann, 2002] and in layer V [Manns et al., 2004]. Similarly, the functional response to a single-whisker deflection is much reduced when the whiskers surrounding it are simultaneously randomly vibrated [Brumberg et al., 1996]. We explored (in collaboration with Sami El Boustani) this issue in more detail in the lightly isoflurane anaesthetized rat by acquiring the receptive field of 14 barrel cortex single units using unitary rostral deflections that were separated by inter-stimulus interval (ISI) ranging from 4 to 50 ms (see fig. 3.1.a). This work reveals that with the exception of a few neurons (fig. 3.1.e), shorter ISI resulted in receptive fields with progressively less significant whiskers (fig. 3.1.b) and with significant responses of lower amplitude, leading up to the disappearance of all significant response in the receptive field at the shortest ISI (fig. 3.1.c-d).

This reduction of the functional response can also be found in the visual cortex [Fournier et al., 2011]. However, it is not as drastic there, and linear components of the receptive fields can be estimated both using sparse [Jones and Palmer, 1987] and dense [Reid and Alonso, 1995; Reid et al., 1997] presentations of ternary noise (random occurrence of black and white pixels on a grey screen), thus making the linear filters a legitimate first order estimate of the visual cortex functional properties. In contrast, the lack of consistency of the linear filters of barrel cortex neurons across experimental conditions adds to the lack of a clear functional role for their "gradient" like PW/AW structure to make the linear receptive field a questionable estimate of the functional properties of barrel cortex neurons.

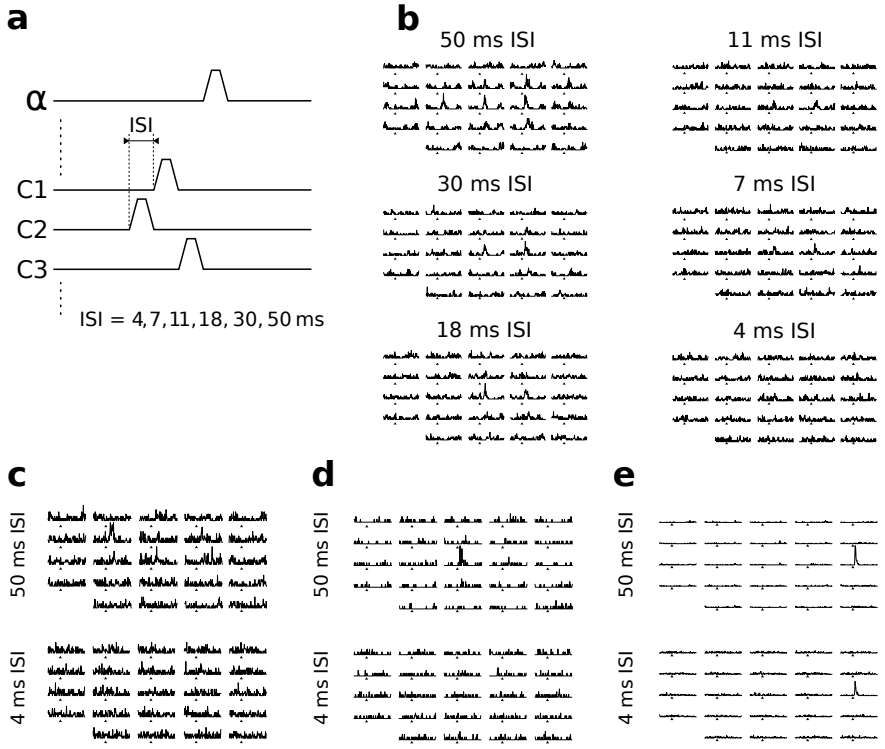

Figure 3.1 – Impact of stimulus density on the measurement of the linear receptive field of barrel cortex neurons. Arrows below PSTHs: stimulus onset. (a) A sparse/dense stimulus transition is produced by varying between 50 ms and 4 ms the inter-stimulus interval (ISI) of impulse stimulations occurring in the different stimulated whiskers. Stimuli are 10ms ramp, 10ms hold and 10ms back. (b) Rostral receptive field of a layer 4 single unit, as measured across decreasing ISI. (c-e) Comparison of the receptive field acquired with 50 ms versus 4 ms ISI for (c) a layer IV single unit, (d) a layer V single unit and (e) a layer IV single unit that is only little affected by stimulus density.

3.2 The sensory-motor hypothesis: coding without complex sensory receptive fields

The difficulty to capture meaningful spatial structure in linear receptive fields of barrel cortex neurons may be due to their involvement in a sensory-motor system. They may thus not encode spatial stimulus properties through purely sensory receptive field properties, but only through interactions between a motor and a sensory components [Ahissar and Knutsen, 2008].

The prominence of whisking behaviours ('nosing' in 1912 parlance) was noted in the first studies of the whisker system [Vincent, 1912, 1913]. However, it was not until the second half of the twentieth century that the coding of object spatial properties through whisking was proposed [Brown and Waite, 1974]. More recently, neurons that specifically report whisking were found in the trigeminal ganglion [Szwed et al., 2003], and whisking related modulations of neuronal activity were observed in the activity of barrel cortex neurons [Fee et al., 1997; Crochet and Petersen, 2006; Curtis and Kleinfeld, 2009],

leading up to the hypothesis that barrel cortex neurons make use of this information in their processing.

This sensori-motor coding hypothesis is also supported by the change in processing and cortical state observed in the barrel cortex between the whisking and non-whisking conditions [Krupa et al., 2004; Fanselow and Nicolelis, 1999; Ferezou et al., 2007; Poulet and Petersen, 2008], including switches in the activation of specific interneuron subtypes [Gentet et al., 2010].

In parallel, behavioural work has demonstrated that the ability of rats to estimate the rostro-caudal position of objects with their whiskers depends on their active whisking behaviour [Mehta et al., 2007] and only to a limited extend on their simultaneous use of multiple whiskers [Knutsen et al., 2006].

Neuronal mechanisms for this sensory-motor coding of the rostro-caudal positioning of objects are currently being investigated and seem to be based on an elaborate and state dependent combination of a whisking-locked subthreshold membrane potential fluctuation with the EPSPs voleys triggered by the contact of whiskers with objects [Crochet and Petersen, 2006; Curtis and Kleinfeld, 2009; Gentet et al., 2010; Crochet et al., 2011].

3.3 But: are they more elaborate receptive fields hidden in the multidimensional whiskerpad sensory space?

A parallel with the visual system - another active sensing system - illustrates well the possibility for a complex sensori-motor system to perform meaningful processing of the stimulus through both the sensori-motor loop - making the eyes track over time the focus of visual attention [Duhamel et al., 1992; Corbetta et al., 1998; Moore and Fallah, 2001] - and through the purely sensory processing carried by the receptive fields of V1 neurons [Hubel and Wiesel, 1962].

Also, although sensory-motor coding of spatial properties is likely to be a central function of the barrel cortex during active whisking, passive whisker contacts also occur in many behavioural situations and can support sensory discrimination tasks [Adibi and Arabzadeh, 2011].

For these two reasons, we hypothesize that both during active and passive whisker use, barrel cortex neurons are actually performing meaningful sensory - and not only sensorimotor - processing of spatial information, notwithstanding the previously described blurry, 'gradient'-like structure of their receptive fields.

One reason for the limited spatial processing reported in previous studies of barrel cortex neurons 'static' receptive field may be that - in contrast with the visual system - the link between the multiple dimensions of the whiskerpad sensory stimuli has been little studied.

In the visual cortex, the most striking examples of functional processing are all built on multiple sensory dimensions, such as the spatial/luminance space of simple/complex V1 neurons [Hubel and Wiesel, 1962]. In MT/V5, 'reinforcing'/'antagonist' neurons [Born and Tootell, 1992; Born, 2000] are integrators/differentiators in a space/direction-of-motion space.

In contrast, studies of barrel cortex neurons have focused on the neurons tuning to a single dimension of the stimulus at a time, such as the direction of whisker deflection [Simons, 1978], the spatial span of receptive fields [Simons, 1978, 1985] or the frequency content of whisker deflections [Ewert et al., 2008], and these studies almost never focused on the neurons functional responses to stimuli that span more than a single dimension

(although [Kida et al., 2005] and [Simons and Carvell, 1989] both looked at the direction selectivity of one principal versus one adjacent whisker).

In the following publication, we explored the receptive fields of barrel cortex neurons across the space/direction sensory dimensions. To this aim we used the first generation of multiwhisker stimulators previously developed in the laboratory and we applied on the right whiskerpad of the rat a sparse set of deflections across the 24 largest macrovibrissae and across two directions of deflection (rostral and caudal). The outcome of this study is presented in the following pages.

Article 2

Spatial structure of multiwhisker receptive fields in the barrel cortex is stimulus dependent

Julie Le Cam,* Luc Estebanez,* Vincent Jacob, and Daniel E. Shulz

Journal of Neurophysiology 106 (2011) 986–998

* *equally contributed to the work*

Abstract: The tactile sensations mediated by the whisker system allow rodents to efficiently detect and discriminate objects. These capabilities rely strongly on the temporal and spatial structure of whisker deflections. Subthreshold but also spiking receptive fields in the barrel cortex encompass a large number of vibrissae, and it seems likely that the functional properties of these multiwhisker receptive fields reflect the multiple-whisker interactions encountered by the animal during the exploration of its environment. The aim of this study was to examine the dependence of the spatial structure of cortical receptive fields on stimulus parameters.

Using a newly developed 24-whisker stimulation matrix, we applied a forward correlation analysis of spiking activity to randomized whisker deflections (sparse noise) to characterize the receptive fields that result from caudal and rostral directions of whisker deflection. We observed that the functionally determined principal whisker — the whisker eliciting the strongest response with the shortest latency — differed according to the direction of whisker deflection. Thus, for a given neuron, maximal responses to opposite directions of whisker deflections could be spatially separated.

This spatial separation resulted in a displacement of the center of mass between the rostral and caudal subfields and was accompanied by differences between response latencies in rostral and caudal directions of whisker deflection. Such direction-dependent receptive field organization was observed in every cortical layer. We conclude that the spatial structure of receptive fields in the barrel cortex is not an intrinsic property of the neuron but depends on the properties of sensory input.

Journal of Neurophysiology

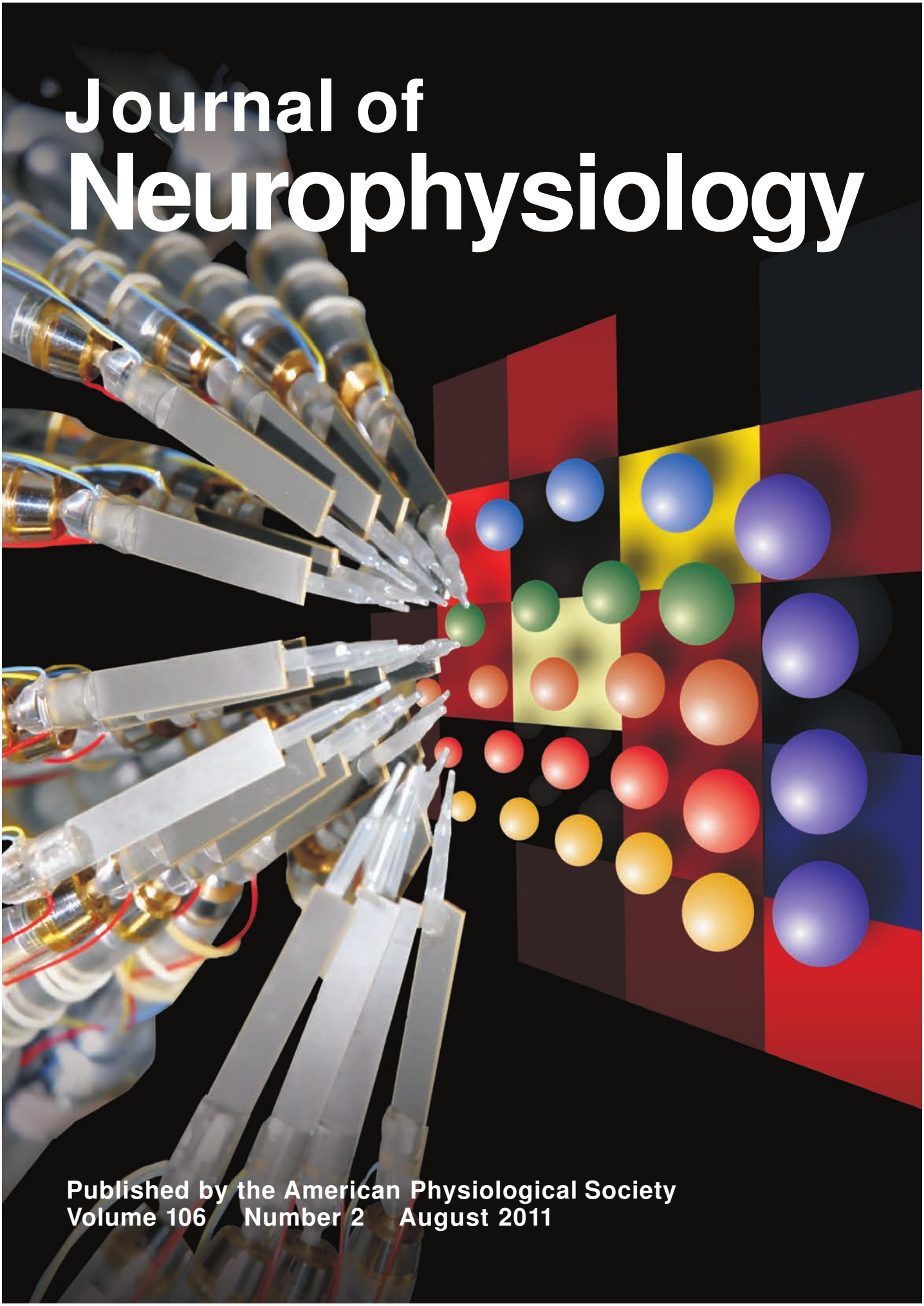

Published by the American Physiological Society
Volume 106 Number 2 August 2011

J Neurophysiol 106: 986–998, 2011.
First published June 8, 2011; doi:10.1152/jn.00044.2011.

Spatial structure of multiwhisker receptive fields in the barrel cortex is stimulus dependent

Julie Le Cam,* Luc Estebanez,* Vincent Jacob, and Daniel E. Shulz
Unité de Neurosciences, Information et Complexité (UNIC), Centre National de la Recherche Scientifique, Gif sur Yvette, France

Submitted 18 January 2011; accepted in final form 26 May 2011

Le Cam J, Estebanez L, Jacob V, Shulz DE. Spatial structure of multiwhisker receptive fields in the barrel cortex is stimulus dependent. *J Neurophysiol* 106: 986–998, 2011. First published June 8, 2011; doi:10.1152/jn.00044.2011.—The tactile sensations mediated by the whisker-trigeminal system allow rodents to efficiently detect and discriminate objects. These capabilities rely strongly on the temporal and spatial structure of whisker deflections. Subthreshold but also spiking receptive fields in the barrel cortex encompass a large number of vibrissae, and it seems likely that the functional properties of these multiwhisker receptive fields reflect the multiple-whisker interactions encountered by the animal during exploration of its environment. The aim of this study was to examine the dependence of the spatial structure of cortical receptive fields on stimulus parameters. Using a newly developed 24-whisker stimulation matrix, we applied a forward correlation analysis of spiking activity to randomized whisker deflections (sparse noise) to characterize the receptive fields that result from caudal and rostral directions of whisker deflection. We observed that the functionally determined principal whisker, the whisker eliciting the strongest response with the shortest latency, differed according to the direction of whisker deflection. Thus, for a given neuron, maximal responses to opposite directions of whisker deflections could be spatially separated. This spatial separation resulted in a displacement of the center of mass between the rostral and caudal subfields and was accompanied by differences between response latencies in rostral and caudal directions of whisker deflection. Such direction-dependent receptive field organization was observed in every cortical layer. We conclude that the spatial structure of receptive fields in the barrel cortex is not an intrinsic property of the neuron but depends on the properties of sensory input.

somatosensory cortex; vibrissa; touch; direction selectivity; rat

LAYER IV of the primary somatosensory cortex (S1) of rodents contains discrete cytoarchitectonic modules called "barrels" (Killackey 1973; Woolsey and van der Loos 1970). Each barrel is in anatomic correspondence with one specific mystacial vibrissa on the snout of the animal (Simons 1985). Functionally, neurons localized in a particular cortical barrel respond preferentially, with shortest response latency, to one whisker, called the principal whisker (PW). However, whole cell and intracellular recordings of synaptic responses to individual whisker deflections showed that the convergence of information onto single neurons of layers II to V of the barrel cortex was extensive, spanning several adjacent whiskers (AWs) from the center of the receptive field (Brecht and Sakmann, 2002b; Brecht et al. 2003; Manns et al. 2004; Moore and Nelson 1998; Zhu and Connors 1999). These large receptive fields represent a potential substrate for response modulation by the context of the peripheral stimulation (Jacob et al. 2008). Here we propose that several basic functional properties of the multiple-whisker receptive fields are affected by simple changes in stimulus properties, specifically along the caudo-rostral axis.

The caudo-rostral axis is important for the whisker-to-barrel system, behaviorally, anatomically, and functionally. Whiskers on the mystacial pad are arranged in a precise geometric pattern of caudo-rostral rows and dorso-ventral arcs. During exploratory behaviors, rats move their vibrissae rostrally, creating a functional asymmetry between rows and arcs. Anatomically, studies have revealed a bias toward within-row connectivity in the intracortical circuitry (Bernardo et al. 1990a, 1990b; Hoeflinger et al. 1995; Kim and Ebner 1999). Additionally, cortical activity patterns induced by single-whisker deflections are elongated along rows (Armstrong-James and Fox 1987; Kleinfeld and Delaney 1996; Simons 1978), and suppressive two-whisker interactions are more prominent when the stimulated whiskers belong to the same row than to the same arc (Ego-Stengel et al. 2005). Consequently, we tested here whether properties of multiwhisker receptive fields change when activating the system with deflections in different directions of movement along the caudo-rostral axis.

In the visual cortex, changes in nonspatial properties of the stimulus, like contrast polarity (ON or OFF light transitions), allow characterization of contiguous but spatially segregated subfields in a subset of neurons called simple cells (Hubel and Wiesel 1962). In the barrel cortex, neurons respond with different magnitudes and latencies to different directions of deflections of the PW (Bruno and Simons 2002; Puccini et al. 2006; Simons 1978; Simons and Carvell 1989; Wilent and Contreras 2005). Neurons with multiwhisker receptive fields do not necessarily respond to the same angle of deflection of the different whiskers. If a neuron shows different directional selectivity to the PW and the AWs, the structure of the receptive field, its center of mass, and its preferred whisker will change with the stimulus direction. Evidence for this dependence is limited and contradictory in the literature. Kida et al. (2005) have shown similar direction preference for the PW and AWs, whereas Hemelt et al. (2010) observed insignificant angular tuning consistencies across vibrissae. Here we tested in the barrel cortex whether a change in the direction of whisker deflection (rostral vs. caudal) can unmask changes in receptive field mapping. Using a new stimulator composed of 24 independent piezoelectric actuators (Jacob et al. 2010) adapted to the five rows and the five most caudal arcs of the rat whisker pad, we have characterized cortical receptive fields using

* J. Le Cam and L. Estebanez contributed equally to this work.

Address for reprint requests and other correspondence: D. E. Shulz, Unité de Neurosciences, Information et Complexité, Centre National de la Recherche Scientifique, 1 Ave. de la Terrasse, bldg 33, 91198 Gif sur Yvette, France (e-mail: shulz@unic.cnrs-gif.fr).

whisker deflections caudally and rostrally from resting position. When comparing one direction of deflection to the other we observed, in most cortical regular spiking neurons, modulations of the spatial structure of the receptive field. These changes included a shift in the center of gravity of the receptive field, differences in the latency of responses to PW and AWs, and even changes in receptive field size.

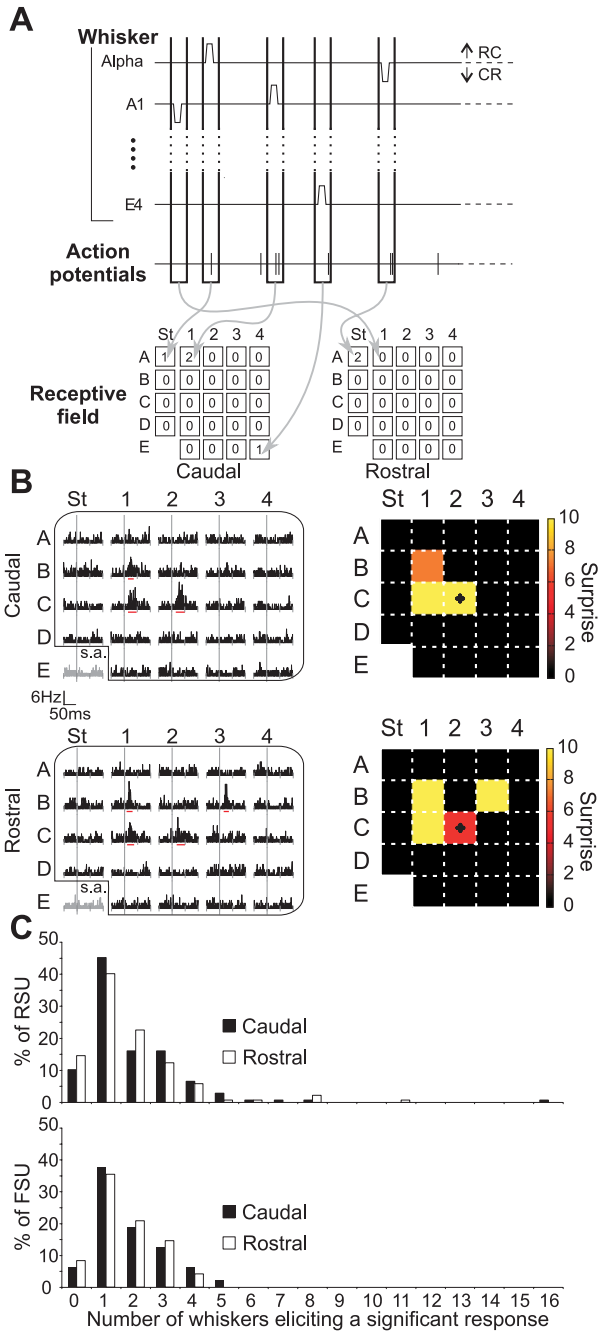

MATERIALS AND METHODS

Experiments were performed in conformity with French (JO 87-848) and European (86/609/CEE) legislation on animal experimentation. All authors have been granted a license from the French Ministry of Agriculture to conduct the animal research described here.

Animal Preparation

Male Wistar rats ($n = 29$, weight = 306 ± 23 g, mean ± SD) were anesthetized with urethane (1.5 g/kg ip). Atropine methyl nitrate (0.3 mg/kg im) was injected to reduce secretions in the respiratory path. Supplementary doses of urethane (0.15 g/kg ip) were administrated when necessary throughout the experiment in order to maintain an adequate level of anesthesia, as indicated by the absence of eye blink reflex, the lack of response to hind paw pinch, and the absence of spontaneous vibrissa movements. ECG and EEG monitoring was performed throughout the experiment. Body temperature was maintained at 37°C by a regulated heating pad. The animal was placed in a stereotaxic frame, and the skull was cemented to a metal bar fixed rigidly to the frame. The snout was held by a modified head holder (Haidarliu 1996) allowing free access to the right vibrissae. The left posteromedial barrel subfield (P0–4, L4–8 from bregma; Chapin and Lin 1984) was exposed. Once the electrode had been inserted into the cortex, the craniotomy was covered with a silicon elastomer (Kwik-Cast, WPI).

Electrophysiological Recordings

Neural activity was recorded extracellularly from 202 neurons with a custom program [Elphy, G. Sadoc, Centre National de la Recherche Scientifique Unité de Neurosciences, Information et Complexité (CNRS-UNIC), **www.unic.cnrs-gif.fr/software.html**] and tungsten electrodes (FHC, 2–10 MΩ at 1 kHz) lowered perpendicularly into cortical columns. Signals were amplified (gain 5,000) and filtered for spike activity (0.3–3 kHz). For each recording site, up to two single units were isolated with a template-matching spike sorter (MSD, Alpha-Omega) and a multiunit signal was recorded simultaneously. Consecutive recordings were performed at least 100 μm away from each other, to avoid recording the same unit twice.

Whisker Stimulation

A recently developed whisker stimulation matrix based on piezoelectric benders (Jacob et al. 2010) was used to deflect independently the 24 most caudal whiskers of the right whisker pad (Fig. 1*A*). Whiskers were trimmed to 10-mm length and were inserted 3 mm into small plastic tubes of calibrated diameter glued on each bender. Benders were driven with RC-filtered (tau = 2 ms) voltage pulses (10 ms forward, 10 ms plateau, 10 ms backward motion, followed by a 20-ms rest period), producing resonance-free deflections of 114 μm at 7 mm from the follicle (93°/s initial velocity) delivered at 20 Hz. One

Fig. 1. Sparse noise analysis of cortical receptive fields. *A*: schematic representation of the sparse noise stimulation and forward correlation analysis. Impulse stimulations of each of the 24 whiskers (10 ms forward, 10-ms plateau, 10 ms backward, followed by 20-ms pause) are repeatedly presented in random sequences for caudal and rostral directions. St, Straddler. *B*: example of a neuron recorded in layer IV of the C2 barrel. *Left*: peristimulus time histograms (PSTHs) for 24 whiskers deflected in the caudal and rostral directions. Activity during the blank period with no stimulation is presented in gray at *bottom left*. s.a., Spontaneous activity. Maximum-surprise maps were built by computing for each PSTH the maximum surprise over time and over integration windows (from 1 to 20 ms, *right*). Surprise values are indicated by the color scale. The anatomically defined principal whisker (PW) is symbolized by a black cross. *C*: histogram of the number of whiskers eliciting a significant response for cells in layers II/III ($n = 56$), IV ($n = 36$), Va ($n = 38$), and Vb ($n = 33$) for caudal and rostral directions of whisker deflection, in the case of regular spiking (RSU, *top*) and fast spiking (FSU, *bottom*) units.

hundred and twenty sequences of randomized caudal and rostral deflections of the 24 whiskers were applied, each including a 50-ms blank with no whisker deflection, providing an estimate of the baseline firing rate of the neuron. Simultaneous recording of the spiking activity allowed the reconstruction of the linear receptive field of the recorded neuron with forward correlation techniques. Briefly, a peristimulus time histogram (PSTH, −50, 150 ms around stimulation time) was reconstructed for both caudal and rostral deflections of each of the 24 stimulated whiskers.

Data Analysis

All off-line data analyses were performed with the Python language (**www.python.org**) and its associated scipy and matplotlib scientific toolkits. 3D Weighted Linear regression and circular statistics were implemented with R and rpy (**http://www.rpy.sourceforge.net**).

Regular spiking unit/fast spiking unit classification. On the basis of bimodal distribution of spikes durations, neurons were classified as fast spiking units (FSUs) or regular spiking units (RSUs). In accordance with previous studies (Bruno and Simons 2002), 75% of the cells (n = 163) were classified as RSUs and 25% (n = 39) were classified as FSUs. The analysis presented here was focused only on RSUs.

Determination of receptive field size. As often reported in the barrel cortex (Armstrong-James et al. 1994), we frequently observed in our recordings a low baseline firing rate; 43% of the cells fired <1 spike/s. Classical methods for the detection of significant responses in PSTHs rely on the assumption that PSTHs are continuous Gaussian processes that can be modeled through their mean and variance. However, this hypothesis may lead to erroneous results when the firing rate of the cells is, as here, too low. Here, to correctly detect significant responses in low-firing rate conditions, we devised a method based on surprise analysis (Legéndy and Salcman 1985). This method takes into account the discrete nature of spiking activity by modeling it as a Poisson process. This is particularly important at low firing rates, a situation frequently found in the barrel cortex. A baseline firing rate was calculated by measuring the average firing rate count in the 150 ms starting at the beginning of "nonstimulation" intervals. The surprise (S)—a measure of the unlikeliness of the occurrence of a given firing rate, given the baseline firing rate—was then measured on the PSTH obtained for stimulations of each whisker and each direction. A high value of surprise corresponds to an unlikely activity of the neuron that is a probable functional response of the neuron. In addition, we took into account firing rates changes both below and above the baseline firing rate by combining the Poisson cumulative density function (CDF) and the Poisson survival function (SF), two functions parameterized by the baseline firing rate (f_b): $S(f) = -\log_{10}\{\min[CDF(f, f_b), SF(f, f_b)]\}$.

Finally, in order to take into account different response dynamics (phasic and tonic) without an a priori on the timescale of the actual functional coding taking place, the surprise was estimated on integration windows spanning from 1 to 20 ms, with 1-ms steps.

To define a threshold above which neuronal responses are considered statistically significant, we built for each time bin a surprise threshold value corresponding to a 1% false positive ratio. We built the distribution of surprise values both with no stimulation and on 150 ms after stimulus onset. The threshold was computed such that false positive responses during the blank period would be below 1% of the count during actual whisker deflections (Fig. 2*A*). To obtain a comparable measurement of response strength across bin sizes, the surprise threshold for a given binning was finally subtracted from the corresponding surprise measurement. For a given neuron, we defined a whisker as triggering a significant response when the computed surprise was at any point of the time positive for at least one of the bin sizes. Detected significant responses were in good agreement with visual inspection of the PSTHs, for both cells with low and cells with high firing baseline levels (see Fig. 2*B*). We illustrated in two case

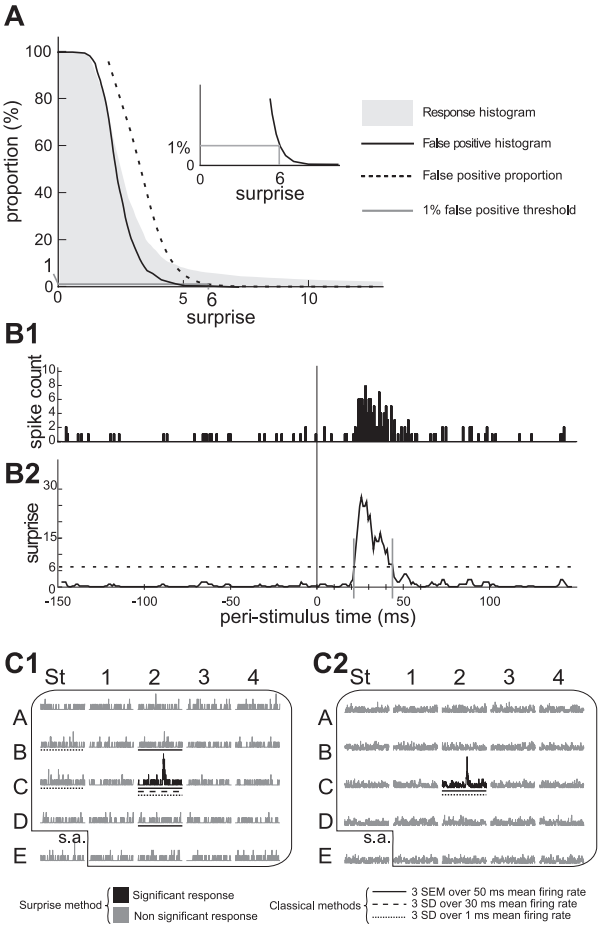

Fig. 2. Surprise method for the detection of significant responses. *A*: determination of the surprise threshold corresponding to a 4-ms integration window. *Inset*: close-up of the determination of the surprise threshold by intersection of the false positive ratio curve. *B*: example of significant responses detection (RSU cell, stimulation of C1 whisker). *B1*: PSTH of response (1-ms bin). *B2*: nonnormalized surprise values over time for a 4-ms integration window. Dashed line corresponds to the 1% false positive threshold. *C*: responses of 2 neurons to rostral deflections of 24 whiskers and comparison of different methods for detection of significant responses. Neuron in *C1* displays a low baseline firing rate, while neuron in *C2* has a higher firing rate. Significant PSTHs detected by the surprise method appear in black; nonsignificant PSTHs are depicted in gray.

studies (Fig. 2*C*) the differences between the surprise method (significant PSTHs are depicted in black) and three classical definitions of a significant sensory response: *1*) the mean response of the neuron on a 30-ms window following stimulus onset goes above a threshold defined as the mean baseline firing rate + 3 SD (significant PSTHs are underlined with a dashed line); *2*) activity in any 1-ms bin goes above mean + 3 SD threshold in a 30-ms window following stimulus onset (significant PSTHs are underlined with a dotted line); *3*) the mean firing rate on a 50-ms window crosses a threshold defined as the mean + 3 SE (significant PSTHs are underlined with a continuous line) (see Jacob et al. 2008).

There are two main differences in the detection of significant responses by these methods versus the surprise method. First, all these classical methods are to some extent tied to the hypothesis that the PSTH can be modeled as a Gaussian process, thus allowing the use of SD or SE to evaluate the firing rate of the neuron. In many cases,

because of the low firing rate observed in barrel cortex neurons, this assumption does not hold, leading to the erroneous detection of significant responses (see, for example, the significant responses detected by *method 2* in Fig. 2*C1*).

Second, these different methods rely on a single binning (e.g., 1 ms, 30 ms, or 50 ms), thus missing responses that do not fit such specific timescales. For instance, very fast responses may be missed by a large bin size (note the response missed by *method 1* in Fig. 2*C2*). In contrast, low-amplitude long responses may be missed by small bin sizes. Such a variety of responses is captured by the multiple bin sizes used in the surprise method.

Response latencies. As in other studies (Armstrong-James et al. 1994; Petersen and Diamond 2000), the response latency was computed across whiskers previously identified as eliciting a significant response by using a dedicated method applied to the few milliseconds between the onset of the stimulation and the beginning of the significant response. To detect the onset of the response, we used the same surprise method as before, but instead of a stringent 1% threshold (which would have resulted in an overestimation of the latencies), we chose a 50% threshold. The latency time for a given bin size was defined as the end time of the first significant bin. The shortest of all these latency measurements was regarded as the whisker latency. Finally, to avoid detecting the onset of small baseline perturbations as the response latency, we made sure that every latency computed with the 50% threshold preceded with 5-ms precision the latency obtained with a 25% threshold (a more stringent measurement of the latency, which brought larger latency estimates). If not, the 25% threshold latency was preferred. Although these thresholds may appear high, they correspond to a false positive rate across the full width of a 150-ms window after stimulus. However, for the calculation of the response latency, the algorithm is used on a much shorter window, going from stimulus onset to response onset (generally $<$20 ms). Within this window, the 25% threshold translates into a 3.3% (20/150 $\times$ 25) false positive error rate.

We compared (Supplemental Fig. S1*A*) our surprise-based latency measurement with the latencies measured with the classical mean + 2 SD method (Foeller et al. 2005; Jacob et al. 2008 for a slightly different method) across all significant neuronal responses obtained in this study.[1] The overall distributions of latencies were similar, although the SD-based latency method failed at low firing rates, resulting in many cases in exceedingly early latency measurements (see case study in Supplemental Fig. S1*B*).

Histology

At the end of the experiments, three small electrolytic lesions (30–50 pulses of 200-ms duration and 10-μA amplitude delivered at 0.3 Hz) were made at known depths, 500 μm apart. The animal was given a lethal dose of pentobarbital (Dolethal) and perfused transcardially with phosphate buffer (0.1 M, pH 7.4) followed by a fixative solution (4% paraformaldehyde in 0.1 M phosphate buffer, pH 7.4). Coronal sections (80-μm width) were cut through the left posteromedial barrel subfield and stained with cresyl violet (n = 10) or with cytochrome oxidase (n = 19) to visualize cortical layers and barrels. The denser staining of L4 combined with the relatively chromogen-free appearance of layers II/III and Va provided a very clear demarcation of the borders between layers II/III and IV and layers IV and Va. From histological examination these borders occurred at a mean depth of 480 μm and 940 μm, respectively. The border between layers Va and Vb was marked by a gradual increase in cytochrome oxidase stain, cell density, and the appearance of larger cell bodies. The transition from layers Va to Vb occurred on average at 1,300 μm.

Electrode tracking and lateral position of recorded cells. Coronal sections were done to unambiguously determine the recording layer. As a consequence, the barrel identity from which the neurons were recorded could not be directly visualized. To recover this information, a functional positioning method was devised. This method relies on the fact that multiunit receptive fields were obtained simultaneously with each cell recording along the electrode track. Each of these multiunit receptive fields was used as the weights in a two-dimensional (2D) grid representing the barrel positions (colored spheres in Fig. 3, *B* and *E*). Such 2D barrel weight grids were positioned vertically in a three-dimensional (3D) space at the recording depth (Fig. 3, *C* and *F*) read on the motorized microelectrode driver (Luigs & Neumann). The weights used for this computation were obtained for a given whisker by taking the maximum of the corresponding surprise value over time (from 0 to 150 ms after stimulation onset) and binning range (1–20 ms) (summing caudal and rostral responses). The weights were then normalized between recordings (the sum of the weights equals 1 for each layer). To estimate the path of the electrode (straight purple line in Fig. 3, *B*, *C*, *E*, and *F*), a weighted least square regression was computed on the 3D distribution of weights. The position of each cell recording within the barrel cortex was finally inferred from this estimated "multiunit" electrode position.

This method was validated by a specific histological control performed on four animals (2 examples are shown in Fig. 3, *A–C* and *D–F*). We recorded multiunit activity at 10 different depths every 100 μm along the electrode track. Animals were then perfused, and the somatosensory cortex was flattened between two microslides. Tangential sections (100 μm) were stained with cytochrome oxidase (histological background in Fig. 3, *A* and *D*) to visualize the layer IV barrels (darker regions) and septa (Land and Simons 1985). Barrel cortices were reconstructed (black outlines in Fig. 3, *A* and *D*) with Neurolucida (MBF Bioscience), and the functional electrode track defined by the method described above was compared with the histologically reconstructed track (green outlines in Fig. 3, *B* and *C* and *E* and *F*). On all four animals and on all recordings, the computed and histologically defined barrel columns were the same.

This functional reconstruction permitted us to determine the anatomic position of our recordings. To avoid any misclassification of layer IV cells between barrel and septum, we considered only those recordings for which the electrolytic lesion was fully within the limits of the cytochrome-rich barrels. All cases in which the electrolytic lesion was in the border between barrels and septa were discarded from further analysis. We targeted the C2 and Straddler barrels, but in some cases, however, recordings were done in another barrel (17%).

Receptive Field Properties

Center of mass. The maximum-surprise map was computed. This grid of values obtained for a given direction of stimulation was used as the set of weights for the computation of the weighted center of the receptive field. This measurement was performed in the rows/arcs coordinates, with the distance between two adjacent barrels/whiskers in a same row or arc defined as the distance unit.

Eccentricity. An eccentricity vector was obtained by linking the center of mass of the receptive field to the whisker defined by the functionally reconstructed position of the recording electrode.

RESULTS

Using a 24-whisker stimulator, we applied deflections in caudal and rostral directions during extracellular recordings of well-isolated (Supplemental Fig. S2) RSUs (n = 163) and FSUs (n = 31). RSUs were subdivided according to their position in the different cortical layers. To characterize the receptive fields of these cells, we used forward correlation techniques and delineated the receptive field corresponding to both directions of stimulation (see MATERIALS AND METHODS and Fig. 1*A*). Among the 163 RSUs, 16% did not respond at all to

[1] Supplemental Material for this article is available online at the Journal website.

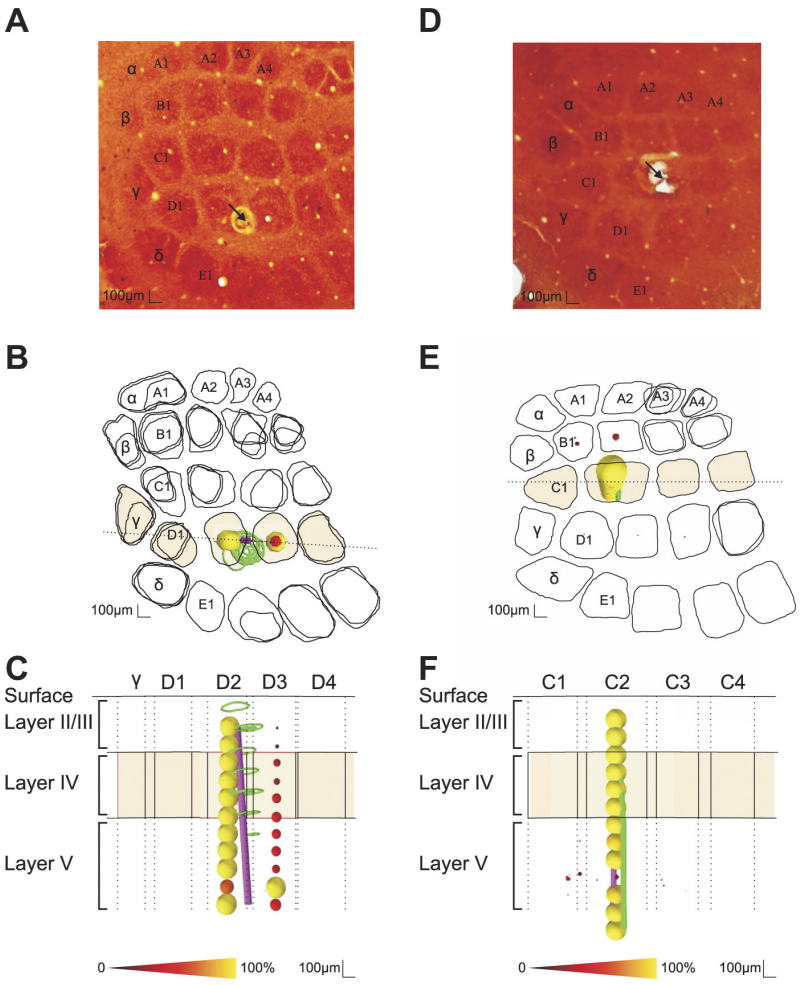

Fig. 3. Functional reconstruction of an electrode track. *A*: photomicrograph of a tangential section at layer IV level with cytochrome oxidase staining and corresponding to the drawings in *B*. *B*: drawings of the barrel field of successive tangential histological slices of the barrel field. The colored barrels correspond to the row of barrels schematized in *A*. *C*: weighted least square fit of a line (purple) with weights provided by the normalized multiunit surprise receptive field at each recording depth (dark red- to yellow-colored spheres). Histological reconstruction of the electrode path using electrolytic lesions is indicated by green lines. Arrow, electrolytic lesion. *D–F*: another example with electrode tracking localized in C2 barrel column. Same convention as *A–C*, respectively.

the sparse noise whisker stimulation (layer II/III: 32%, layer IV: 3%, layer Va: 5%, and layer Vb: 15%). Of the remaining 137 single units that showed significant responses to whisker deflections, 67% responded significantly to the deflection of 2–16 adjacent whiskers (see an example in Fig. 1*B*). The whiskers in multiple-whisker receptive fields were always contiguously located in the mystacial pad.

The distribution of the number of whiskers for which a significant response was elicited per neuron was not different for caudal and rostral receptive fields (Fig. 1*C*, Kolmogorov-Smirnoff test, $P = 0.89$). FSUs displayed receptive field size distributions almost identical to the RSU distribution (Kolmogorov-Smirnoff test, $P = 0.99$). A quantitative examination of the receptive fields obtained with the two deflection directions showed that several of these functional properties were affected by the direction of whisker deflection, including the receptive field size, which is the number of whiskers eliciting a significant response, and the response latencies. Moreover, the well-established link between the functional representation of PW and the anatomic identity of the barrel cortex column from which the recordings were made was also influenced by the direction of whisker deflection.

Relation Between Receptive Field Center and Anatomic Identity of Recorded Barrel is Influenced by Direction of Whisker Deflection

S1 cortex is organized with such a strict anatomic topography (McCasland and Woolsey, 1988; Simons 1978; Woolsey and van der Loos 1970) that the center of a receptive field is thought to provide a reasonable estimate of the location of an electrode within S1 cortex. This observation is often considered as sufficient to conclude that a given cell is located within the barrel column that matches the functionally defined central or principal whisker. However, by comparing the responses to whisker deflection in one direction and the other we have observed that the center of the receptive field defined functionally is not such a good estimate of the anatomic location of the recording site, since it changes with the direction of whisker deflection. To study the link between the center of the receptive field and the anatomic identity of the recording site according to the direction of deflection of the whiskers, we localized the barrel column from which the cells had been recorded in each experiment (see MATERIALS AND METHODS). Cells did not systematically show a significant response to the stimulation of the

whisker corresponding to the recording barrel column (i.e., the anatomic whisker). Two examples are presented in Fig. 4*A*. In Fig. 4*A1*, a neuron recorded in layer IV of barrel C2 showed the strongest response for whisker C3 in the rostral direction and for whisker C2 in the opposite direction. Similarly, in the example shown in Fig. 4*A2* of a neuron recorded in layer Va of the alpha cortical column, the whisker eliciting the strongest response was indeed alpha in the caudal receptive field but beta in the rostral receptive field. These examples illustrate that the PW defined functionally was shifted according to the angle of whisker deflection and was not tied to the position of the anatomic whisker. We quantified the strength of this link to the anatomic whisker by computing the proportion of neurons that displayed a significant response to the anatomic whisker in both directions of stimulation (Fig. 4*B*). This analysis confirmed that layer II/III and layer V RSU neurons have receptive fields only mildly related to the position of the anatomic whisker: only 26% of layer II/II, 31% of layer Va, and 40% of layer Vb included significant responses to the stimulation of the anatomic whisker in both directions. In contrast, FSU neurons and layer IV barrel RSU neurons (respectively 49% and 47% of neurons with anatomic whisker significant for both directions) corresponded more often to the position of the anatomic whisker.

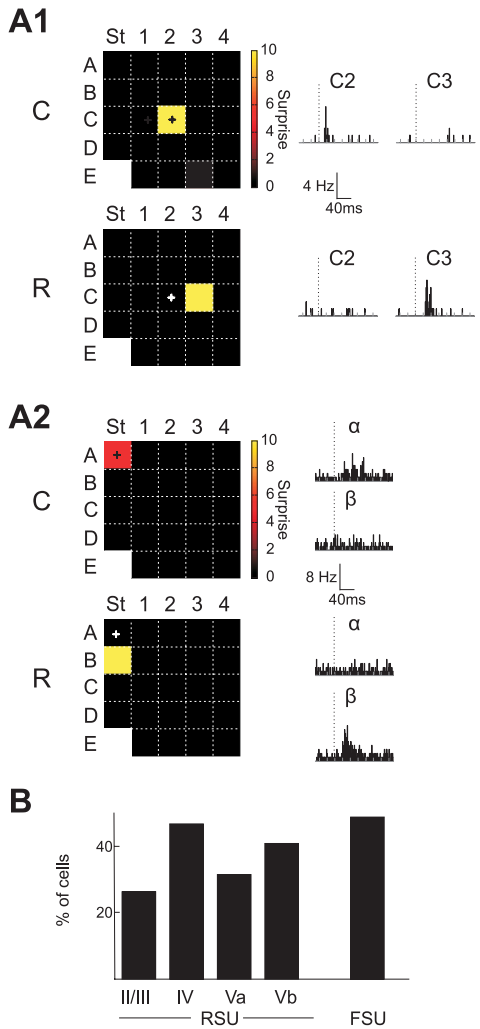

Fig. 4. The functional principal whisker (PW) of cortical receptive fields differed according to the direction of deflection. *A1*: caudal (C) and rostral (R) receptive fields of a layer IV cell. Cross indicates the PW. PSTHs of responses to whiskers C2 and C3 are shown on *right*. *A2*: Same as in *A1* for a layer Vb cell. PSTHs of response to whiskers α and β are shown on *right*. *B*: % of RSU and FSU neurons with shifts in the PW in caudal and rostral receptive fields. Only neurons fulfilling the following 2 conditions were considered: *1*) a significant response to the whisker matching the recorded barrel column in 1 of the receptive fields and *2*) no response to that whisker but to an adjacent whisker (AW) in the other receptive field.

Since we only explored the rostro-caudal axis of deflection and no other angles to which the neuron might respond best, the number of instances in which the anatomically matching whisker did not elicit a significant response might be overestimated. However, our results show that in a certain subset of cortical neurons, particularly in layers II/III and V, the functional definition of the PW is not directly tied to the anatomic position of the neuron.

Receptive Field Size is Modulated by Direction of Whisker Deflection

Receptive field size was measured by counting the number of whiskers eliciting a statistically significant response. Receptive field sizes were quantified for RSUs across all cortical layers as well as for FSUs. As reported previously (Armstrong-James and Fox 1987; Ghazanfar and Nicolelis 1999 Simons 1978), many S1 cortical neurons exhibited a multiwhisker receptive field in our recording conditions. Here we quantified and compared statistically the receptive field size in response to caudal versus rostral deflections. Figure 5*A* shows three typical examples of layer IV and layer Va cells where the number of whiskers eliciting significant responses varied as a function of the direction of whisker movement. For example, *cell 1* exhibited a caudal receptive field of four whiskers, whereas the rostral receptive field of the same neuron showed only two whiskers eliciting significant responses. In some instances, the receptive fields were only partially in correspondence (see *cell 3* in Fig. 5*A*) and, as described before, the PW—the whisker that evoked the strongest response—was not necessarily the same for the two receptive fields of the same neuron. *Cell 2* in Fig. 5*A* is an example of such a case (see also Fig. 1*B*).

To study this difference at the population level, we plotted the distributions of the number of whiskers eliciting a significant response for caudal and rostral deflections for every cortical layer and a joint 2D histogram (Fig. 5*B*). Deviations from the diagonal in this histogram indicate differences in the number of whiskers constituting the caudal and rostral receptive fields. A majority of responsive RSU neurons (93 of 137) displayed a difference in size between caudal and rostral receptive fields. This was the case for 63% (n = 24/38) of layer II/III RSU cells, 63% (n = 22/35) of layer IV RSU cells, 61% (n = 23/36) of layer Va RSUs, and 85% (n = 24/28) of layer Vb RSUs. Similarly, FSUs displayed in 61% (19/31) of the cases a different number of significant whiskers for rostral and caudal stimulations. The distributions of the size of caudal and rostral receptive fields were not significantly different, either for RSU or for FSU neurons (see Fig. 1*C*; RSU: Kolmogorov-

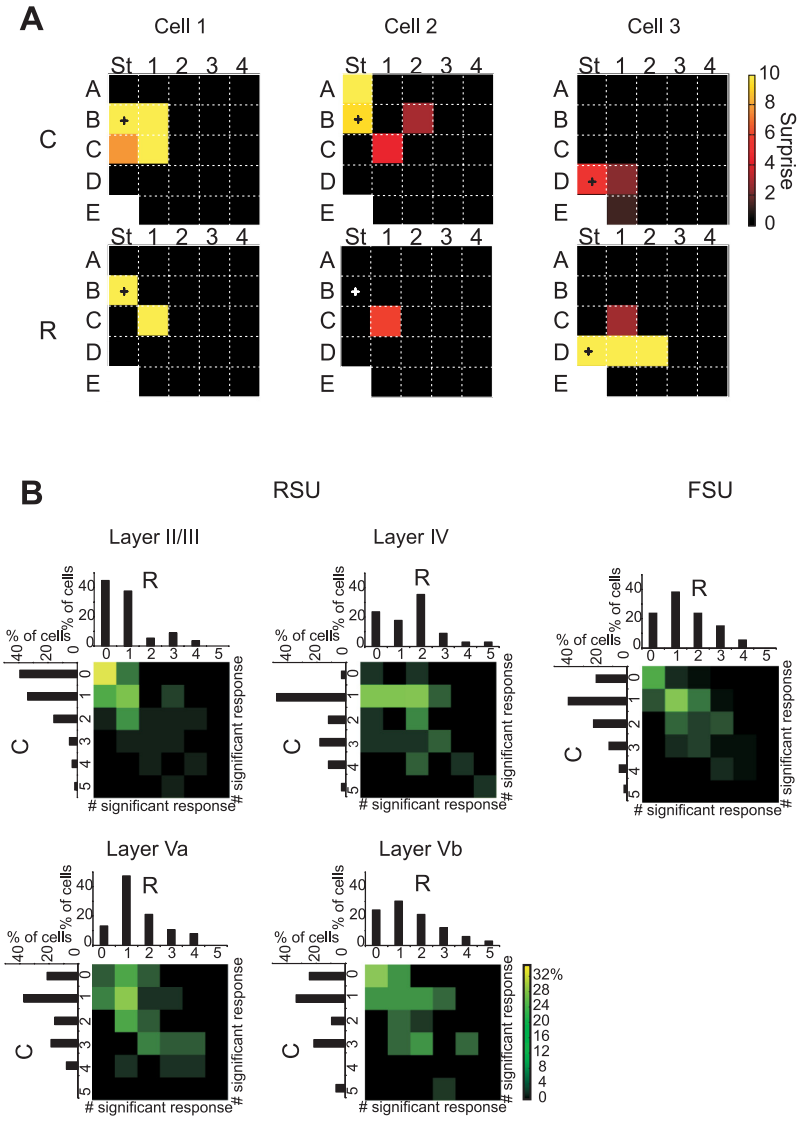

Fig. 5. Size of the receptive field varies with the directions of whisker deflection. *A*: examples of layer IV (*cell 1*) and layer Va (*cell 2* and *cell 3*) RSU receptive fields obtained with caudal (C) and rostral (R) directions of whisker deflection. Same conventions as Fig. 1*B*. *B*: cross-distribution of the number of whiskers eliciting a significant response in caudal vs. rostral receptive fields for RSU neurons in each layer and for all FSU neurons grouped. The proportion of cells is indicated by the color scale.

Smirnoff, $P = 0.89$; FSU: Kolmogorov-Smirnoff test, $P = 0.99$).

Receptive Field Mismatch as Function of Direction of Whisker Deflection

Classically, neurons encountered in a given electrode penetration are maximally activated by the deflection of the same vibrissa, the PW. Other AWs can also activate neurons, but the strength of the response is generally weaker (Simons 1985). This is indeed what we have observed here using one direction of whisker deflection. However, we also observed striking differences between receptive fields of a given neuron determined with caudal and rostral deflections. These differences included, as we have already seen, the number and identity of the whiskers eliciting a significant response, but also the displacement of the receptive field center of mass.

We determined the position of the centers of mass of caudal and rostral receptive fields and calculated the distance between them (see Fig. 6*A* and MATERIALS AND METHODS). A value equal to 1 means that the centers of mass in the two receptive fields were separated by one whisker. The displacement was calculated only for cells showing at least one whisker eliciting significant responses in each receptive field (RSU, $n = 106$; FSU, $n = 29$). Figure 6*A* shows an example RSU neuron with a displacement of the center of mass of 1.13 whiskers. This is because the caudal receptive field includes only whisker C1, whereas the rostral receptive field includes whiskers C2 and C3, introducing an elongation of the receptive field away from C1. Several more examples of caudal and rostral receptive fields for neurons recorded in the different cortical layers are presented in Fig. 6*B*. This figure illustrates on one hand the diversity of multiwhisker cortical receptive fields and on the other hand several examples of shifts of the PW between caudal and rostral

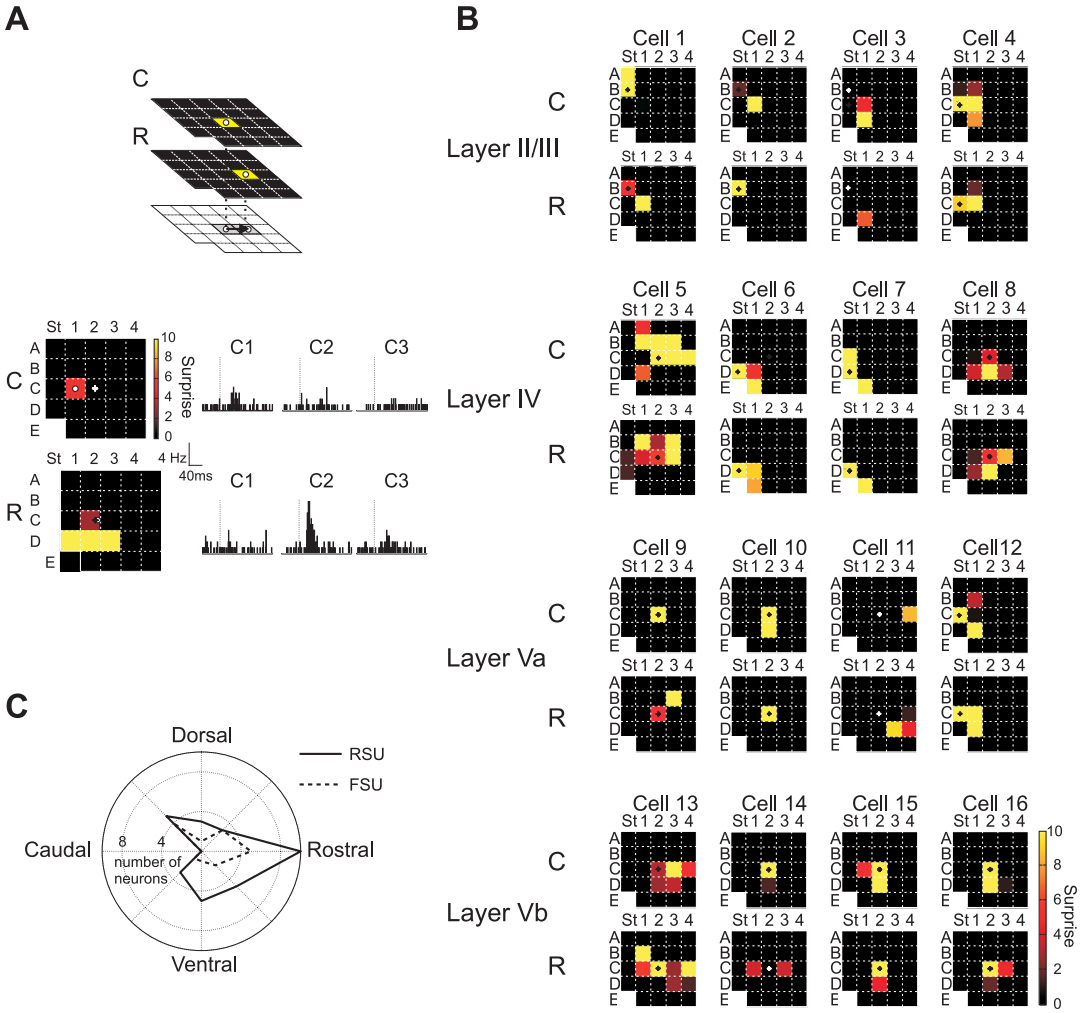

Fig. 6. Quantitative differences between caudal and rostral receptive fields. *A*, *top*: distance vector (black arrow) is computed by linking the center of mass of the caudal (C) and the rostral (R) receptive fields. *Bottom*: example of a layer IV neuron showing a displacement of the center of mass of 1.13 whiskers. Same convention as Fig. 3*B*. Corresponding PSTHs of the significant responses are shown on *right*. Principal whisker C2 is indicated by a cross and the center of mass by a white dot. *B*: caudal and rostral receptive fields of 16 cells recorded across the different layers. Same convention as Fig. 1*B*. *C*: polar distribution of the direction of displacement of the center of mass between rostral and caudal receptive fields. Note the significant bias toward the rostral direction, both for RSUs and FSUs.

receptive fields (see *cells 1*, *2*, *5*, *9*, *11*, *13*, and *14* in Fig. 6*B*). For the other examples presented in Fig. 6*B* the PW is the same for both directions of deflection, although neurons exhibit significant changes in the receptive field structure and span (see, for example, *cells 7*, *8*, *15*, and *16*). The whiskers in multiple-whisker receptive fields were always contiguously located in the mystacial pad.

The distribution of the displacements of the center of mass across the population of recorded neurons is shown in Fig. 7 for the different cortical layers. We observed that 26% (n = 27) of layer II/III, 7% (n = 27) of layer IV, 32% (n = 27) of layer Va, and 18% (n = 25) of layer Vb cells exhibited a displacement of the center of mass of more than one whisker. The mean displacement for RSU neurons was 0.61 ± 0.74 in layer II/III, 0.37 ± 0.39 in layer IV, 0.68 ± 0.63 in layer Va, and 0.61 ± 0.49 in layer Vb. As expected, the displacement was significantly smaller in layer IV compared with layer V (Va and Vb merged vs. IV, Mann-Whitney test, $P < 0.05$). Finally, FSU displacement was also low (0.48 ± 0.55), although not significantly smaller than the displacement of RSU neurons. These results showed that the spatial extent of caudal and rostral receptive fields could be spatially separated. The spatial separation between responses to opposite directions of whisker deflections is reminiscent of the structure of simple cell receptive fields in the primary visual cortex (DeAngelis et al. 1995; see DISCUSSION). These results indicate that the receptive field can shift spatially as a function of the direction of whisker deflection. In addition, the displacement occurring in layer V, but not in other layers, was significantly (Rayleigh test $P < 0.03$) biased toward the horizontal direction, with a circular mean displacement angle of 3.8°. A polar distribution of the motion direction of the center of mass between caudal

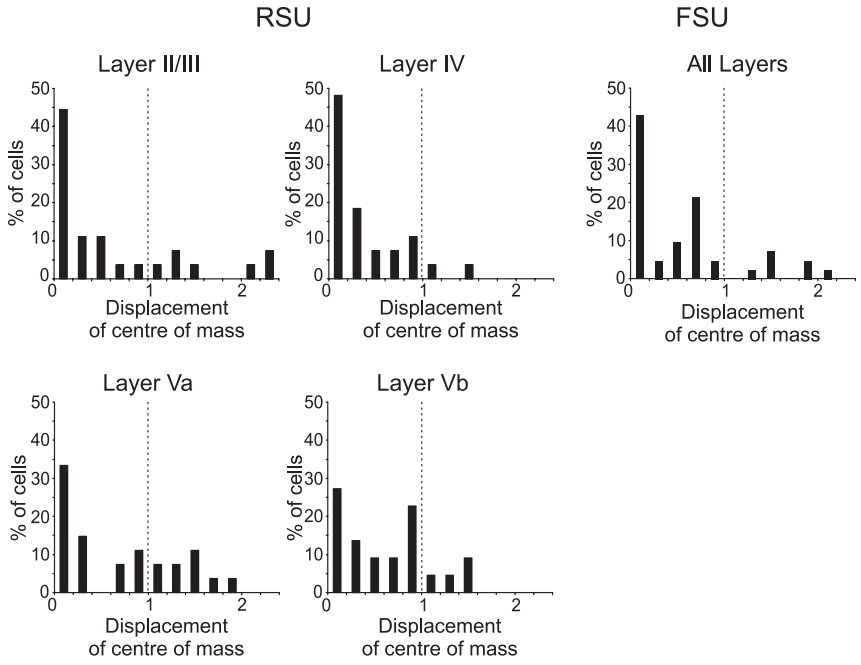

Fig. 7. Caudal and rostral receptive fields can be spatially segregated. Distribution of the distance vector between the center of mass of caudal and rostral receptive fields (layer II/III: $n = 27$, layer IV: $n = 27$, layer Va: $n = 27$ layer Vb: $n = 22$; all FSU: $n = 31$). Dashed line indicates a displacement of 1 whisker. The displacement vector was smaller in layer IV compared with layer V (Va and Vb merged vs. IV, Mann-Whitney test, $P < 0.05$).

and rostral stimulations, with the caudal receptive field as the reference (Fig. 6*C*), illustrates the orientation bias: rostral receptive fields were often more rostrally positioned within the barrel cortex than the corresponding caudal receptive fields. This observation was true both for RSU and for FSU.

The direction-dependent changes in the receptive field structure observed here could have been explained by an "iceberg" effect where a given direction could activate a global inhibitory input that would reduce responses globally to a point where no significant response would be detected. If this were the case, the receptive fields defined with one direction of whisker deflection should always be a shrunken version of the receptive field defined with the other direction. However, we observed many instances where the receptive fields of a given neuron were very dissimilar in shape, such as *cells 13* and *14* in Fig. 6*B*, thus ruling out this possibility as the sole explanation for the changes.

Latency of Responses to PW and AWs Changes in Caudal and Rostral Receptive Fields

Cortical neurons show responses that are selective to the angular direction of whisker deflection (Simons and Carvell 1989; Wilent and Contreras 2005). The angle of whisker movement might be represented also in the cortex by the temporal properties of responses, such as the minimal response latency. Here we determined and compared the response latency for two directions of whisker deflection for the PW and AWs. In this analysis, we took into account only cells with the anatomically matching whisker eliciting a significant response (RSU: $n = 53$; FSU: $n = 16$). For cells with multiple AWs, only the AW eliciting the strongest response was considered (RSU: $n = 40$; FSU: $n = 14$). Latencies were calculated in a time window corresponding to the response of the cells to the first ramp of the stimulus (from 0 to 35 ms). Overall, the latency of PW responses was significantly shorter for FSU than for RSU (Kolmogorov-Smirnoff, $P = 0.007$) when grouping across layers, suggesting that FSUs receive more direct thalamic input than RSUs (Fig. 8*A*). Looking at the effect of the direction of stimulation, we noted that it could impact latency. Two examples of responses to opposite directions of deflections of the PW are presented in Fig. 8*B*. In both cases the shortest response latencies were clearly different, with a gap of several milliseconds. For both PW and AW, large latency differences, up to 12 ms, were often observed (Fig. 8, *D* and *E*). However, differences in latency were highly variable both for PW and AW, and no systematic bias toward one direction was observed.

Finally, the relationship between response latencies for PW and AW pairs for caudal and rostral directions of deflection is depicted for RSUs in layer IV in Fig. 8*C*. PW latencies were significantly shorter than AW latencies for RSUs in layer IV (Mann-Whitney $P = 0.001$) and in layer Va (Mann-Whitney $P = 0.002$), as well as for FSUs grouped across layers (Mann-Whitney $P = 0.02$). In contrast, the difference in latency of response between PW and AWs was significant neither in layer II/III nor in layer Vb for RSU neurons. The noticeable difference in latency values for the PW against the AW in both directions correlates more consistently with the identity of the whisker than with the directions of deflections, even if there is a significant temporal shift in responses for caudal and rostral angles that might be used by the system to represent the direction of whisker movement (but see Kida et al. 2005).

DISCUSSION

Receptive fields of barrel cortex neurons were spatially characterized for two opposite directions of whisker deflection in the caudo-rostral axis by using randomized sequences of 24

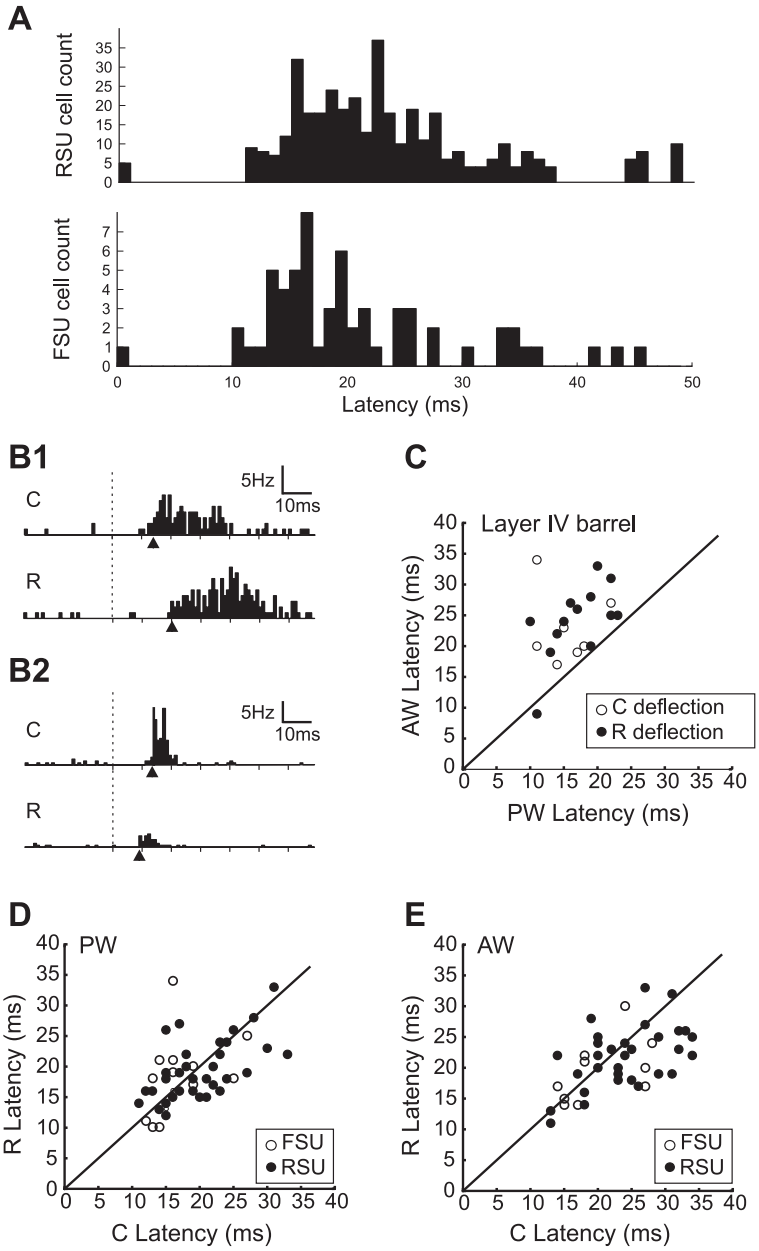

Fig. 8. Latency of responses is affected by the direction of whisker movement. *A*: population histogram of the latency response of the PW for RSU neurons (*top*) and FSU neurons. *B1*: example of a layer II/III RSU cell showing a difference between caudal (C, 10 ms) and rostral (R, 14 ms) latencies for the deflection of the PW. Dashed line indicates the onset of the stimulation. Arrowhead indicates the minimal response latency. *B2*: example of a layer Vb RSU neuron showing a difference between caudal (21 ms) and rostral (14 ms) latencies for the PW. *C*: scatterplot of the PW response latency as a function of the AW response latency for the caudal and the rostral movement. *D* and *E*: scatterplots of the rostral response latency as a function of the caudal response latency for the PW (*D*) and for the AW (*E*).

whisker deflections (sparse noise) and forward correlation analysis. In agreement with previous studies (Armstrong-James and Fox 1987; de Kock et al. 2007; Ghazanfar and Nicolelis 1999; Simons 1978), the majority of cortical neurons (67%) across the different cortical layers, including layer IV, exhibited multiwhisker suprathreshold receptive fields. Moreover, the neuronal responses of RSUs to two opposite directions of whisker deflection show no consistency across the vibrissae that compose the receptive fields (see also Hemelt et al. 2010 for a similar observation in layer IV neurons). Thus the size and position of the group of whiskers on the snout eliciting significant spiking responses was modulated by the direction of whisker movement. In many instances (23% of RSUs), this modulation resulted in a clear spatial separation of caudal and rostral receptive fields. In those cases, we observed a mismatch between the anatomically and the functionally defined PW for one of the directions of whisker movement. In contrast, FSUs showed very similar receptive field structures for the two opposite directions of whisker deflection. The main finding of this work is that several properties of the receptive field of RSUs, such as the size, the response latency, and the center of mass, are stimulus dependent, meaning that they varied as a function of the direction of whisker deflection (see below).

White Noise Analysis and Receptive Field Mapping

In the visual system, a variety of methods have been used to map visual receptive fields quantitatively, from the plot of receptive fields by hand used by Hubel and Wiesel as early as 1962 (Hubel and Wiesel 1962) to line-weighting functions (Field and Tolhurst 1986) and response plane techniques (Palmer and Davis 1981). More recently, sophisticated receptive field mapping approaches have been developed based on the use of a modified version of white noise analysis (i.e., randomized spatiotemporal stimuli). In this approach, a rapid succession of impulse stimuli (spots of light for the visual system or short whisker deflections here) are presented randomly and the spiking activity that results from the stimulation is correlated to the stimulus sequence. This analysis leads to the definition of the transfer function of the recorded neuron and has the advantage of being very efficient in terms of the experimental time needed to explore the receptive field, since the stimuli are presented discontinuously at frequencies usually higher than 20 Hz (see review in DeAngelis et al. 1995 of an application of this analysis to the visual system). In principle, this analysis can provide a full characterization of input-output functions of linear and nonlinear systems (Marmarelis and Marmarelis 1978).

To our best knowledge this is the first attempt to apply such a system-analysis approach to the whisker/barrel cortex system. Applying this approach requires the use of a stimulation device that allows deflecting consecutively most whiskers in a random order. We dispensed such sparse noise stimulation in two opposite directions of whisker movements by using a 24-whisker stimulator (Jacob et al. 2010) centered on whisker C2. We established spatiotemporal receptive fields of well-isolated single neurons across different cortical layers from layer II/III to layer V. Since we integrated the spiking activity over a time window of several tens of milliseconds after the stimulation, we only considered here the 2D spatial projection of the spatiotemporal receptive field. Of particular concern was the possibility that the high-frequency stimulation of adjacent whiskers used here would produce a generalized lateral inhibition that would suppress the activity of the recorded neuron. However, we could determine significant receptive fields for the great majority of the recorded neurons, strongly suggesting that this approach is efficient in obtaining a complete description of the input-output relationship of cortical neurons.

Receptive Field Center is Modulated by Direction of Whisker Deflection

The classical anatomic description of the barrel cortex corresponds to a one-to-one mapping of facial whiskers into layer IV barrels (Woolsey and van der Loos 1970). This anatomic observation is reinforced by functional studies showing that the majority of cortical neurons in layer IV exhibit monowhisker receptive fields (Armstrong-James and Fox, 1987; Simons 1978).

The inverse relationship (the fact that neurons in a barrel column are more sensitive to the corresponding PW) has been often used as an indication of the anatomic identity of the recording site (see, e.g., Kida et al. 2005). At odds with this assertion, we have found that the PW, corresponding to the anatomic barrel column where the cell was recorded from, did not necessarily elicit a significant response. Our results are in agreement with Wright and Fox (2010), who showed that the whisker eliciting the strongest response may often differ from the anatomically defined PW, mainly in layer Va. Similar observations were made by Armstrong-James and Fox (1987), showing by histological analysis that the principal vibrissa was not synonymous with the appropriate vibrissae in 14% of occasions. It must be taken into account that all of the recordings included in our study correspond to barrel column locations and not to septa, where strong influences of several surrounding whiskers are expected.

Difference in Direction Preference for PW and AWs

Barrel cortex cells exhibit direction selectivity in response to PW and AW stimulation (Bruno and Simons 2002; Puccini et al. 2006; Simons 1978; Simons and Carvell 1989; Wilent and Contreras 2005). Several models exist for the relation between the angular preference of the PW and of the AWs in the receptive field. Preferred angles can be correlated, meaning that all whiskers in a receptive field share the same preference, can be anticorrelated where whiskers show opposite angular preference, or may show no particular interdependence. Experimental support for these hypotheses is scarce but has been recently provided. In agreement with the first possibility, Kida et al. (2005) have shown that the direction preference of responses in the rostro-caudal axis to one or multiple AW stimulations is consistent with that of the PW. More recently, Hemelt and colleagues (2010) have reported, however, that most layer IV neurons that respond to several adjacent vibrissae show a wide range of tuning similarity across the receptive field, in support of the third hypothesis. In agreement with that report, we observed here in all cortical layers that the direction selectivity to stimulation of AWs often differed from the direction selectivity of the PW in the rostro-caudal axis. From our data, however, we cannot exclude the anticorrelated hypothesis because we did not study the full direction tuning curve.

Tuning to the direction of whisker deflection has been reported also in thalamic (Brecht and Sakmann 2002a; Minnery and Simons 2003; Shosaku et al. 1985; Timofeeva et al. 2003; Waite 1973) and subthalamic (Bellavance et al. 2010; Furuta et al. 2006) nuclei. Indexes of directionality for the PW are globally decreasing along the whisker-to-cortex pathway, while the impact of AWs is increasing.

Since the cortical direction selectivity in response to PW stimulation most probably derives from converging thalamic inputs (Minnery and Simons 2003) but that of AWs from combined thalamic inputs and intracortical connections (Armstrong-James and Callahan 1991; Fox et al. 2003; Goldreich et al. 1999; Wright and Fox 2010), the processing of information by the two sources do not seem to operate in a coordinate manner to produce similar direction selectivity. Interestingly, cortical FSUs are thought to receive convergent inputs from thalamic cells with various angular preferences (Swadlow and Gusev 2002). As a consequence, their angular tuning is broad and their receptive field is not modulated by the direction of whisker deflection. For RSUs, we observed a laminar difference with stronger modulation of the receptive field structure of nongranular neurons, suggesting that cortico-cortical connections are involved.

The spatial properties of receptive fields we explored here in the barrel cortex could serve, as in the visual cortex, to detect spatial contrasts between stimulations arising in AWs and, consequently, the detection of object edges. For example, it has been reported that the movement of AWs can diverge (Sachdev et al. 2002). During contact with objects, one whisker can move while the adjacent one remains stationary or the two whiskers can simultaneously move in opposite directions. Moreover, one whisker can be maintained in contact with an object while the other is retracted and protracted. In all these situations, responses of a cortical neuron to the movement of the PW in one direction and to an AW in the opposite direction will combine synergistically to produce a maximal response.

In conclusion, our results show that although the whisker-barrel system is somatotopically arranged in functional vertical modules (Woolsey and van der Loos 1970) receiving inputs from the somatotopically corresponding whisker (Welker 1976), the functionally defined receptive field is stimulus dependent. Thus not only the response level but also the spatial structure of S1 receptive fields can differ in a significant way with different input patterns.

ACKNOWLEDGMENTS

We thank V. Ego-Stengel for helpful comments on the manuscript and G. Hucher for helping with the histology.

Present address of V. Jacob: School of Biosciences, Cardiff University, Cardiff CF10 3US, UK.

GRANTS

Supported by CNRS, Agence Nationale de la Recherche (NATACS and TRANSTACT), and EU contracts FACETS (FP6-015879) and BrainScaleS (FP7-269921).

DISCLOSURES

No conflicts of interest, financial or otherwise, are declared by the author(s).

REFERENCES

Armstrong-James M, Callahan CA. Thalamo-cortical processing of vibrissal information in the rat. II. Spatiotemporal convergence in the thalamic ventroposterior medial nucleus (VPm) and its relevance to generation of receptive fields of S1 cortical "barrel" neurones. *J Comp Neurol* 303: 211–224, 1991.

Armstrong-James M, Diamond ME, Ebner FF. An innocuous bias in whisker use in adult rats modifies receptive fields of barrel cortex neurons. *J Neurosci* 14: 6978–6991, 1994.

Armstrong-James M, Fox K. Spatiotemporal convergence and divergence in the rat S1 "barrel" cortex. *J Comp Neurol* 263: 265–281, 1987.

Bellavance MA, Demers M, Deschenes M. Feedforward inhibition determines the angular tuning of vibrissal responses in the principal trigeminal nucleus. *J Neurosci* 30: 1057–1063, 2010.

Bernardo KL, McCasland JS, Woolsey TA. Local axonal trajectories in mouse barrel cortex. *Exp Brain Res* 82: 247–253, 1990a.

Bernardo KL, McCasland JS, Woolsey TA, Strominger RN. Local intra- and interlaminar connections in mouse barrel cortex. *J Comp Neurol* 291: 231–255, 1990b.

Brecht M, Roth A, Sakmann B. Dynamic receptive fields of reconstructed pyramidal cells in layers 3 and 2 of rat somatosensory barrel cortex. *J Physiol* 553: 243–265, 2003.

Brecht M, Sakmann B. Whisker maps of neuronal subclasses of the rat ventral posterior medial thalamus, identified by whole-cell voltage recording and morphological reconstruction. *J Physiol* 538: 495–515, 2002a.

Brecht M, Sakmann B. Dynamic representation of whisker deflection by synaptic potentials in spiny stellate and pyramidal cells in the barrels and septa of layer 4 rat somatosensory cortex. *J Physiol* 543: 49–70, 2002b.

Bruno RM, Simons DJ. Feedforward mechanisms of excitatory and inhibitory cortical receptive fields. *J Neurosci* 22: 10966–10975, 2002.

Chapin JK, Lin CS. Mapping the body representation in the SI cortex of anesthetized and awake rats. *J Comp Neurol* 229: 199–213, 1984.

de Kock CPJ, Bruno RM, Spors H, Sakmann B. Layer- and cell-type-specific suprathreshold stimulus representation in rat primary somatosensory cortex. *J Physiol* 581: 139–154, 2007.

DeAngelis GC, Ohzawa I, Freeman RD. Receptive-field dynamics in the central visual pathways. *Trends Neurosci* 18: 451–458, 1995.

Ego-Stengel V, Mello e Souza T, Jacob V, Shulz DE. Spatiotemporal characteristics of neuronal sensory integration in the barrel cortex of the rat. *J Neurophysiol* 93: 1450–1467, 2005.

Field DJ, Tolhurst DJ. The structure and symmetry of simple-cell receptive-field profiles in the cat's visual cortex. *Proc R Soc Lond B Biol Sci* 228: 379–400, 1986.

Foeller E, Celikel T, Feldman DE. Inhibitory sharpening of receptive fields contributes to whisker map plasticity in rat somatosensory cortex. *J Neurophysiol* 94: 4387–4400, 2005.

Fox K, Wright N, Wallace H, Glazewski S. The origin of cortical surround receptive fields studied in the barrel cortex. *J Neurosci* 23: 8380–8391, 2003.

Furuta T, Nakamura K, Deschenes M. Angular tuning bias of vibrissa-responsive cells in the paralemniscal pathway. *J Neurosci* 26: 10548–10557, 2006.

Ghazanfar AA, Nicolelis MA. Spatiotemporal properties of layer V neurons of the rat primary somatosensory cortex. *Cereb Cortex* 9: 348–361, 1999.

Goldreich D, Kyriazi HT, Simons DJ. Functional independence of layer IV barrels in rodent somatosensory cortex. *J Neurophysiol* 82: 1311–1316, 1999.

Haidarliu S. An anatomically adapted, injury-free headholder for guinea pigs. *Physiol Behav* 60: 111–114, 1996.

Heggelund P. Quantitative studies of the discharge fields of single cells in cat striate cortex. *J Physiol* 373: 277–292, 1986.

Hemelt ME, Kwegyir-Afful EE, Bruno RM, Simons DJ, Keller A. Consistency of angular tuning in the rat vibrissa system. *J Neurophysiol* 104: 3105–3112, 2010.

Hoeflinger BF, Bennett-Clarke CA, Chiaia NL, Killackey HP, Rhoades RW. Patterning of local intracortical projections within the vibrissae. Representation of rat primary somatosensory cortex. *J Comp Neurol* 354: 551–563, 1995.

Hubel DH, Wiesel TN. Receptive fields, binocular interaction and functional architecture in the cat's visual cortex. *J Physiol* 160: 106–154, 1962.

Jacob V, Estebanez L, Cam JL, Tiercelin JY, Parra P, Parésys G, Shulz DE. The matrix: a new tool for probing the whisker-to-barrel system with natural stimuli. *J Neurosci Methods* 189: 65–74, 2010.

Jacob V, Le Cam J, Ego-Stengel V, Shulz DE. Emergent properties of tactile scenes selectively activate barrel cortex neurons. *Neuron* 60: 1112–1125, 2008.

Kida H, Shimegi S, Sato H. Similarity of direction tuning among responses to stimulation of different whiskers in neurons of rat barrel cortex. *J Neurophysiol* 94: 2004–2018, 2005.

Killackey HP. Anatomical evidence for cortical subdivisions based on vertically discrete thalamic projections from the ventral posterior nucleus to cortical barrels in the rat. *Brain Res* 51: 326–331, 1973.

Kim U, Ebner FF. Barrels and septa: separate circuits in rat barrels field cortex. *J Comp Neurol* 408: 489–505, 1999.

Kleinfeld D, Delaney KR. Distributed representation of vibrissa movement in the upper layers of somatosensory cortex revealed with voltage-sensitive dyes. *J Comp Neurol* 375: 89–108, 1996.

Land PW, Simons DJ. Cytochrome oxidase staining in the rat SmI barrel cortex. *J Comp Neurol* 238: 225–235, 1985.

Legéndy CR, Salcman M. Bursts and recurrences of bursts in the spike trains of spontaneously active striate cortex neurons. *J Neurophysiol* 53: 926–939, 1985.

Manns ID, Sakmann B, Brecht M. Sub- and suprathreshold receptive field properties of pyramidal neurones in layers 5a and 5b of rat somatosensory barrel cortex. *J Physiol* 556: 601–622, 2004.

Marmarelis PZ, Marmarelis VZ. *Analysis of Physiological Systems: the White Noise Approach*. New York: Plenum, 1978.

McCasland JS, Woolsey TA. High-resolution 2-deoxyglucose mapping of functional cortical columns in mouse barrel cortex. *J Comp Neurol* 278: 555–569, 1988.

Minnery BS, Simons DJ. Response properties of whisker-associated trigeminothalamic neurons in rat nucleus principalis. *J Neurophysiol* 89: 40–56, 2003.
Moore CI, Nelson SB. Spatio-temporal subthreshold receptive fields in the vibrissa representation of rat primary somatosensory cortex. *J Neurophysiol* 80: 2882–2892, 1998.
Palmer LA, Davis TL. Receptive-field structure in cat striate cortex. *J Neurophysiol* 46: 260–276, 1981.
Petersen RS, Diamond ME. Spatial-temporal distribution of whisker-evoked activity in rat somatosensory cortex and the coding of stimulus location. *J Neurosci* 20: 6135–6143, 2000.
Puccini GD, Compte A, Maravall M. Stimulus dependence of barrel cortex directional selectivity. *PLoS One* 1: e137, 2006.
Sachdev RNS, Sato T, Ebner FF. Divergent movement of adjacent whiskers. *J Neurophysiol* 87: 1440–1448, 2002.
Shosaku A. A comparison of receptive field properties of vibrissa neurons between the rat thalamic reticular and ventro-basal nuclei. *Brain Res* 347: 36–40, 1985.
Simons DJ. Response properties of vibrissa units in rat SI somatosensory neocortex. *J Neurophysiol* 41: 798–820, 1978.
Simons DJ. Temporal and spatial integration in the rat SI vibrissa cortex. *J Neurophysiol* 54: 615–635, 1985.
Simons DJ, Carvell GE. Thalamocortical response transformation in the rat vibrissa/barrel system. *J Neurophysiol* 61: 311–330, 1989.
Swadlow HA, Gusev AG. Receptive-field construction in cortical inhibitory interneurons. *Nat Neurosci* 5: 403–404, 2002.
Timofeeva E, Mérette C, Edmond C, Lavallée P, Deschênes M. A map of angular tuning preference in thalamic barreloids. *J Neurosci* 23: 10717–10723, 2003.
Waite PM. The responses of cells in the rat thalamus to mechanical movements of the whiskers. *J Physiol* 228: 541–561, 1973.
Welker C. Receptive fields of barrels in the somatosensory neocortex of the rat. *J Comp Neurol* 166: 173–189, 1976.
Wilent WB, Contreras D. Dynamics of excitation and inhibition underlying stimulus selectivity in rat somatosensory cortex. *Nat Neurosci* 8: 1364–1370, 2005.
Woolsey TA, der Loos HV. The structural organization of layer IV in the somatosensory region (SI) of mouse cerebral cortex. *Brain Res* 17: 205–242, 1970.
Wright N, Fox K. Origins of cortical layer V surround receptive fields in the rat barrel cortex. *J Neurophysiol* 103: 709–724, 2010.
Zhu JJ, Connors BW. Intrinsic firing patterns and whisker-evoked synaptic responses of neurons in the rat barrel cortex. *J Neurophysiol* 81: 1171–1183, 1999.

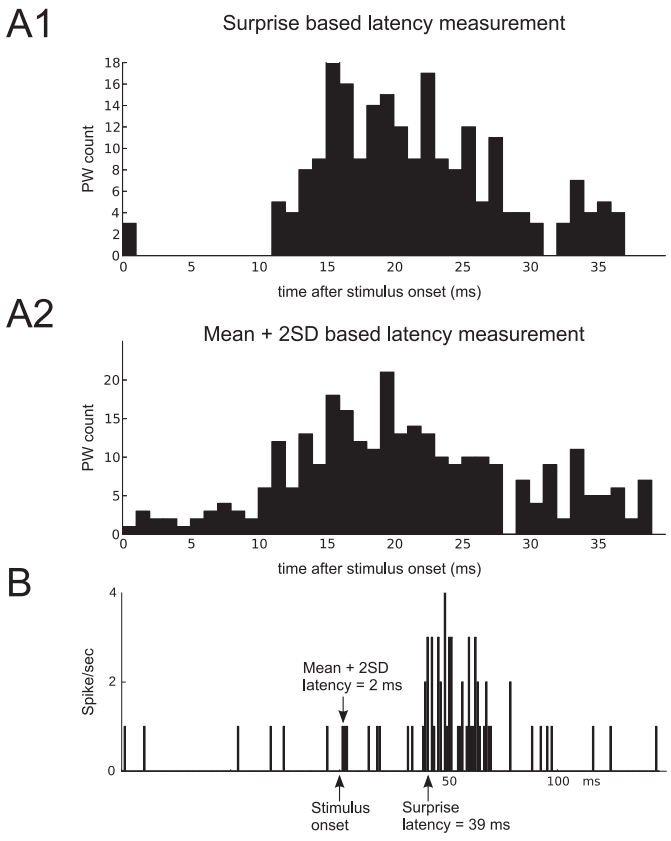

Le Cam et al. Supplementary Figure 1

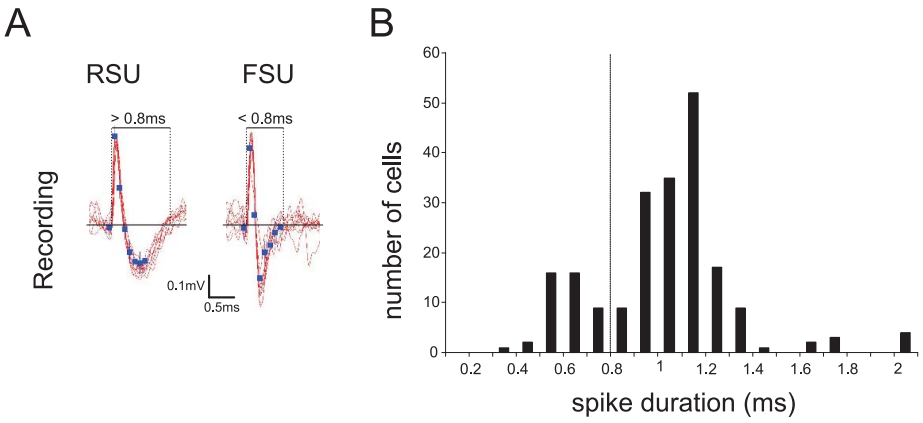

Le Cam et al. Supplementary Figure 2

Supplementary Figure 1. Comparison of latency measurements obtained by a Surprise method and by a traditional mean + SD measurement. (A1) Histogram of all latency measurements, computed with the surprise based measurement (see methods). (A2) Histogram of all latency measurements, computed as the first time the PSTH reaches a value above the prestimulus mean firing rate + 2SD, on two consecutive bins. Note the many latency estimates lower than 5ms when using this method. (B) Case study. Low firing rate leads to spurious latency measurements by the mean + 2SD method, in contrast with the Surprise method.

Supplementary Figure 2. Distinction of RSU and FSU neurons based on the shape of the extracellularly recorded spike. (A) Spike shapes of RSU (left) and FSU (right) neurons. Notice the slower rebound observed in the case of RSU neurons. (B) Population histogram of spike duration across all neurons. We clusted RSU (large spike duration) and FSU neurons (small spike duration) on the basis of this bimodal distribution (vertical line: threshold).

Chapter 4

Non-linear facilitations and suppressions in barrel cortex neurons support context-dependent cortical processing

In contrast with barrel cortex linear filters, non-linear interactions in this cortex have striking functional implications, ranging from strong suppression up to clear facilitation of the neurons functional responses. Here we review the diversity of these non-linear interactions as characterized by stimulating subsets of whiskers in passive (anaesthetized/paralysed) rat preparations. So far, all studies of barrel cortex non-linearities have been carried in the context of a forward correlation approach (meaning PSTH based) by studying the difference between functional responses to independent versus synchronous or dephased stimulations of a set of whiskers (up to 6). The reported non-linearities are the difference between the linear summation of the responses to independent stimulation of each studied whisker versus the actual response to a combination in time of their deflections. Interactions are "suppressive" when the the actual response is surpassed by the linear sum, and "facilitative" in the opposite situation.

4.1 Barrel cortex functional responses depend non-linearly on the time sequence of whisker deflections

4.1.1 A dominant suppressive interaction

Initial studies of this phenomenon have been carried in the awake paralysed rat [Simons, 1985] and subsequently in layer IV neurons recorded in the fentanyl anaesthetized rat [Simons and Carvell, 1989]. These works have looked at how the functional response to a 7 ms long, 11° amplitude ramp and hold deflection applied on the principal whisker (PW) is affected by applying an earlier (identical) stimulation on one of the adjacent whiskers and by varying the inter-stimulus interval (ISI) from 0 ms to 100 ms. In these two studies,

PW responses were generally suppressed by the preceding stimulation, with the strongest suppression occurring at 10 ms and 20 ms ISI: for this delay, up to 55% of the recorded units were suppressed (meaning that an 45% of the neurons were either unaffected or facilitated by this protocol).

In addition, in a subset of neurons (3% of barrel cortex regular spiking units), 50 ms ISI and larger ISI resulted in a clear facilitation of the functional response. However, no other facilitations were reported in these studies.

In good match with these initial studies, other works have reproduced the full suppression curve [Boloori and Stanley, 2006] or have focused on the properties of barrel cortex neurons at 20 ms ISI, the stimulation delay that lead to suppression in the largest possible population of barrel cortex neurons [Higley and Contreras, 2005]. More recently, a similar ISI approach was used to build a quantitative model of the response of a barrel cortex neuron to sequential PW impulse deflections (combined with the neuron tuning curve for stimulus amplitude). In this case where consecutive stimulations were applied on the same whisker and not on adjacent whiskers, a strong suppression was also observed, followed by facilitative ISI. However, there, suppressive ISI extended on a much larger duration (from around 10 ms up to 90 ms) and the follow-up facilitation was stronger and more consistent across the recorded pool of neurons [Boloori et al., 2010].

4.1.2 Functional responses are facilitated at shorter ISI

However, further study of the AW→PW ISI paradigm showed that not only are barrel cortex neurons response to PW suppressed by preceding stimulations of one AW, but they may also be enhanced. Indeed, shorter ISI (from 5 ms to 0 ms) resulted in a facilitation of the functional response in 69% of layer II/III, in 15% of layer IV and in 24% of the layer V barrel cortex neurons recorded in the barrel cortex of lightly (1.25 mg/kg) urethane anaesthetized rats [Shimegi et al., 1999, 2000]. More recently, at a different frequency of stimulation, a comparable protocol has been carried out [Ego-Stengel et al., 2005] using slightly deeper urethane anaesthetized rats (1.5 mg/kg). Although not coherent with [Shimegi et al., 1999] regarding the proportion of suppression/facilitation across layers, this work also found both facilitation (11% in layer II/III, 20% in layer IV, 7% in layer V, there, fig. 13.a) and suppression (5% in layer II/III, 30% in layer IV, 40% in layer V) of functional responses in the AW→PW ISI paradigm. In addition, the ISI corresponding to the peaks in facilitation turned out to be comparable across studies, with only short ISI triggering facilitation across layers (3 to 10 ms ISI) except in layer V where a wide distribution of ISI from 0 to 40 ms could result in facilitation in both studies.

However, when performing control analysis with the same *ad hoc* criterion as [Shimegi et al., 1999] (the so called "facilitation index"), [Ego-Stengel et al., 2005] found a much more comparable proportions of facilitation across experiments, while when using a more rigorous statistical measurement (the classical condition-test ratio [Simons, 1985; Simons and Carvell, 1989]), the proportion of facilitation observed in the population was strongly reduced, thus suggesting that the large proportion of facilitation reported in [Shimegi et al., 1999, 2000] may be overestimated due to the lack of a well defined statistical analysis in this study.

4.1.3 Intracellular recordings suggest a competition between a divisive and an additive mechanism

Initial intracellular sharp recordings carried in the awake paralysed rat with again the same protocol suggested that single whisker deflections result in an EPSP (Excitatory

Post-Synaptic Potential) followed by an prolonged hyperpolarization of the membrane potential, thus making it harder for the EPSP triggered by an additional whisker deflection to result in a spike [Carvell and Simons, 1988].

However, a more recent intracellular study in the deeply isoflurane anaesthetized rat proposes a different subthreshold mechanism for AW→PW facilitation and suppression [Higley and Contreras, 2005]. In this study, whisker stimulations were also found to trigger an EPSP, followed by a slow hyperpolarization. However, in contrast with the previous study, here, suppression of the PW response was shown to be mainly due to the division of the amplitude of the response to the PW with respect to the response to an isolated PW stimulation (average division by 2.42), and not due to an hyperpolarization of the V_m: on average, the membrane potential was actually *depolarized* and not hyperpolarized at the time of the second ("test") whisker stimulation.

In the same study, the response to a 3 ms AW→PW ISI was examined. There, similar to the 20 ms ISI, the PW stimulation was divided (in this case by 2.8 on average) and seated on top of the depolarized membrane potential resulting from the preceding the AW stimulation. However, at this 3 ms ISI, the membrane potential was much more depolarized than for a 20 ms ISI with respect to baseline V_m (on average 73% of the depolarization induced by an independent PW stimulation). As a consequence, neurons responded to the PW stimulation either in a linear fashion or in a supralinear manner. Such combination of EPSP with the ongoing membrane potential may fit with the general mechanism for EPSP summation in the barrel cortex. Indeed, in this cortex, the amplitude of EPSPs was shown to be linearly proportional to the value of the ongoing V_m [Wilent and Contreras, 2005; Crochet et al., 2011], including when the ongoing V_m value was sitting on top of a membrane potential set by an EPSP from a previous deflection of the same whisker [Crochet et al., 2011].

4.2 Non-linear interactions are amplified by increasing the number of stimulated whiskers

4.2.1 Even remote whiskers strongly impact responses to consecutive PW stimulations

What is the spatial extent of the whiskers involved by such non-linear interaction ? Barrel cortex neurons have been shown to receive EPSP in response to the deflection of virtually any of the rat whiskerpad vibrissae [Moore and Nelson, 1998; Brecht and Sakmann, 2002; Brecht et al., 2003; Manns et al., 2004]. To test the involvement of theses remote vibrissae in the non-linear processing of whisker stimulations, a group of whiskers 2 rows or 2 arcs away from the PW was stimulated by piezoelectric actuators [Brumberg et al., 1999] or an air puff [Higley and Contreras, 2003]. This stimulation turned out to affect non-linearly the PW response to the same extent as a similar stimulation of whiskers immediately adjacent to the PW. Subthreshold EPSPs resulting from remote versus adjacent whisker stimulations were also highly comparable in time course and amplitude [Higley and Contreras, 2003]. Such results show that barrel cortex non-linearities span over the whole whiskerpad. They also suggest that even remote parts of the whiskerpad have a prominent role in the non-linear processing carried by barrel cortex neurons. Non-linear processing should thus (also) be studied at this whiskerpad wide scale.

4.2.2 Most multiwhisker stimulations lead to the suppression of PW functional responses

The first strategy used to study the properties of multiwhisker non-linearities was to focus on their spatial spread, regardless of any precise stimulus timing. Such a study was carried by producing a centre-surround situation where a principal whisker was stimulated with a ramp and hold deflections, in contrast with the 4 adjacent whiskers that were stimulated with an identical dorsoventral white noise (noise with an uneven power spectrum) [Brumberg et al., 1996]. This stimulus resulted in a strong suppression of the response to the PW. A follow-up study found that such stimulation of all adjacent whiskers with common noise has a limited impact in layer II/III, but a much stronger one in layer IV and V [Brumberg et al., 1999].

The effect of this surround white noise protocol seems actually highly comparable to the impact of a progressive reduction of the ISI used during the acquisition of receptive fields across multiple whiskers using a sparse protocole. This experiment has been reported in the literature for two ISI (5 s and 0.1 s, [Hirata and Castro-Alamancos, 2008]) and that we tested for several shorter ISI (50 ms, 30 ms, 18 ms 11 ms, 7 ms, 4 ms. see fig. 3.1). Indeed, large functional responses were observed when no white noise was applied on surround whisker as well as during the acquisition of the receptive field with long ISI. When white noise was applied/when the ISI was decreased, these receptive fields turned spatially smaller and remaining functional responses were smaller.

Actually, these two protocols (sparse→dense and white noise) are fundamentally similar in their design: in both cases, an independent PW stimulation situation (because there is no white noise stimulus in the surround or because the ISI is so large that stimulation on different whiskers do not interact) is compared with a situation where this same PW stimulus is combined with randomly occurring whisker deflections in the surround (white noise or densely packed dirac deflections randomly occurring across surround whiskers for receptive field acquition). We argue that to explain these two results, it could be sufficient to consider the same ISI-dependent mechanism that is engaged by AW→PW 2 whiskers non-linear interactions. Indeed, when faced with random surround stimulations (read: dense PW-AW whisker stimulations with equal probability of occurrence for any ISI), such non-linear interactions will result in a systematic global suppression of the functional response due to the comparatively much smaller range of ISI that resulted in a facilitation versus suppression in the AW→PW interaction curve.

4.2.3 Simultaneous multiwhisker stimulations lead to large increases in firing rate in a subset of neurons

As we have just seen, random patterns of multiwhisker stimulations (such as white noise or dense random stimulations) result regardless of their precise temporal sequence in a reduction of the extent and strength of the neurons functional response. Still, based on the model previously obtained for AW→PW 2 whiskers non-linear interactions, other patterns of multiwhisker stimulation should result in facilitation (for instance multiwhisker stimuli that concentrate AW-PW ISIs in the 0-5 ms facilitative range for all whiskers).

Several studies have indeed attempted to better control the timing of multiwhisker deflection. All such studies have been carried under 1.5 mg/kg urethane anaesthesia and have opted for identical and synchronous deflection of all surround whiskers as a manner to limit the dimensionality of the stimulus.

When performing such synchonous multiwhisker stimulations, multiunit activity was always a subliminal summation of the functional response to independent functional re-

sponse [Mirabella et al., 2001]. In contrast, single unit responses always revealed in a proportion of neurons either a multiwhisker response stronger than the PW response [Hirata and Castro-Alamancos, 2008; Brecht and Sakmann, 2002; Manns et al., 2004], or even a multiwhisker response stronger than the sum of independent responses to all stimulated whiskers (supralinear responses [Ghazanfar and Nicolelis, 1997]). In addition, such simultaneous multiwhisker stimulations resulted in shorter latencies and sharper subthreshold EPSPs, as well as a deeper post-EPSP hyperpolarization [Hirata and Castro-Alamancos, 2008]. As for 2-whisker interactions, the proportion of "supra-PW" neurons (neurons that show a response to a multi-whisker deflection that is stronger than the response to the PW alone) differed across cortical layers: few neurons showed multiwhisker facilitation in layer II/III [Brecht et al., 2003] in contrast with layer IV where a majority of barrel pyramidal neurons were facilitated [Brecht and Sakmann, 2002; Hirata and Castro-Alamancos, 2008] (if layer IV is the 500 μm to 900 μm deep cortical layer), while septum neurons were not [Brecht and Sakmann, 2002].

Finally, a comparable proportion of supralinear and infralinear neurons were found in layer V [Ghazanfar and Nicolelis, 1997; Manns et al., 2004] where striking case studies demonstrate the presence in this layer of neurons that have almost no functional response to independent whisker stimulations and a strong response to synchronous deflections of several whiskers at a time [Ghazanfar and Nicolelis, 1997].

As predicted by the AW→PW ISI non-linearity curve, the enhancement of the principal whisker functional response was dependent on the precise coincidence of the multiple whisker stimulations. As soon as delays were introduced in the whisker stimulation, the PW response went back to a reduced response [Hirata and Castro-Alamancos, 2008], an observation that comes to support our hypothesis that multiwhisker non-linear interactions are carried by the same set of subthreshold mechanisms as 2-whiskers non-linear interactions.

4.3 Non-linear multiwhisker interactions may be involved in higher order barrel cortex processing

Due to the non-linearity of their response to multiwhisker stimulations, barrel cortex neurons respond in markedly different manners to different multiwhisker stimulation time courses. If coupled with the asymmetric spatial structure of their linear receptive fields [Simons, 1985; Le Cam et al., 2011], such non-linearities could explain the demonstrated selectivities for the direction [Jacob et al., 2008] (by taking into account non-linearities beyond the second order, see discussion therein) and onset [Drew and Feldman, 2007] of a multiwhisker stimulus that mimics the displacement of a rod through the whiskerpad.

Barrel cortex neurons nonlinear functional responses to multiwhisker stimulation could also be the basis of a stimulus "context-dependent" change in their processing properties. Indeed, the statistical properties of two tactile stimuli such as an homogeneously textured wall and the edge of a bar are largely different on many respect.

In the visual system, such effects have been demonstrated when going from a spatially unstructured white noise to a spatially structured natural image. Indeed, going from the first to the second stimulus resulted in the appearance of a marked antagonist surround in the receptive field of these neurons [Lesica et al., 2007] and lead to a strong increase in the sharpness and time precision of EPSPs [Vinje and Gallant, 2002; Baudot, 2006; El Boustani et al., 2009] and in the reliability of much sparser spike trains across stimulus repetitions [Baudot, 2006; Haider et al., 2010].

We hypothesized that similar context-dependent processing indeed takes place in the barrel cortex when it is submitted to changing stimulus statistics. Since natural multi-whisker stimulations are not sufficiently characterized at the moment, we studied the response of barrel cortex neurons to white noise stimulations across the 24 largest whiskers of the rat by the mean of reverse correlation analysis, and we changed the large scale statistics of the input by increasing the level of interwhisker correlation in the stimulation.

The impact of this 'toy' change of sensory statistics on the processing carried by barrel cortex neurons is presented in the following manuscript - currently undergoing a major revision at Nature Neuroscience.

Chapter 4 will appear shortly in a scientific journal

Chapter 5

A topographical organization for barrel cortex neurons tunings

The intracortical connectivity of pyramidal neurons decreases strongly with increasing distance to the soma (with a 100 µm characteristic distance) as seen in the rat S1 cortex using simultaneous patch clamp recordings [Lefort et al., 2009; Perin et al., 2011] as well as using glutamate uncaging connectivity mapping [Bureau et al., 2006].

Such dominance of local connectivity results in neighbouring cortical cells being key contributors to the processing carried by any given neurons. Thus, the identification of any rule that structures the functional properties of these neighbourhood neurons is extremely useful to the understanding of the sensory processing carried by cortical neurons.

In particular, the identification of the spatial organization of tunings on the cortical volume (so called "sensory maps") makes it possible to study the cortical processing with a good knwoledge of the neurons functional inputs.

For instance, in the cat V1 cortex, a strikingly accurate and systematic topographical organization of orientation tuning — including sharp 'pinwheel' singularities — has been observed [Hubel and Wiesel, 1963; Bonhoeffer et al., 1991; Ohki et al., 2006]. In this cortical area, this knowledge of the spatial organization of orientation tunings has allowed the comparison of the processing carried by functionally homologous neurons, but that receive input either from an homogeneous or from heterogeneous set of inputs. This has been achieved by recording neurons with comparable tunings, either at a "smooth" position in the orientation map, or near the centre of a pinwheel singularity, where nearby neurons have extremely different orientation tunings [Marino et al., 2005; Nauhaus et al., 2008].

In a similar fashion, any accurate mapping that would be present in the barrel cortex may be key to unveil some of the processing performed by the neurons of this cortical area.

5.1 Introduction

5.1.1 The whisker to barrel topy

The dominant topy in the barrel cortex — as in the visual cortex — is the direct mapping of the spatial extend of the peripheral sensory apparatus into the cortical surface: retinotopy in the case of the visual cortex, and the faithfully mapping of the whiskerpad onto the

barrel cortex in the case of the whisker system (compare whiskers in fig 1.1.a and barrels in layer IV of the barrel cortex in fig 1.1.b).

In contrast with the continuum of V1 retinotopy, this barrel cortex mapping is spotted: blobs — the barrels — receiving a dominant input from the dorso-medial area of the VPM (and from the POm in layer V) are separated by areas that receive their input from the ventrolateral VPM (see review in [Diamond et al., 2008]). However, if in terms of anatomy the barrel/septum map is striking, it is not as much the case in terms of functional properties: it is hard to tell if a neuron pertains to the barrel or to the septum on the sole basis of its linear receptive field.

Indeed, in one hand, layer IV septum neurons show broad receptive fields and they lack a well defined dominant whisker, at least in the urethane anaesthetize rat [Brecht and Sakmann, 2002]. Similarly broad receptive fields with a limited principal whisker response were also generally observed in septum related neurons of layer II/III, as recorded in urethane anaesthetized rats [Brecht et al., 2003]. Such receptive fields properties match well with the wide receptive fields of the dominant input to septa: POm [Koralek et al., 1988; Yu et al., 2006].

However, in the other hand, although barrel neurons have been classically reported as responding chiefly to a single, principal whisker both in the in-vivo [Simons, 1978] and in the slice preparation [Petersen and Sakmann, 2000, 2001], such reduced receptive fields have not been observed consistently. Indeed, in many other studies (including ours, see Chapter 3), barrel cortex layer IV neurons responded to the stimulations of several adjacent whiskers [Chapin, 1986; Ghazanfar and Nicolelis, 1999; Jacob et al., 2008] and were hard to squarely distinguish from septal receptive fields.

Thus, overall, the anatomical split that can be noted in layer IV of the barrel cortex does not seem to be complemented by a comparably strong functional devide in the response to whisker stimulations.

5.1.2 A directional tuning topy in the barrel

An additional dimension of the barrel cortex feature space is whisker direction of deflection [Simons, 1978]. Sharp tuning within this sensory dimension are often reported as being widely shared by neurons across layers [Simons, 1978; Lee and Simons, 2004; Kida et al., 2005] but systematic evaluations of the proportion of significantly tuned neurons are scarce and yield contradictory results: in the same condition (isoflurane anaesthetized juvenile rats) and with the same technique (two photon imaging in layer II/III) one study found that only 21% of barrel cells and 15% of septum cells were direction tuned [Kerr et al., 2007], while another observed a significant tuning in 79% of barrel cortex neurons [Kremer et al., 2011].

Still, the potential mapping of the tunings to this additional stimulus dimension on the barrel cortex surface has been explored by several studies. Initial electrophysiology recordings coupled with histological reconstructions of barrel cortex border suggested in fentanyl anaesthetized adult rats that clusters of nearby layer IV neurons share similar directional tuning [Bruno et al., 2003], although in this study the directional tuning of adjacent neurons was not correlated. A followup study looked both at layers II/III and IV with similar methods, using isoflurane anaesthetized adult rat grown in an enriched environment. In that particular study, a weak radial mapping of the directional tuning was observed in neurons of layer II/III, but not in layer IV [Andermann and Moore, 2006]: in layer II/III, a correlation was observed between the preferred direction of PW deflection and the position of the neuron with respect to the centre of the barrel.

More recently, the development of two-photon [Denk et al., 1990] calcium imaging of the local neuronal network spiking activity [Stosiek et al., 2003] has brought a valuable method to explore the spatial organization of functional tunings. This attractive method has been successfully applied to the exploration of potential mappings present in superficial layers of the visual [Ohki et al., 2005, 2006], auditory [Rothschild et al., 2010], piriform (olfactory) [Stettler and Axel, 2009] and gustatory cortex.In the latter case, this method revealed a clear spatial split of the areas devoted to the different basic tastes [Chen et al., 2011].

Similar to the work on these different cortices, efforts have also been undertaken to image the spatial organization of S1 cortex barrel neurons with respect to their direction tuning. Remarkably, a first two-photon study of this direction mapping in juvenile isoflurane anesthetized rats didn't show the expected, instead revealing a spatially disorganized layer II/III with respect to directional tuning [Kerr et al., 2007]. However, more recently, an additional study has shown that a certain level of radial organization of the neurons in function of their direction tuning is present in the layer II/III of adult rats, but not in juveniles [Kremer et al., 2011]. Such unexpectedly late emergence of the directional mapping is likely to be the reason for the diverging observation made across electrophysiology and two-photon based studies of this property.

5.1.3 Barrel cortex neurons tuning: beyond direction

In the previous chapter (see Article 3), we have explored the linear filters that best trigger spiking activity in barrel cortex neurons when applied in the rostrocaudal orientation. We have shown that across all studied neurons, these optimal linear filters are part of a common *phase* space that is sufficient to capture 76% of their variance (see Article 3, fig. 1 as well as fig 5.4.a of this chapter). Similar to the direction of whisker deflection, this additional stimulus dimension - orthogonal to the direction of stimulation (see fig 5.4.b) - is encoded in a sharp manner by a subset of highly selective neurons (so called 'simple cells' in our work) but also modulates in a limited way the firing of most other neurons ('complex cells'). We hypothesize that the network mechanisms engaged in the buildup of phase selectivity may be the same as those involved in direction selectivity, with the excitatory component of the sensory response being constant and the tuning of the neuron spiking output being solely modulated by a direction (and phase ?) dependent delay of the inhibitory component [Wilent and Contreras, 2005].

In the same study, we also observed another, *high order* dimension of the sensory space to which barrel cortex neurons are tuned: inter-whisker correlation (see Article 3, fig. 3). Indeed, we found that two different populations of neurons were either sensitive only to correlated stimulations at the scale of the whiskerpad ('global' neurons), or to uncorrelated stimulus as well as local contrasts ('local' neurons).

These two additional barrel cortex neurons tunings (phase and local/global) were strong in our hands and may thus be good candidates for a spatial mapping, at least not less than the tuning to the direction of deflection.

To explore in the barrel cortex the presence of spatial maps in response to this widened stimulus space (from direction of deflection up to phase/orientation/correlation), we carried in collaboration with Julien Bertherat (a PhD student, École Normale Supérieure, also co-directed by Laurent Bourdieu and Daniel Shulz) a two-photon calcium imaging study of the functional response of barrel cortex layer II/III neurons during a whiskerpad-wide systematic forward correlation exploration of (1) two orthogonal orientations (the rotro-caudal and ventrodorsal axes), (2) four cardinal phases for each orientation (3) two

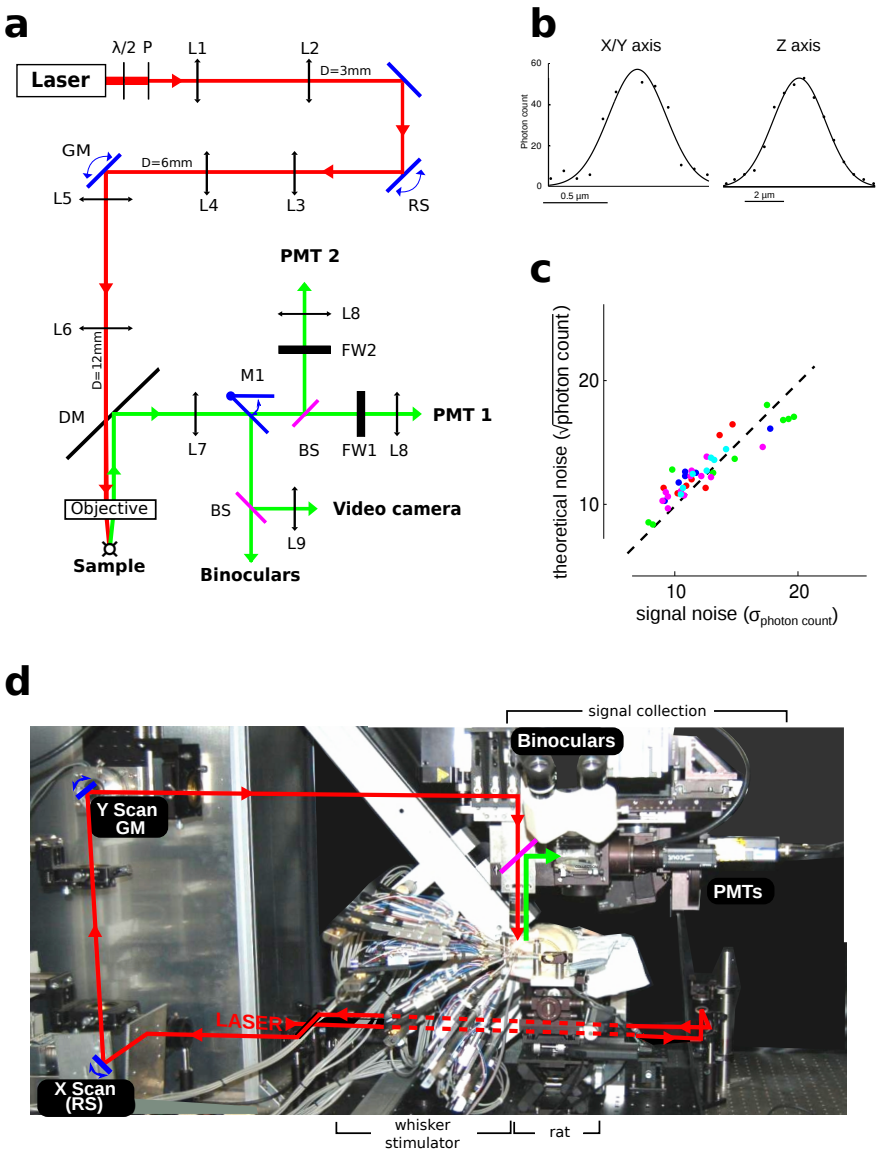

Figure 5.1 – A custom made two-photon microscope. (a) optical schematic of the microscope. Red path: femtosecond pulsed IR excitation beam generated by the laser. Green path: fluorescence collection path aiming at photon counting photomultipliers 1 and 2 ("PMT1" and "PMT2"). Mirrors are in blue. RS: Resonant Scanner (horizontal scan). GM: Galvanometric Mirror (vertical scan). M1: retractable mirror to switch between PMT and binocular collection paths. DM: Dichroic mirror (to separate the excitation and collection paths). BS: Beam spliter. $\lambda/2$: Motorized wave plate (tunes laser power). P: polarizer. L1-L9: lenses. FW: filter wheel holding OGB1 and SR101 selective filters. (b) X/Y and Z sections of the miscroscope point spread function. Full width at half maximum are X/Y: 0.5 µm and Z: 5 µm. (c) Comparison of measured noise on neuron somas (abscissa, see text) versus theoretical photon noise (ordinate) across 4 experiments, following stabilization (different point colours).

levels of interwhisker-correlation (0% and 100% correlation) across all orientations and phases.

5.2 Methods

5.2.1 Surgery

All surgical procedures were in accordance with the European Community guidelines on the care and use of animals (86/609/CEE, CE official journal L358, 18th December 1986). Adult rats (P81–112; weight 350 g) male wistar rats were anaesthetized with isoflurane (1–1.5%) in 20% O_2, 80% N_2O and placed on a heating blanket. A light anaesthesia level (stage III, planes 1/2) was carefully maintained through the experiment with the help of constant breathing and EEG monitoring.

On a stereotactic frame, a metal post was glued with dental cement on the rat left skull, tangent to the bone at the stereotactic position of the barrel cortex (centered at 2.5 mm from bregma and 5.5 mm laterally). The rat was then transferred on the surgery and imaging frame where it was held by the metal post, with the head but not the body approximately 45° tilted. A craniotomy was then performed at the centre of the recording chamber, and the dura mater was removed. Following this step, the craniotomy was kept moisturized with artificial cerebrospinal fluid (ACSF).

5.2.2 Two-photon microscopy.

Multicellular bolus loading of Oregon-Green BAPTA 1-AM (OGB1-AM) was performed using a protocol adapted from [Stosiek et al., 2003]. Instead of a classical pressure control on the dye injection, a glass micropipette (tip diameter 10 µm) was filled with the OGB1-AM/Pluronic/Alexa fluor standard bolus injection mix and advanced into the craniotomy under a fluorescence stereo-microscope. At the selected injection site, the teflon coated piston of a gastight microsyringe (Exmire, Japan) was progressively inserted into the micropipette to inject a controlled 1 pL dye volume into the cortical tissue.

To specifically stain astrocytes, a drop of sulforhodamine 101 (100 µM in ACSF) was then applied on the cortex and washed 2 min later [Nimmerjahn et al., 2004]. Finally, the craniotomy was filled with agarose gel (1.5%; type III-A, Sigma-Aldrich) and sealed with a glass coverslip secured with cyanoacrylate glue.

Fluorescence was monitored with a custom two-photon microscope (fig. 5.1.a, see picture in fig. 5.1.d) powered by a Mai-Tai broadband laser (Spectra Physics). 150 µm fields of view were scanned at 40 Hz using a X axis resonant scanner (CRS-Series, GSI) combined with a Y axis galvanometric scanner (M-Series, 9 x 20 mm, GSI). Experiments were performed with an Olympus XLum 20X, NA 0.95 objective. Fluorescence photons were epi-collected by imaging the objective back aperture onto two H7421 photon counting photomultiplier (PMT) modified to allow linear photo-counting up to a photon incident rate of 10MHz. Each PMT was equipped with a motorized filter wheel with sets of fluorescence filters selective for OGB1 and SR101 fluorescence.

5.2.3 Whisker stimulation

A multiwhisker/multidirection whisker stimulation device (full details in Patent and Article 1) was set within the frame of the two-photon microscope (see picture in fig. 5.1.d) to allow the delivery of independent multidirectional arbitrary deflections across 24 whiskers

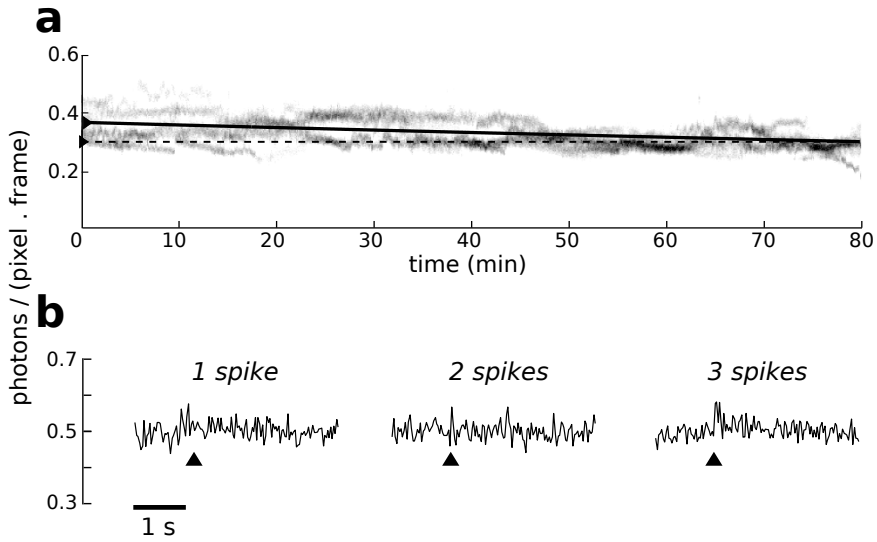

Figure 5.2 – A tradeoff in photon collection. (a) Grey shades: mean photon count per 40 Hz frame and per pixel included in neurons ROI, across five 80 min recording session obtained during different experiments. Black curve: exponential fit. Arrows and dashed line: mean photon count at the begining and end of the recording session. (b) For a comparable photon flow, modeled effect of 1,2 or 3 spikes on the signal extracted from a typical neuron ROI. Arrow: spike time.

on the animal right whiskerpad. If a follicle contained two whiskers, the smaller one was removed, and all remaining whiskers were cut to 1 cm length. Whisker were then inserted 5 mm into their corresponding whisker stimulator.

To obtain an adequate reproduction of the chosen stimulus, stimulus waveforms were pre-multiplied by the inverse transfer function of the piezoelectric actuators. Resulting whisker stimulations were validated by comparing the input signal wit the actual movement of the actuator measured with a high speed laser telemeter (Micro-ϵ OptoNCDT 1700).

5.2.4 Histology

At the end of the recordings, rats were killed by pentobarbital overdose and transcardially perfused. The left barrel cortex was flattened. 100 μm thick slices were cut tangentially and stained for cytochrome oxydase to visualize layer IV barrels.

5.3 Results

5.3.1 A two-photon imaging setup with photon noise sensitivity

One specificity of the miscroscope used in these experiments is that the collection of fluorescent light is performed by two photomultipliers (PMT) used in their photon-counting mode and not in analog mode.

To better understand the impact of this technological choice on the quality of the resulting recordings of neuronal activity, we characterized the recording noise obtained in four different isoflurane anaesthetized rats using our standard recording conditions: OGB-1 stained barrel cortex neurons soma fluorescence was recorded across a 150 µm field of view at a 40 Hz frame rate. In these fluorescence traces, we selected all 2 s epochs that were devoid of any visible calcium transients (selection criterium: signal skewness $< 5.10^{-4}$). Due to the photon-counting nature of the PMTs, we could then compare the actual noise found in these epochs (their standard deviation $\sigma_{\text{photon count}}$) to the expected level of the photon noise ($\sqrt{\text{photon count}}$) based on the observed photon count (fig. 5.1.c). These two values were always highly similar, thus suggesting that our two-photon imaging setup offers the highest theoretically possible level of signal/noise ratio for a given number of collected fluorescence photons.

This two-photon miscroscope will soon be more fully described in a manuscript currently being written ("Fast image scanning, efficient photon collection and photon counting in two photon microscopy.", Julien Bertherat, Luc Estebanez *et al.*).

5.3.2 Minimization of photobleaching at the expense of single spike detection

Hour long recordings with a steady flow of calcium dependent fluorescence were needed to build up significant functional responses across the many explored stimulus dimensions (phases, directions, correlation). We obtained such steady fluorescence (average reduction of collected fluorescence after 80 min recordings: 20%) by starting from an initially low level that produced limited photobleaching, and by progressively increasing the IR light excitation power along the recording (as little as 25 mW excitation power reached the craniotomy at the beginning of the recording).

However, a reduced excitation beam power to minimize bleaching also resulted in a limited flow of collected fluorescence (on average a 2 MHz green photon flow across the 150 µm wide field of view). To understand the consequence of this reduced photon flow on the detection of neuron soma calcium transients, a modelling study was carried in the laboratory. We studied the impact of pure photon noise (the only identified noise source in our microscope) on standard calcium transients (as reported in [Grewe et al., 2010]) corresponding to 1, 2 ou 3 spikes. The photon flow, ROI and neuron soma size mimicked our experimental conditions.

On these model calcium signals, attempts to detect back the spike times using a state of the art "peeling algorithm" [Grewe et al., 2010] failed for the 1 spike condition (S/N ratio: 1.43), in contrast with the 2 and 3 spikes condition (respective S/N ratio: 2.74 and 4.07).

We conclude from this modelling study that, to best extract functional information from data acquired during our experiments, a spike extraction approach may not be optimal. Instead, we chose to create peri-stimulus time histograms (PSTH) of the fluorescence traces: a procedure that averages out photon noise without losing the information corresponding to the low S/N action potential evoked calcium transients.

5.3.3 40Hz full frame imaging based acquisition allows high-frequency noise removal on hours long acquisitions

The microscope excitation laser scanning was carried by a pair of galvanometers, with the X axis galvanometer being resonant and tuned at 8 kHz, thus making possible the

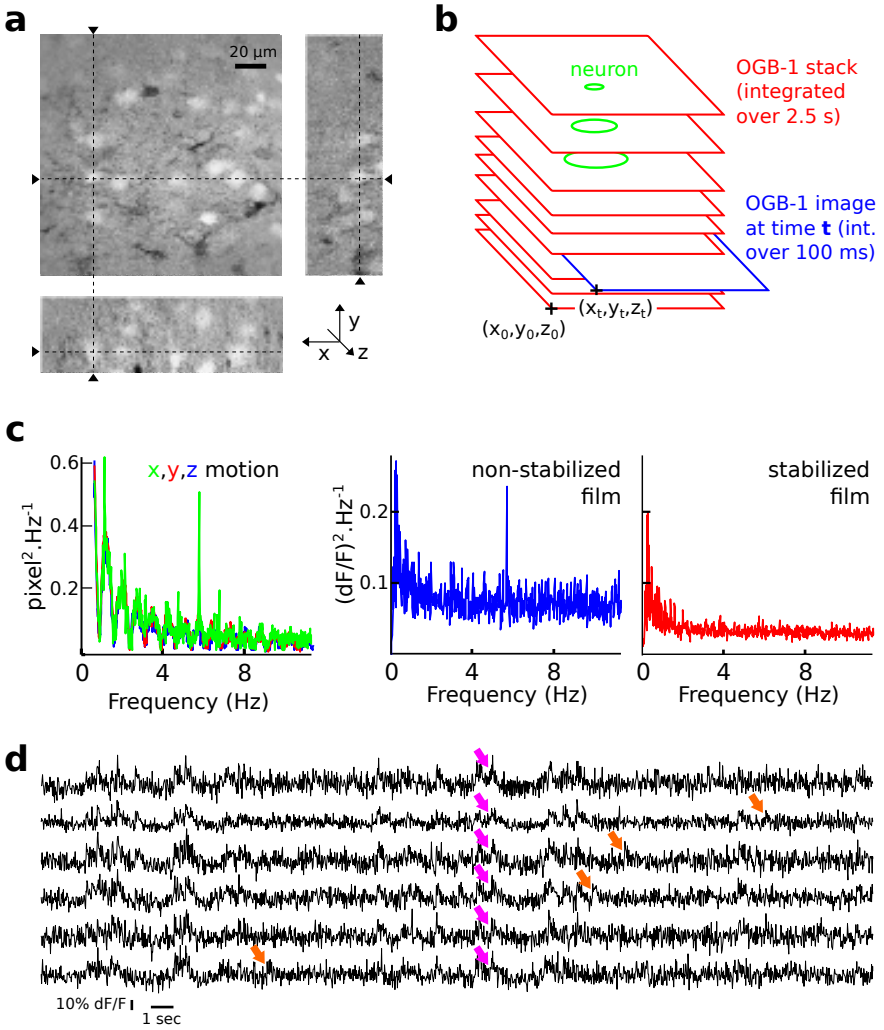

Figure 5.3 – Image-based acquisition makes for a temporally and spatially resolved signal registration. (a) A 60 µm thick reference stack centered around the acquisition plane is acquired both in the OGB-1 channel and in the SR101 channel (not shown) to differentiate neurons and astrocytes. (b) Principle of frames registration with respect to the stack. (c) Left: Power spectrum density (PSD) of the x,y,z position of the recorded images within the stack. Middle: PSD of neurons fluorescence collected without carrying the registration. Right: signal collected with registration. Note the disappearance of the heartbeat peak at 5 Hz and overall reduction in signal power. (d) OGB-1 fuorescence signal collected simultaneously on 6 neurons of the stack presented in a. Purple arrows: synchronous calcium transients across neurons. Orange arrows: single neuron calcium transients.

acquisition of images in the XY plan at rates going up to 80 Hz. However, based on a model of the expected single frame S/N ratio at such frequency, and in order to limit file size, we chose instead to carry our experiments at a 40 Hz frame rate.

One advantage of full frame microscopes — in contrast with their "smart-scanning"

counterparts [Gobel et al., 2006; Reddy et al., 2008; Otsu et al., 2008; Grewe et al., 2010] — is that this method allows a systematic and precise registration of the collected signal (acquired images at time *t*) into an initially collected stack of reference structural images of the recorded area (in our case a 400 x 400 pixels, 150 µm wide and 60 µm thick reference stack, see fig. 5.3.a).

Neurons ROI selection

Offline, using a dedicated software [Peng et al., 2010], neuron soma volumes were selected as spherical ROIs on the basis of this OGB-1 stack combined with a matching SR101 stack (reporting astrocytes). These ROIs were then reduced to vertical cylinders of same diameter and only half height. We chose to apply this change in the ROI volumes for two reasons.

First, as classically noted with other two-photon microscopes designs [Denk et al., 1990], our custom-built microscope has a much wider point spread function in the Z axis (5 µm full width at half maximum, FWHM) than in the X/Y axis (0.5 µm FWHM, see fig. 5.1.b). The ROIs Z extrema were thus contaminated by extraneuronal (neuropil) signal. The suppression of the top and bottom half of the initial ROI sphere corresponded in most neurons (with 10 µm diameter) to the removal of this neuropil contaminated area.

Second, we found that the large jumps in pixel count that occur when a spherical ROI is sectioned at changing depths (Z) over time produced a vast increase in the level of noise present in the recorded fluorescence signals. By transforming the initial sphere into a vertical cylinder, we removed altogether this noxious source of noise.

Image registration mechanism

To increase the S/N ratio during the registration process, binning was applied: a $3\times$ spatially and $4\times$ temporally binned version of the activity film was registered on an X/Y $3\times$ binned version of the OGB-1 stack. This was done by looking, at each frame, for the X,Y,Z position in the stack that maximized image/stack correlation.

Such procedure resulted in an (X,Y,Z) 1 µm precise and 10 Hz temporally precise registering of the 40 Hz fluorescence film onto the neurons ROI defined by the initially acquired stack.

This level of spatial and time precision was sufficient to detect (left panel fig. 5.3.c) movements on the 3 axes up to 10 Hz (including 5 Hz heart-beat related movements), and to remove the corresponding artefacts in the fluorescence signal (mid and right panels in fig. 5.3.c). Crucially, it also took into account large scale driftings of the imagings plan into the stack over 80 min recordings, thus ensuring an accurate identification of the recorded neurons through the experiment.

Following this registration, the neurons fluorescence traces displayed eye-visible calcium transients, more likely due to spiking bursts than to temporally isolated spike – single spikes are masked by photon noise in our conditions (see section 5.3.2 and fig. 5.3.c for further explanations).

5.3.4 A topographically organized cortex

Observations presented here are preliminary as only a limited subset of data could be analysed in time for the submission of this thesis. To characterize the spatial organization on the barrel cortex surface of the functional coding of the stimulus direction, phase

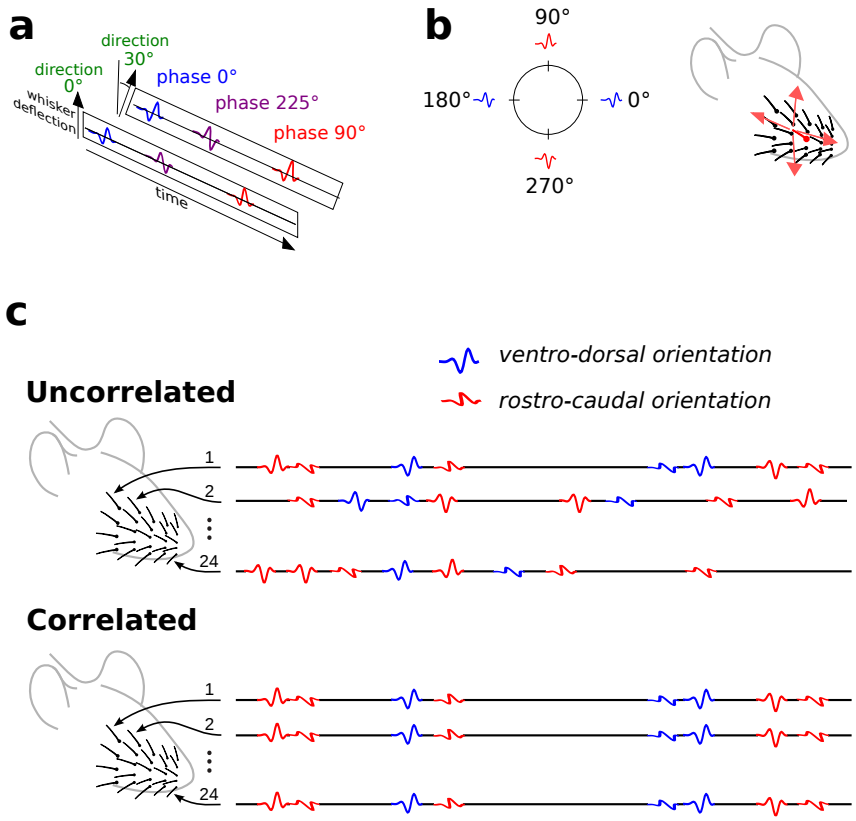

Figure 5.4 – A forward correlation protocol for the exploration of orientation, phase and correlation sensitivity across 24 whiskers. (a) Direction and phase are orthogonal dimensions that can be freely combined. (b) Included in the stimulation protocol are the four cardinal phases (left) and two cardinal orientations (rostro-caudal and ventro-dorsal, right). (c) Stimuli corresponding to a specific phase and orientation are occurring as a Poissonian sequence on each whisker. Uncorrelated and correlated versions of the stimulus are obtained by applying on the different whiskers either different (top) or identical (bottom) stimulations.

(fig. 5.4.a) as well as sensitivity to correlation, we designed a forward correlation protocol that extensively explored the cardinal dimensions of this wide sensory space (fig. 5.4.b-c).

We had previously found that forward correlation analysis of a 2D stimulus subpace using extracellular recording techniques could be resolved in a 10 min recording time. In addition, we hypothetized that to sufficiently sample an 8 times larger space (4 phases, 2 orientations, 2 degrees of inter-whisker correlation) a 8 times longer recording time was required. We thus carried 80 min long two-photon recordings on the barrel cortex of rats subjected to our multiwhisker forward correlation stimulus, with all parameters of the two-photon acquisition identical to those chosen during the method development (see previous subsections).

The calcium activity that we recorded during these experiments (fig. 5.4.d) was more dense than what is classically reported in the barrel cortex, with a mixture of synchronous (pink arrows) and asynchronous (orange arrows) transients across the cortex. We expect that one reason for this higher firing rate is that we used multiwhisker stimulations. Indeed,

such stimulations have been recently found to trigger (by the mean of air puffs) strong bursting activity in layer II/III of the barrel cortex [Lutcke et al., 2010]. Another potential reason is that we maintained a very light level of anaesthesia through the experiment.

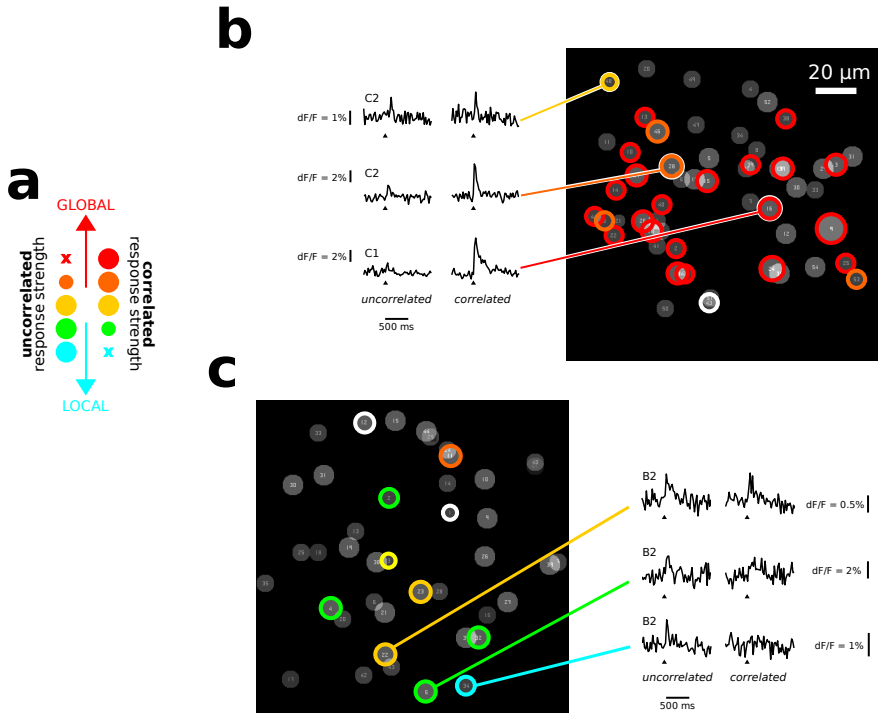

Figure 5.5 – Local and global neurons are aggregated in layer II/III of the barrel cortex. (a) Diagram describing the conventions used to color label the neurons in function of their functional response to uncorrelated and correlated multiwhisker stimulations. Global neurons (orange to red) are specifically sensitive to correlated multiwhisker stimulation and respond at most residually to uncorrelated stimulations. In contrast, most local neurons (yellow to blue) are suppressed by correlated multiwhiskers stimulations but in all cases respond clearly to uncorrelated stimulations. (b) Representative examples of the functional responses collected across one field of view where only global functional responses were collected. Uncircled neurons: neurons present in the stack but unsampled during the acquisition of the receptive field. Neurons circled in white: neurons properly sampled during the receptive field acquisition, but functionally unresponsives. (c) Same as b, for a different field where local responses dominate.

5.3.5 Local and global responses are strongly spatially segregated

We first analysed the functional response to correlated versus uncorrelated whisker stimulations. To this aim, for each neuron ROI, we built two PSTH by grouping the responses to all phase and orientations. One PSTH grouped the whisker stimulations that were presented in a correlated context, while the other grouped responses to stimuli obtained in a correlated context.

Across recorded fields, we observed an aggregations either of correlation sensitive neurons (fig.5.5.b, 'global' neurons) or of neurons responsive to uncorrelated stimulations

but suppressed by correlated input (fig.5.5.c, 'local' neurons). We hypothesize that these two types of functional response aggregates (see Article 3 for their in-depth exploration) match different histological compartments, such as the septum and barrel related areas of the layer II/III. Indeed, we have previously observed using electrophysiological recordings a similar aggregation of local/global neurons in septum/barrel areas in the deeper layers of the barrel cortex (see supp. fig. 3 of the manuscript in Chapter 4).

A precision reconstruction of the position of our recordings with respect to barrel and septum is currently being carried on the basis of the cytochrome oxydase histology that was performed immediately after each experiment. Such additional structural information should provide us with the needed data to test our hypothesis.

5.3.6 The complex phase/orientation co-tuning is visibly organized in space.

To study the neurons tuning to the phase/orientation of stimulations, PSTHs were built independently for each of the explored phase/orientation combination. Overall, we thus obtained 8 PSTHs exploring two extrema of each of the 4 phase/orientation dimensions of the stimulus (two spatial orientations and for each orientation two phase families).

It was clear from the collected data that:

- the phase/orientation subspace is represented in layers II/III in a spatially structured manner, with neighbouring neurons sharing a similar tuning to the subspace. This spatial coherence extended across the 150 µm wide field of view of the microscope (see case study in fig. 5.6).

- the neurons tuning within the phase/orientation subspace cannot be reduced to a simple tuning either to an orientation subspace or to a phase subspace. Instead, neurons responded to a complex combination of these two dimensions. In particular, from the few cases that were studied in depth so far, it seems that markedly phase tuned neurons for one spatial orientation are much less so in the other orientation.

Overall, this mapping of orientation and direction seems both a strong and complex phenomenon that will require a full analysis of the available data before any conclusions are drawn. We don't see this complex link between phase and direction as a surprise. Indeed, one should note that a given phase stimulus is actually a sequence of temporal combinations of whisker deflections with opposite directions. It should thus be expected that the direction tuning [Simons, 1978] is combining in an intricate manner with the phase tuning when explored together as in this work.

5.4 Discussion

The observation of a clear mappings in layer II/III of the barrel cortex seems at odd with the much lower clarity of the previously reported spatial mappings in this cortical area [Andermann and Moore, 2006; Kremer et al., 2011]. We hypothesize that a major reason for such a discrepancy is the difference between the stimulus shapes used to carry the forward correlation analysis in these different studies. Indeed, in the two previous studies that reported a spatial mapping of direction tuning, a "ramp followed by a slow decay", sawtooth-like stimulus was used. Although classical in the literature [Simons, 1978], such

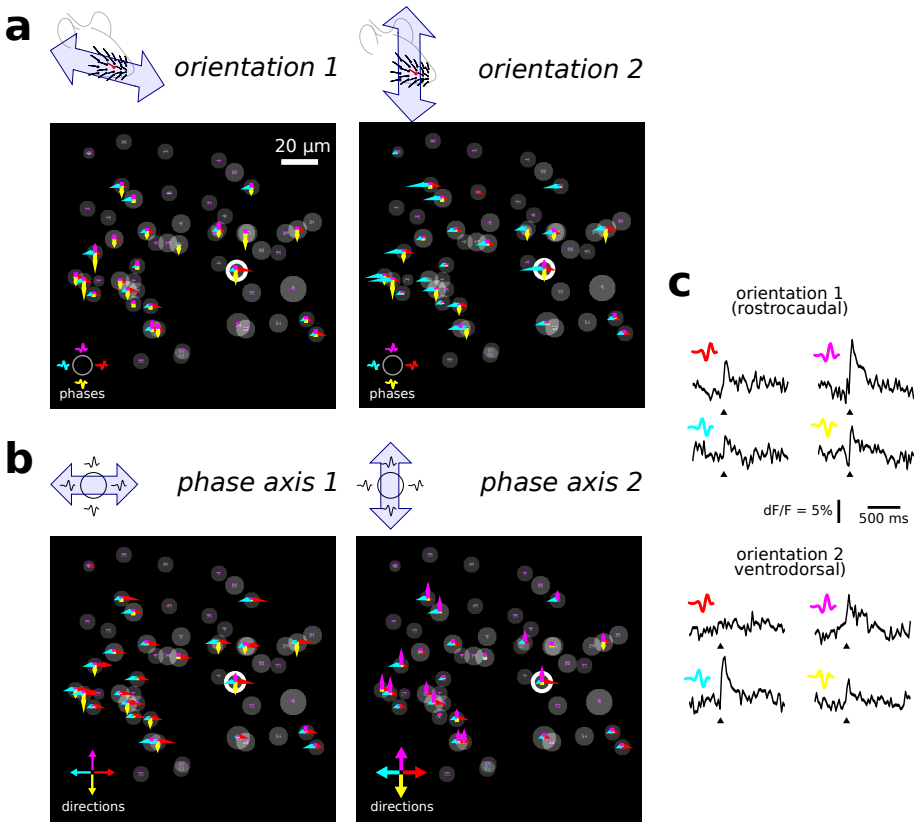

Figure 5.6 – The tuning of neurons to the phase/orientation sensory dimensions is complex but is spatially coherent across recorded 150 µm fields. For one case study obtained during correlated epochs, a systematic visualization of the eight dimensions of the stimulus is provided though four views corresponding to stimuli with (a) the same orientation, either rostrocaudal (left) or ventrodorsal (right). Different phases are in different arrow colors. (b) The same stimulus shape (the so called 'phase axis') and different directions of stimulation (arrow colors). (c) example PSTHs collected for the 8 stimulsu dimensions: two orientations and four phases for each orientation, explored in the neuron ROI circled in white across all panels.

stimulation shapes choice is only supported by an unverified hypothesis regarding the role of whiskers as speed/acceleration event detectors.

In contrast, in our study, we chose to explore a specific phase/orientation/correlation subspace on the basis of a previous electrophysiological study of barrel cortex neurons (Article 3) that identified — with a method that limit bias (reverse correlation) — the stimulation subspace that best triggers their functional response. We hypothesize that the spatial mapping of neurons tunings observed in this specific subspace may appear much less prominent if explored with another, *ad-hoc* set of stimuli such as sawtooth deflections.

The data we presented here is a limited subset of all recordings that we collected using the same protocol: overall, we obtained data in the same conditions in 13 experiments, and we combined each experiment with cytochrome oxydase histology. During these experiments, we sytematically carried 80 min recordings and we acquired on average four

different 150 µm fields per animal. Once analysed, such data should thus provide us with a sufficiently rich data set to properly characterize the spatial organization of local/global neurons. It should also give us a large pool of data to understand the link between phase and orientation, as well as the spatial organization of that particular tuning.

If fully confirmed at the population level, the observations of strict spatial mappings of the local/global and phase-orientation tunings will set the stage for an in-depth exploration of the mechanisms that support the direction and phase tuning in the barrel cortex: are the direction and phase tuning mechanisms purely feed-forward or instead are they supported by a lateral cortico-cortical propagation of similary tuned inputs at the subthresholdd level [Bringuier et al., 1999]? What is the spatial organization of the inhibitory network in charge of direction selectivity [Wilent and Contreras, 2005]? Is there a similar mapping for inhibitory neurons, and/or are inhibitory neurons involved in a purely non-selective iceberg effect [Hirsch et al., 2003] ?

Regarding local and global neurons, the question of the contribution of nearby global neurons clusters to the antagonist surround of local neurons (see manuscript in Chapter 4) could also be better explored once a clear view of the spatial organization of local and global neurons will be known.

Chapter 6

Sensori-motor integration in the rodent barrel cortex

The different experimental approaches and the results obtained during the course of this thesis are all focusing on the whisker system as a purely sensory modality. However, it is known for a long time that this view of the whisker system is partial: when exploring their environment, rodents are actually often actively moving their whiskers by the mean of the whiskerpad musculo-skeletal apparatus [Vincent, 1912; Welker, 1964; Carvell and Simons, 1990].

6.1 Whisker movements: whisking, and more

Such movements are produced by the activation of two families of muscles: intrinsic whiskerpad muscles [Carvell et al., 1991] that protract (move on the rostral direction) the whiskers, while extrinsic whiskerpad muscles [Berg and Kleinfeld, 2003] actively retract them (move them on the caudal direction).

Among the most often reported active whisker movement is "whisking", a fast (5-15 Hz in the rat) alterning cycle of whiskerpad-wide protractions and retractions of the whiskers on both sides of the animal snout [Vincent, 1912; Welker, 1964; Carvell and Simons, 1990].

6.1.1 The whisking CPG hypothesis

These "whisking" oscillatory movements are thought to be driven by a brainstem central pattern generator (CPG, [Gao et al., 2001]). This is the same CPG that also seems to support the rodent rhythmic sniffing behaviour. Indeed, whisking and sniffing have been found to be strikingly synchronized [Welker, 1964]. Actually, it turns out that if whisking is always coupled with sniffing, in contrast sniffing can still occur in the absence of whisking in rats [Deschenes et al., 2011]. This conditionality of whisking on sniffing suggest that a base function of the rats — sniffing — has been reused as a whisking CPG, and that it has been put under the control of an additional gating mechanism.

Remarkably, the activation of this hypothetized CPG is correlated with a deep change in the characteristics of the ongoing cortical state of the barrel cortex [Krupa et al., 2004; Fanselow and Nicolelis, 1999; Ferezou et al., 2007]. Such change in cortical state is

internally driven [Poulet and Petersen, 2008], potentially by the same gating mechanism that is responsible for allowing the whiskers to be entrained by the sniffing rhythms.

Still, the precise anatomical identification of this whisking CPG is currently lacking. The mechanism responsible for its activation and supression are so far limited to the observation of the occurence of whisking bursts following M1 microstimulations [Brecht et al., 2004; Matyas et al., 2010], thus suggesting an involvement of M1 in the opening of whisking gate hypothesized in the previous paragraph.

6.1.2 Large modulation of the whisking basal properties during rodents active environment exploration

Despite their likely drive by a CPG, whisking movements are far from stereotyped. Instead, they are vastly modulated by rodents during their active exploration of the environment: the right and the left whiskerpad whisking cycles can desynchronize [Towal and Hartmann, 2006; Mitchinson et al., 2007] ; individual whisker positions are adjusted in function of the position of the contacted objects [Grant et al., 2009] ; the angle they make with adjacent whiskers can be widely modulated by the animal, resulting in whisking cycles that are delayed and have different amplitudes for different, adjacent whiskers [Sachdev et al., 2002].

Similar degrees of modulation over the base CPG rythmic pattern have been previously described in other systems. The walking CPG of quadrupeds [Sherrington, 1910; Brown, 1911] illustrates well the two main sources of such modulations: (1) internal control (for instance gait switching, a phenomenon that deeply impacts the dynamic equilibrium of the CPG, see [Ijspeert et al., 2007]) and (2) sensory perception, such as the detection of obstacles.

6.2 Cortical control on whisker movements

Following many striking demonstrations of the unique role of the primary motor area (M1) in body motor control [Penfield and Boldrey, 1937; Georgopoulos et al., 1986; Wessberg et al., 2000; Graziano et al., 2002; Brecht et al., 2004], a consensus view had emerged, stating that primary motor functions were located solely in M1.

In particular, in mammals, the modulation of CPGs by sensory inputs is thought to involve the primary motor cortex. Indeed, in the M1 area of cats engaged in a walking behavior, patterns of neuronal activity correlate with the ongoing gait rhythm. When no obstacles are set on the animals path, their gait is very regular and they manage to walk even when their M1 cortical area is tetrodotoxin suppressed. In contrast, when obstacles are set in the animals path, M1 activity becomes critical, as tetrodotoxin on M1 makes them unable to modulate their gait and to succeed in the walking task [Beloozerova and Sirota, 1998]).

6.2.1 Cortical control on whisker movements is carried by a distributed network comprising at least M1 and S1

However, recently, the barrel cortex itself has been shown to be involved in the direct motor control of whisker retraction [Matyas et al., 2010], while M1 itself appears to control whisker protractions and to be involved in the onset of whisking [Matyas et al., 2010; Brecht et al., 2004]. Further, the strong anatomical connectivity between M1 and the barrel cortex [Ferezou et al., 2007; Matyas et al., 2010; Mao et al., 2011] suggests that

they are in fact forming together a unitary cortical module that is in charge of the sensory driven adjustments of whisker positions.

6.2.2 Tight cortical sensori-motor integration may support optimal sensing strategies

The fact that this whisker cortical motor module includes the barrel cortex — the primary sensory cortex for the whisker tactile modality — opens intriguing possibilities concerning a potentially rich integration of whisker motor control with previously described whisker sensory processings that are carried by barrel cortex neurons. For instance, one could envision that an object contact on a whisker would drive different motor responses (retraction, protraction of the whisker) depending on the strength of the sensed contact, thus allowing the efficient whisker sensing of a wide range of sensory stimuli (from fine grained textures to large irregularities that may potentially produce more powerful whisker movements).

Such kind of motor-regulated sensing strategies may be implemented in different manners: one way would be a movement amplification mechanism resembling the one used by the cochlea. Indeed, in this auditory sensory apparatus, outer hair cells actively amplify weak sounds signals by generating a mechanically amplified version of the sound waves that they detect (reviewed in [Hudspeth, 1997]).

Another strategy is the so called "minimal impingement" [Mitchinson et al., 2007]. This hypothesis states that the sensori-motor loop simply ensures that a light but steady contact is kept with the sensed texture at all times. Such sensori-motor rule is simpler (it does not implement an active amplification of the precise whisker micromotions) and it is supported by phenomenological observations made on behaving rodents [Mitchinson et al., 2007; Grant et al., 2009]. It may also be sufficient to explain the sensitivity the whisker system shows over a wide range of texture granulometries [Guic-Robles et al., 1989; Carvell and Simons, 1990; Morita et al., 2011], as well as the lack of difference in the firing rate of barrel cortex neurons when awake behaving rats touch rough versus smooth textures [Prigg et al., 2002].

One should also note that these different "simple" sensory-motor feedback loops could be compared to the gain-control strategies that have been previously observed in the barrel cortex of a purely sensory model: the urethane anaesthetized rat [Maravall et al., 2007]

6.2.3 Towards attention-driven whisking patterns

More elaborate sensori-motor algorithms may also be implemented by the M1-S1 module. For instance, the processing carried by the barrel cortex 'local' cell types increases the salience of whiskers that touch irregularities on an otherwise homogeneous object surface (see Article 3). We thus hypothesize that rodents may (1) increase the sensori-motor "amplification gain" of those specific whiskers, but also (2) focus other adjacent whiskers onto these information rich spots once they have been found at the surface of the explored object. One clear benefit of such strategy would be the creation of a foveal point in the whiskerpad that could be a focusing point for certain cognitive processes, similar to the way the attention is carried across a visual scene in correlation with eye movements [Duhamel et al., 1992; Corbetta et al., 1998; Moore and Fallah, 2001].

6.3 Roadblocks in the study of the whisker S1-M1 cortical module

To carry such fine-grained integration of the sensory and motor processes in the whisker system S1-M1 loop, one major non-resolved difficulty is the current lack of a mean to simultaneously control the multiwhisker sensory input provided to an awake behaving rat whiskerpad (see Chapter 1) while measuring back voluntary whisker movements.

However, beyond this challenging technical issue, we believe that the main roadblocks in this study are (1) a lack of theoretical tools to represent in a common frame both sensory and motor related neuronal activity; and (2) our currently poor knowledge of the different functional roles of the primary motor cortex, and the corresponding neuronal circuits thereof.

6.3.1 Mismatching motor and sensory representations preclude the study of the interactions between these two components

The somatosensory system is fundamentally different from the motor system. One system measures movements, while the other produces them. One has a periphery made of an array of *independent* sensors, while the other has effectors made of a set of highly *interconnected* muscles [Dorfl, 1982] that build movement with respect to rigid skeletal parts and — adding to the complexity — an elaborate semi-rigid collagen support structure [Haidarliu et al., 2011].

Such fundamental differences between the functional properties of motor and sensory systems have lead to an increasing division between the approaches and knowledge garnered from these two systems.

In one side, sensory systems have been seen through the prism of increasingly complex receptive fields properties and mappings (see Chapters 3 and 4).

In contrast, while the initial large scale views of the motor system were also somatotopic [Penfield and Boldrey, 1937], such mapping in fact turned out to be blurry at smaller scales [Dombeck et al., 2009] and topographic 'motor receptive field' never fully materialized [Rathelot and Strick, 2006].

Instead, more adequate *kinetic* models either of the whole limb/body motion [Georgopoulos et al., 1986] or of single motor units [Todorov, 2000] were proposed to describe the functional properties of motor cortex neurons. However, such functional representations are devoid of the topographic aspect that makes sensory receptive fields attractive and easy to work with.

Even further, a large proportion of the more recent research on motor cortex has focused on brain machine interfacing [Wessberg et al., 2000; Serruya et al., 2002; Taylor et al., 2002; Moritz et al., 2008; Velliste et al., 2008]. These engineering developments went one step further in the suppression of all direct reference to classical structure/function linkage between motor neurons spiking activity and the body spatial organization. Indeed, in such studies, any functional mapping of the motor neurons activity is left to a machine learning algorithm: an information processing black box.

Such "implicit" approaches where functional models are built and stored as the weights of a Kalman filter are now being extended to the whole sensory-motor loop [O'Doherty et al., 2011] by the mean of microstimulations of the somato-sensory cortex [Romo et al., 2000; Talwar et al., 2002] in correlation with contacts of the prosthesis with objects. Without attempting to build any explicit functional representation of the recorded or microstimulated neurons, this approach has demonstrated its hability to sup-

port a functional brain-controlled prosthesis with sensory feedback. Nevertheless, it gives only limited clues to understand the coding mechanims used both by the primary motor cortex and by the primary somatosensory cortex.

In contrast, we argue that to really understand the sensory-motor processing taking place in the M1-S1 loop, further attempts to model the motor system with representations that are as powerful as the sensory receptive fields will be more valuable than the current trend towards the use of efficient but blind encoding and decoding algorithms.

6.3.2 The many functional circuits of M1 are poorly known

Even before such theoretical issues can be tackled, knowledge of the precise M1 neuronal networks involved in sensory-motor processing should be advanced.

Indeed, in contrast with the relatively simple and well identified set of inputs that feeds sensory cortices, motor cortex is a major brain *output* area, and as such it receives input from many cognitive modules, supporting a diversity of functions that take place at different time scales:

(1) Premotor areas driven long and medium term goals leading up to the build up of complex motor plans — such as goal directed limb movements [Georgopoulos et al., 1986] — are at least partly prepared and them executed by the primary motor cortex [Scott, 2004].

(2) At much shorter time scales, direct sensory input has been shown to promote 'cortical reflexes' [Evarts, 1973; Beloozerova and Sirota, 1998]: quick M1 driven motor action in response to sensory feedback on a limb.

(3) Finally, also at a very short time scale, internally driven 'stop' decisions arising from a network that includes prefrontal cortex and basal ganglia network are able to quickly suppresses previously planned actions [Slater-Hammel, 1960; Voss et al., 2006; Stinear et al., 2009] that have become suddenly irrelevant in the light of the current environment.

The circuit implementation within M1 of these several functions is still poorly known. We see the proper characterization of the neuronal networks engaged in these several functions (particularly 2 and 3) as an urgent and key first step towards a functional description of the cortical sensory-motor loop.

Bibliography

Adibi, M. and Arabzadeh, E. (2011). A comparison of neuronal and behavioral detection and discrimination performances in rat whisker system. *J Neurophysiol*, 105(1):356--365.

Ahissar, E. and Knutsen, P. (2008). Object localization with whiskers. *Biological cybernetics*, 98(6):449--458.

Ahissar, E., Sosnik, R., Bagdasarian, K., and Haidarliu, S. (2001). Temporal frequency of whisker movement. ii. laminar organization of cortical representations. *Journal of neurophysiology*, 86(1):354.

Ahl, A. (1986). The role of vibrissae in behavior: a status review. *Veterinary Research Communications*, 10(1):245--268.

Andermann, M. L. and Moore, C. I. (2006). A somatotopic map of vibrissa motion direction within a barrel column. *Nat Neurosci*, 9(4):543--551.

Andermann, M. L., Ritt, J., Neimark, M. A., and Moore, C. I. (2004). Neural correlates of vibrissa resonance; band-pass and somatotopic representation of high-frequency stimuli. *Neuron*, 42(3):451--463.

Anjum, F., Turni, H., Mulder, P., Van Der Burg, J., and Brecht, M. (2006). Tactile guidance of prey capture in etruscan shrews. *Proceedings of the National Academy of Sciences*, 103(44):16544.

Arabzadeh, E., Panzeri, S., and Diamond, M. (2004). Whisker vibration information carried by rat barrel cortex neurons. *The Journal of neuroscience*, 24(26):6011.

Arabzadeh, E., Petersen, R. S., and Diamond, M. E. (2003). Encoding of whisker vibration by rat barrel cortex neurons: implications for texture discrimination. *J Neurosci*, 23(27):9146--9154.

Armstrong-James, M. and Callahan, C. (1991). Thalamo-cortical processing of vibrissal information in the rat. ii. spatiotemporal convergence in the thalamic ventroposterior medial nucleus (vpm) and its relevance to generation of receptive fields of s1 cortical "barrel" neurones. *The Journal of Comparative Neurology*, 303(2):211--224.

Axelrad, H., Verley, R., and Farkas, E. (1976). Responses evoker in mouse and rat si cortex by vibrissa stimulation. *Neuroscience Letters*, 3:265--274.

Baudot, P. (2006). *Computation naturelle, beaucoup de bruit pour rien ?* PhD thesis, École doctorale de l'UPMC.

Beloozerova, I. and Sirota, M. (1998). Cortically controlled gait adjustments in the cat. *Annals of the New York Academy of Sciences*, 860(1):550--553.

Berg, R. and Kleinfeld, D. (2003). Rhythmic whisking by rat: retraction as well as protraction of the vibrissae is under active muscular control. *Journal of neurophysiology*, 89(1):104.

Berger, H. (1929). Uber das elektrenkephalogramm des menschen. *Arch Psychiatr Nervenkr*, 87:527--570.

Betz, V. (1874). Anatomischer nachweis zweier gehirncentra. *Centralblatt für die medizinischen Wissenschaften*, 12:578--580.

Boloori, A., Jenks, R., Desbordes, G., and Stanley, G. (2010). Encoding and decoding cortical representations of tactile features in the vibrissa system. *The Journal of Neuroscience*, 30(30):9990.

Boloori, A. and Stanley, G. (2006). The dynamics of spatiotemporal response integration in the somatosensory cortex of the vibrissa system. *The Journal of neuroscience*, 26(14):3767.

Bonhoeffer, T., Grinvald, A., et al. (1991). Iso-orientation domains in cat visual cortex are arranged in pinwheel-like patterns. *Nature*, 353(6343):429--431.

Born, R. T. (2000). Center-surround interactions in the middle temporal visual area of the owl monkey. *J Neurophysiol*, 84(5):2658--2669.

Born, R. T. and Tootell, R. B. (1992). Segregation of global and local motion processing in primate middle temporal visual area. *Nature*, 357(6378):497--499.

Brecht, M., Preilowski, B., and Merzenich, M. (1997). Functional architecture of the mystacial vibrissae. *Behavioural brain research*, 84(1-2):81--97.

Brecht, M., Roth, A., and Sakmann, B. (2003). Dynamic receptive fields of reconstructed pyramidal cells in layers 3 and 2 of rat somatosensory barrel cortex. *The Journal of physiology*, 553(1):243.

Brecht, M. and Sakmann, B. (2002). Dynamic representation of whisker deflection by synaptic potentials in spiny stellate and pyramidal cells in the barrels and septa of layer 4 rat somatosensory cortex. *J Physiol*, 543(Pt 1):49--70.

Brecht, M., Schneider, M., Sakmann, B., and Margrie, T. (2004). Whisker movements evoked by stimulation of single pyramidal cells in rat motor cortex. *Nature*, 427(6976):704--710.

Bringuier, V., Chavane, F., Glaeser, L., and Frégnac, Y. (1999). Horizontal propagation of visual activity in the synaptic integration field of area 17 neurons. *Science*, 283(5402):695.

Broca, P.-P. (1861). Remarques sur le siege de la faculte du langage articule, suivies d'une observation d'aphemie (perte de la parole). *Bulletin de la Société Anatomique*, 6:330--357.

Brodmann (1909). *Brodmann's Localisation in the cerebral cortex: The principles of comparative localisation in the cerebral cortex based on the cytoarchitectonics*. Springer Verlag.

Brown, A. and Waite, P. (1974). Responses in the rat thalamus to whisker movements produced by motor nerve stimulation. *The Journal of Physiology*, 238(2):387.

Brown, T. (1911). The intrinsic factors in the act of progression in the mammal. *Proceedings of the Royal Society of London. Series B, Containing Papers of a Biological Character*, 84(572):308--319.

Brumberg, J., Pinto, D., and Simons, D. (1999). Cortical columnar processing in the rat whisker-to-barrel system. *Journal of neurophysiology*, 82(4):1808.

Brumberg, J. C., Pinto, D. J., and Simons, D. J. (1996). Spatial gradients and inhibitory summation in the rat whisker barrel system. *J Neurophysiol*, 76(1):130--140.

Bruno, R., Khatri, V., Land, P., and Simons, D. (2003). Thalamocortical angular tuning domains within individual barrels of rat somatosensory cortex. *The Journal of neuroscience*, 23(29):9565.

Bureau, I., von Saint Paul, F., and Svoboda, K. (2006). Interdigitated paralemniscal and lemniscal pathways in the mouse barrel cortex. *PLoS biology*, 4(12):e382.

Carvell, G. and Simons, D. (1988). Membrane potential changes in rat smi cortical neurons evoked by controlled stimulation of mystacial vibrissae* 1. *Brain research*, 448(1):186--191.

Carvell, G. and Simons, D. (1995). Task-and subject-related differences in sensorimotor behavior during active touch. *Somatosensory & Motor Research*, 12(1):1--9.

Carvell, G., Simons, D., Lichtenstein, S., and Bryant, P. (1991). Electromyographic activity of mystacial pad musculature during whisking behavior in the rat. *Somatosensory & motor research*, 8(2):159--164.

Carvell, G. E. and Simons, D. J. (1990). Biometric analyses of vibrissal tactile discrimination in the rat. *J Neurosci*, 10(8):2638--2648.

Caton, R. (1875). The electric currents of the brain. *Br. Med. J.*, 2:278.

Chapin, J. K. (1986). Laminar differences in sizes, shapes, and response profiles of cutaneous receptive fields in the rat si cortex. *Exp Brain Res*, 62(3):549--559.

Chen, X., Gabitto, M., Peng, Y., Ryba, N., and Zuker, C. (2011). A gustotopic map of taste qualities in the mammalian brain. *Science*, 333(6047):1262--1266.

Chen, X., Han, F., Poo, M., and Dan, Y. (2007). Excitatory and suppressive receptive field subunits in awake monkey primary visual cortex (v1). *Proceedings of the National Academy of Sciences*, 104(48):19120.

Corbetta, M., Akbudak, E., Conturo, T., Snyder, A., Ollinger, J., Drury, H., Linenweber, M., Petersen, S., Raichle, M., Van Essen, D., et al. (1998). A common network of functional areas for attention and eye movements. *Neuron*, 21(4):761--773.

Crochet, S. and Petersen, C. C. H. (2006). Correlating whisker behavior with membrane potential in barrel cortex of awake mice. *Nat Neurosci*, 9(5):608--610.

Crochet, S., Poulet, J., Kremer, Y., and Petersen, C. (2011). Synaptic mechanisms underlying sparse coding of active touch. *Neuron*, 69(6):1160--1175.

Curtis, J. and Kleinfeld, D. (2009). Phase-to-rate transformations encode touch in cortical neurons of a scanning sensorimotor system. *Nature neuroscience*, 12(4):492.

Daugman, J. (1985). Uncertainty relation for resolution in space, spatial frequency, and orientation optimized by two-dimensional visual cortical filters. *Optical Society of America, Journal, A: Optics and Image Science*, 2:1160--1169.

Daugman, J. (1988). Complete discrete 2-d gabor transforms by neural networks for image analysis and compression. *Acoustics, Speech and Signal Processing, IEEE Transactions on*, 36(7):1169--1179.

De Ruyter Van Steveninck, R. and Bialek, W. (1988). Real-time performance of a movement-sensitive neuron in the blowfly visual system: Coding and information transfer in short spike sequences. *Proc. R. Soc. Lond. B*, 234:379--414.

Dehnhardt, G. and Ducker, G. (1996). Tactual discrimination of size and shape by a california sea lion (zalophus californianus). *Learning & behavior*, 24(4):366--374.

Dehnhardt, G., Mauck, B., and Bleckmann, H. (1998). Seal whiskers detect water movements. *Nature*, 394(6690):235--236.

Dehnhardt, G., Mauck, B., Hanke, W., and Bleckmann, H. (2001). Hydrodynamic trail-following in harbor seals (phoca vitulina). *Science*, 293(5527):102.

Denk, W., Strickler, J., and Webb, W. (1990). Two-photon laser scanning fluorescence microscopy. *Science*, 248(4951):73.

der Loos, H. V. and Woolsey, T. A. (1973). Somatosensory cortex: structural alterations following early injury to sense organs. *Science*, 179(71):395--398.

Deschenes, M., Moore, M., and Kleinfeld, D. (2011). Sniffing and whisking in rodents.

Diamond, M. E., von Heimendahl, M., Knutsen, P. M., Kleinfeld, D., and Ahissar, E. (2008). 'where' and 'what' in the whisker sensorimotor system. *Nat Rev Neurosci*, 9(8):601--612.

Dombeck, D., Graziano, M., and Tank, D. (2009). Functional clustering of neurons in motor cortex determined by cellular resolution imaging in awake behaving mice. *The Journal of Neuroscience*, 29(44):13751.

Dorfl, J. (1982). The musculature of the mystacial vibrissae of the white mouse. *Journal of anatomy*, 135(Pt 1):147.

Drew, P. and Feldman, D. (2007). Representation of moving wavefronts of whisker deflection in rat somatosensory cortex. *Journal of neurophysiology*, 98(3):1566.

Duhamel, J., Colby, C., and Goldberg, M. (1992). The updating of the representation of visual space in parietal cortex by intended eye movements. *Science*, 255(5040):90.

Ego-Stengel, V., e Souza, T. M., Jacob, V., and Shulz, D. E. (2005). Spatiotemporal characteristics of neuronal sensory integration in the barrel cortex of the rat. *J Neurophysiol*, 93(3):1450--1467.

El Boustani, S., Marre, O., Béhuret, S., Baudot, P., Yger, P., Bal, T., Destexhe, A., and Frégnac, Y. (2009). Network-state modulation of power-law frequency-scaling in visual cortical neurons. *PLoS computational biology*, 5(9):e1000519.

Erchova, I., Lebedev, M., and Diamond, M. (2002). Somatosensory cortical neuronal population activity across states of anaesthesia. *European Journal of Neuroscience*, 15(4):744--752.

Evarts, E. (1973). Motor cortex reflexes associated with learned movement. *Science*, 179(4072):501.

Ewert, T. A. S., Vahle-Hinz, C., and Engel, A. K. (2008). High-frequency whisker vibration is encoded by phase-locked responses of neurons in the rat's barrel cortex. *J Neurosci*, 28(20):5359--5368.

Fanselow, E. and Nicolelis, M. (1999). Behavioral modulation of tactile responses in the rat somatosensory system. *Journal of Neuroscience*, 19 (17):7603--7616.

Fee, M. S., Mitra, P. P., and Kleinfeld, D. (1997). Central versus peripheral determinants of patterned spike activity in rat vibrissa cortex during whisking. *J Neurophysiol*, 78(2):1144--1149.

Felleman, D. and Van Essen, D. (1991). Distributed hierarchical processing in the primate cerebral cortex. *Cerebral cortex*, 1(1):1.

Ferezou, I., Bolea, S., and Petersen, C. (2006). Visualizing the cortical representation of whisker touch: Voltage-sensitive dye imaging in freely moving mice. *Neuron*, 50:617--629.

Ferezou, I., Haiss, F., Gentet, L. J., Aronoff, R., Weber, B., and Petersen, C. C. H. (2007). Spatiotemporal dynamics of cortical sensorimotor integration in behaving mice. *Neuron*, 56(5):907--923.

Fournier, J., Monier, C., Pananceau, M., and Frégnac, Y. (2011). Adaptation of the simple or complex nature of v1 receptive fields to visual statistics. *Nature Neuroscience*, 14(8):1053--1060.

Fraser, G., Hartings, J., and Simons, D. (2006). Adaptation of trigeminal ganglion cells to periodic whisker deflections. *Somatosensory & motor research*, 23(3-4):111--118.

Friedberg, M., Lee, S., and Ebner, F. (1999). Modulation of receptive field properties of thalamic somatosensory neurons by the depth of anesthesia. *Journal of neurophysiology*, 81(5):2243.

Fritsch, G. and Hitzig, E. (1870). Electric excitability of the cerebrum. *Arch Anat Physiol Wissen*, 37:300–332.

Galvez, R., Weiss, C., Cua, S., and Disterhoft, J. (2009). A novel method for precisely timed stimulation of mouse whiskers in a freely moving preparation: Application for delivery of the conditioned stimulus in trace eyeblink conditioning. *Journal of neuroscience methods*, 177(2):434--439.

Gao, P., Bermejo, R., and Zeigler, H. (2001). Whisker deafferentation and rodent whisking patterns: behavioral evidence for a central pattern generator. *The Journal of Neuroscience*, 21(14):5374.

Gentet, L., Avermann, M., Matyas, F., Staiger, J., and Petersen, C. (2010). Membrane potential dynamics of gabaergic neurons in the barrel cortex of behaving mice. *Neuron*, 65(3):422--435.

Georgopoulos, A. P., Schwartz, A. B., and Kettner, R. E. (1986). Neuronal population coding of movement direction. *Science*, 233(4771):1416--1419.

Gerdjikov, T., Bergner, C., Stüttgen, M., Waiblinger, C., and Schwarz, C. (2010). Discrimination of vibrotactile stimuli in the rat whisker system: behavior and neurometrics. *Neuron*, 65(4):530--540.

Ghazanfar, A. and Nicolelis, M. (1997). Nonlinear processing of tactile information in the thalamocortical loop. *Journal of neurophysiology*, 78(1):506.

Ghazanfar, A. and Nicolelis, M. (1999). Spatiotemporal properties of layer v neurons of the rat primary somatosensory cortex. *Cerebral Cortex*, 9(4):348.

Gobel, W., Kampa, B., and Helmchen, F. (2006). Imaging cellular network dynamics in three dimensions using fast 3d laser scanning. *Nature Methods*, 4(1):73--79.

Goldreich, D., Peterson, B. E., and Merzenich, M. M. (1998). Optical imaging and electrophysiology of rat barrel cortex. ii. responses to paired-vibrissa deflections. *Cereb Cortex*, 8(2):184--192.

Grant, R. A., Mitchinson, B., Fox, C. W., and Prescott, T. J. (2009). Active touch sensing in the rat: anticipatory and regulatory control of whisker movements during surface exploration. *J Neurophysiol*, 101(2):862--874.

Graziano, M., Taylor, C., and Moore, T. (2002). Complex movements evoked by microstimulation of precentral cortex. *Neuron*, 34(5):841--851.

Grewe, B., Langer, D., Kasper, H., Kampa, B., and Helmchen, F. (2010). High-speed in vivo calcium imaging reveals neuronal network activity with near-millisecond precision. *Nat. Methods*, 7(5):399--405.

Guic-Robles, E., Valdivieso, C., and Guajardo, G. (1989). Rats can learn a roughness discrimination using only their vibrissal system. *Behavioural Brain Research*, 31(3):285--289.

Haidarliu, S., Simony, E., Golomb, D., and Ahissar, E. (2011). Collagenous skeleton of the rat mystacial pad. *The Anatomical Record: Advances in Integrative Anatomy and Evolutionary Biology*.

Haider, B., Krause, M. R., Duque, A., Yu, Y., Touryan, J., Mazer, J. A., and McCormick, D. A. (2010). Synaptic and network mechanisms of sparse and reliable visual cortical activity during nonclassical receptive field stimulation. *Neuron*, 65(1):107--121.

Hartmann, M. (2001). Active sensing capabilities of the rat whisker system. *Autonomous Robots*, 11(3):249--254.

Hartmann, M., Johnson, N., Towal, B., and Assad, C. (2003). Mechanical characteristics of rat vibrissae: Resonant frequencies and damping in isolated whiskers and in the awake behaving animal. *The Journal of Neuroscience*, 23 (16):6510--6519.

Hayward, J. (1975). Response of ventrobasal thalamic cells to hair displacement on the face of the waking monkey. *The Journal of Physiology*, 250(2):385.

Higley, M. and Contreras, D. (2003). Nonlinear integration of sensory responses in the rat barrel cortex: an intracellular study in vivo. *The Journal of neuroscience*, 23(32):10190.

Higley, M. and Contreras, D. (2005). Integration of synaptic responses to neighboring whiskers in rat barrel cortex in vivo. *Journal of neurophysiology*, 93(4):1920.

Hirata, A. and Castro-Alamancos, M. A. (2008). Cortical transformation of wide-field (multiwhisker) sensory responses. *J Neurophysiol*, 100(1):358--370.

Hirsch, J., Martinez, L., Pillai, C., Alonso, J., Wang, Q., and Sommer, F. (2003). Functionally distinct inhibitory neurons at the first stage of visual cortical processing. *Nature Neuroscience*, 6(12):1300--1308.

Horton, J. (1984). Cytochrome oxidase patches: a new cytoarchitectonic feature of monkey visual cortex. *Philosophical Transactions of the Royal Society of London. Series B, Biological Sciences*, pages 199--253.

Hubel, D. and Wiesel, T. (1963). Shape and arrangement of columns in cat's striate cortex. *The Journal of Physiology*, 165(3):559.

Hubel, D. H. and Wiesel, T. N. (1959). Receptive fields of single neurones in the cat's striate cortex. *J Physiol*, 148:574--591.

Hubel, D. H. and Wiesel, T. N. (1962). Receptive fields, binocular interaction and functional architecture in the cat's visual cortex. *J Physiol*, 160:106--154.

Hudspeth, A. (1997). Mechanical amplification of stimuli by hair cells. *Current opinion in neurobiology*, 7(4):480--486.

Ijspeert, A., Crespi, A., Ryczko, D., and Cabelguen, J. (2007). From swimming to walking with a salamander robot driven by a spinal cord model. *Science*, 315(5817):1416.

Ito, M. (1981). Some quantitative aspects of vibrissa-driven neuronal responses in rat neocortex. *Journal of Neurophysiology*, 46:705--715.

Ito, M. (1985). Processing of vibrissa sensory information within the rat neocortex. *Journal of neurophysiology*, 54(3):479.

Jacob, V., Cam, J. L., Ego-Stengel, V., and Shulz, D. E. (2008). Emergent properties of tactile scenes selectively activate barrel cortex neurons. *Neuron*, 60(6):1112--1125.

Jacob, V., Estebanez, L., Cam, J. L., Tiercelin, J.-Y., Parra, P., Parésys, G., and Shulz, D. E. (2010). The matrix: a new tool for probing the whisker-to-barrel system with natural stimuli. *J Neurosci Methods*, 189(1):65--74.

Jadhav, S. P., Wolfe, J., and Feldman, D. E. (2009). Sparse temporal coding of elementary tactile features during active whisker sensation. *Nat Neurosci*, 12(6):792--800.

Jin, T., Witzemann, V., and Brecht, M. (2004). Fiber types of the intrinsic whisker muscle and whisking behavior. *The Journal of neuroscience*, 24(13):3386.

Jones, J. and Palmer, L. (1987). The two-dimensional spatial structure of simple receptive fields in cat striate cortex. *Journal of Neurophysiology*, 58(6):1187.

Jones, L. M., Depireux, D. A., Simons, D. J., and Keller, A. (2004). Robust temporal coding in the trigeminal system. *Science*, 304(5679):1986--1989.

Kenet, T., Bibitchkov, D., Tsodyks, M., Grinvald, A., and Arieli, A. (2003). Spontaneously emerging cortical representations of visual attributes. *Nature*, 425(6961):954--956.

Kerr, J., de Kock, C., Greenberg, D., Bruno, R., Sakmann, B., and Helmchen, F. (2007). Spatial organization of neuronal population responses in layer 2/3 of rat barrel cortex. *Journal of Neuroscience*, 27(48):13316 –13328.

Kida, H., Shimegi, S., and Sato, H. (2005). Similarity of direction tuning among responses to stimulation of different whiskers in neurons of rat barrel cortex. *Journal of neurophysiology*, 94(3):2004.

Knutsen, P., Derdikman, D., and Ahissar, E. (2005). Tracking whisker and head movements in unrestrained behaving rodents. *Journal of neurophysiology*, 93(4):2294.

Knutsen, P., Pietr, M., and Ahissar, E. (2006). Haptic object localization in the vibrissal system: behavior and performance. *The Journal of neuroscience*, 26(33):8451.

Koralek, K., Jensen, K., and Killackey, H. (1988). Evidence for two complementary patterns of thalamic input to the rat somatosensory cortex. *Brain research*, 463(2):346--351.

Kremer, Y., Léger, J.-F., Goodman, D., Brette, R., and Bourdieu, L. (2011). Late emergence of the vibrissa direction selectivity map in the rat barrel cortex. *Journal of Neuroscience*, 31(29):10689 –10700.

Krupa, D., Brisben, A., and Nicolelis, M. (2001). A multi-channel whisker stimulator for producing spatiotemporally complex tactile stimuli. *Journal of neuroscience methods*, 104(2):199--208.

Krupa, D., Wiest, M., Shuler, M., Laubach, M., and Nicolelis, M. (2004). Layer-specific somatosensory cortical activation during active tactile discrimination. *Science*, 304(5679):1989.

Le Cam, J., Estebanez, L., Jacob, V., and Shulz, D. (2011). The spatial structure of multi-whisker receptive fields in the barrel cortex is stimulus-dependent. *Journal of Neurophysiology*.

Lee, S. and Simons, D. (2004). Angular tuning and velocity sensitivity in different neuron classes within layer 4 of rat barrel cortex. *Journal of neurophysiology*, 91(1):223.

Lefort, S., Tomm, C., Floyd Sarria, J., and Petersen, C. (2009). The excitatory neuronal network of the c2 barrel column in mouse primary somatosensory cortex. *Neuron*, 61(2):301--316.

Lesica, N. A., Jin, J., Weng, C., Yeh, C.-I., Butts, D. A., Stanley, G. B., and Alonso, J.-M. (2007). Adaptation to stimulus contrast and correlations during natural visual stimulation. *Neuron*, 55(3):479--491.

Lottem, E. and Azouz, R. (2009). Mechanisms of tactile information transmission through whisker vibrations. *The Journal of Neuroscience*, 29(37):11686.

Lutcke, H., Murayama, M., Hahn, T., Margolis, D., Astori, S., zum Alten Borgloh, S., Gobel, W., Yang, Y., Tang, W., Kugler, S., et al. (2010). Optical recording of neuronal activity with a genetically-encoded calcium indicator in anesthetized and freely moving mice. *Frontiers in neural circuits*, 4.

Manns, I., Sakmann, B., and Brecht, M. (2004). Sub-and suprathreshold receptive field properties of pyramidal neurones in layers 5a and 5b of rat somatosensory barrel cortex. *The Journal of physiology*, 556(2):601--622.

Mao, T., Kusefoglu, D., Hooks, B., Huber, D., Petreanu, L., and Svoboda, K. (2011). Long-range neuronal circuits underlying the interaction between sensory and motor cortex. *Neuron*, 72(1):111--123.

Maravall, M., Petersen, R. S., Fairhall, A. L., Arabzadeh, E., and Diamond, M. E. (2007). Shifts in coding properties and maintenance of information transmission during adaptation in barrel cortex. *PLoS Biol*, 5(2):e19.

Marino, J., Schummers, J., Lyon, D., Schwabe, L., Beck, O., Wiesing, P., Obermayer, K., and Sur, M. (2005). Invariant computations in local cortical networks with balanced excitation and inhibition. *Nature neuroscience*, 8(2):194--201.

Matyas, F., Sreenivasan, V., Marbach, F., Wacongne, C., Barsy, B., Mateo, C., Aronoff, R., and Petersen, C. C. H. (2010). Motor control by sensory cortex. *Science*, 330(6008):1240--1243.

Mehta, S., Whitmer, D., Figueroa, R., Williams, B., and Kleinfeld, D. (2007). Active spatial perception in the vibrissa scanning sensorimotor system. *PLoS biology*, 5(2):e15.

Melzer, P., Loos, H. V. D., Dorfl, J., Welker, E., Robert, P., Emery, D., and Berrini, J.-C. (1985). A magnetic device to stimulate selected whiskers of freely moving or restrained small rodents: its application in a deoxyglucose study. *Brain Research*, 348:229--240.

Mirabella, G., Battiston, S., and Diamond, M. E. (2001). Integration of multiple-whisker inputs in rat somatosensory cortex. *Cereb Cortex*, 11(2):164--170.

Mitchinson, B., Martin, C. J., Grant, R. A., and Prescott, T. J. (2007). Feedback control in active sensing: rat exploratory whisking is modulated by environmental contact. *Proc Biol Sci*, 274(1613):1035--1041.

Moore, C. (2004). Frequency-dependent processing in the vibrissa sensory system. *Journal of neurophysiology*, 91(6):2390.

Moore, C. I. and Nelson, S. B. (1998). Spatio-temporal subthreshold receptive fields in the vibrissa representation of rat primary somatosensory cortex. *J Neurophysiol*, 80(6):2882--2892.

Moore, T. and Fallah, M. (2001). Control of eye movements and spatial attention. *Proceedings of the National Academy of Sciences*, 98(3):1273.

Moreno, C., Vivas, O., Lamprea, N. P., Lamprea, M. R., Múnera, A., and Troncoso, J. (2010). Vibrissal paralysis unveils a preference for textural rather than positional novelty in the one-trial object recognition task in rats. *Behav Brain Res*, 211(2):229--235.

Morita, T., Kang, H., Wolfe, J., Jadhav, S., and Feldman, D. (2011). Psychometric curve and behavioral strategies for whisker-based texture discrimination in rats.

Moritz, C., Perlmutter, S., and Fetz, E. (2008). Direct control of paralysed muscles by cortical neurons. *Nature*, 456(7222):639--642.

Mountcastle, V. B. (1957). Modality and topographic properties of single neurons of cat's somatic sensory cortex. *J Neurophysiol*, 20(4):408--434.

Mountcastle, V. B., Davies, P. W., and Berman, A. L. (1957). Response properties of neurons of cat's somatic sensory cortex to peripheral stimuli. *J Neurophysiol*, 20(4):374--407.

Nauhaus, I., Benucci, A., Carandini, M., and Ringach, D. (2008). Neuronal selectivity and local map structure in visual cortex. *Neuron*, 57(5):673--679.

Neimark, M., Andermann, M., Hopfield, J., and Moore, C. (2003). Vibrissa resonance as a transduction mechanism for tactile encoding. *The Journal of neuroscience*, 23(16):6499.

Nelken, I., Rotman, Y., and Yosef, O. (1998). Responses of auditory-cortex neurons to structural features of natural sounds. In *Proc. R. Soc. Lond. B*, volume 265, pages 221--225.

Nicolelis, M. and Chapin, J. (1994). Spatiotemporal structure of somatosensory responses of many-neuron ensembles in the rat ventral posterior medial nucleus of the thalamus. *The Journal of neuroscience*, 14(6):3511.

Nimmerjahn, A., Kirchhoff, F., Kerr, J., and Helmchen, F. (2004). Sulforhodamine 101 as a specific marker of astroglia in the neocortex in vivo. *Nature methods*, 1(1):31--37.

O'Doherty, J. E., Lebedev, M. A., Ifft, P. J., Zhuang, K. Z., Shokur, S., Bleuler, H., and Nicolelis, M. A. L. (2011). Active tactile exploration using a brain-machine-brain interface. *Nature*.

Ohki, K., Chung, S., Ch'ng, Y., Kara, P., and Reid, R. (2005). Functional imaging with cellular resolution reveals precise micro-architecture in visual cortex. *Nature*, 433(7026):597--603.

Ohki, K., Chung, S., Kara, P., Hubener, M., Bonhoeffer, T., and Reid, R. (2006). Highly ordered arrangement of single neurons in orientation pinwheels. *NATURE-LONDON-*, 442(7105):925.

Otsu, Y., Bormuth, V., Wong, J., Mathieu, B., Dugué, G., Feltz, A., and Dieudonné, S. (2008). Optical monitoring of neuronal activity at high frame rate with a digital random-access multiphoton (ramp) microscope. *Journal of neuroscience methods*, 173(2):259--270.

Penfield, W. and Boldrey, E. (1937). Somatic motor and sensory representation in the cerebral cortex of man as studied by electrical stimulation. *Brain*, 60(4):389.

Peng, H., Ruan, Z., Long, F., Simpson, J., and Myers, E. (2010). V3d enables real-time 3d visualization and quantitative analysis of large-scale biological image data sets. *Nature biotechnology*, 28(4):348--353.

Perin, R., Berger, T., and Markram, H. (2011). A synaptic organizing principle for cortical neuronal groups. *Proceedings of the National Academy of Sciences*, 108(13):5419.

Petersen, C. (2007). The functional organization of the barrel cortex. *Neuron*, 56(2):339--355.

Petersen, C. and Sakmann, B. (2000). The excitatory neuronal network of rat layer 4 barrel cortex. *The Journal of Neuroscience*, 20(20):7579.

Petersen, C. and Sakmann, B. (2001). Functionally independent columns of rat somatosensory barrel cortex revealed with voltage-sensitive dye imaging. *The journal of Neuroscience*, 21(21):8435.

Petersen, R., Brambilla, M., Bale, M., Alenda, A., Panzeri, S., Montemurro, M., and Maravall, M. (2008). Diverse and temporally precise kinetic feature selectivity in the vpm thalamic nucleus. *Neuron*, 60(5):890--903.

Pinto, D. J., Brumberg, J. C., and Simons, D. J. (2000). Circuit dynamics and coding strategies in rodent somatosensory cortex. *J Neurophysiol*, 83(3):1158--1166.

Poulet, J. and Petersen, C. (2008). Internal brain state regulates membrane potential synchrony in barrel cortex of behaving mice. *Nature*, 454(7206):881--885.

Prigg, T., Goldreich, D., Carvell, G., and Simons, D. (2002). Texture discrimination and unit recordings in the rat whisker/barrel system. *Physiology & behavior*, 77(4-5):671--675.

Rathelot, J. and Strick, P. (2006). Muscle representation in the macaque motor cortex: an anatomical perspective.

Reddy, G., Kelleher, K., Fink, R., and Saggau, P. (2008). Three-dimensional random access multiphoton microscopy for functional imaging of neuronal activity. *Nature neuroscience*, 11(6):713.

Reid, R. and Alonso, J. (1995). Specificity of monosynaptic connections from thalamus to visual cortex. *Nature*, 378(6554):281--283.

Reid, R., Victor, J., and Shapley, R. (1997). The use of m-sequences in the analysis of visual neurons: linear receptive field properties. *Visual Neuroscience*, 14:1015--1028.

Ritt, J. T., Andermann, M. L., and Moore, C. I. (2008). Embodied information processing: vibrissa mechanics and texture features shape micromotions in actively sensing rats. *Neuron*, 57(4):599--613.

Rodgers, K., Benison, A., and Barth, D. (2006). Two-dimensional coincidence detection in the vibrissa/barrel field. *Journal of neurophysiology*, 96(4):1981.

Romo, R., Hernández, A., Zainos, A., Brody, C., and Lemus, L. (2000). Sensing without touching:: Psychophysical performance based on cortical microstimulation. *Neuron*, 26(1):273--278.

Rothschild, G., Nelken, I., and Mizrahi, A. (2010). Functional organization and population dynamics in the mouse primary auditory cortex. *Nature neuroscience*, 13(3):353--360.

Sachdev, R., Sato, T., and Ebner, F. (2002). Divergent movement of adjacent whiskers. *Journal of neurophysiology*, 87(3):1440.

Sachdev, R., Sellien, H., and Ebner, F. (2001). Temporal organization of multi-whisker contact in rats. *Somatosensory & motor research*, 18(2):91--100.

Saig, A., Arieli, A., and Ahissar, E. (2010). What is it like to be a rat? sensory augmentation study. *Haptics: Generating and Perceiving Tangible Sensations*, pages 298--305.

Schubert, D., Kötter, R., and Staiger, J. (2007). Mapping functional connectivity in barrel-related columns reveals layer-and cell type-specific microcircuits. *Brain Structure and Function*, 212(2):107--119.

Schultz, W., Galbraith, G., Gottschaldt, K., and Creutzfeldt, O. (1976). A comparison of primary afferent and cortical neurone activity coding sinus hair movements in the cat. *Experimental Brain Research*, 24(4):365--381.

Schwartz, O., Pillow, J. W., Rust, N. C., and Simoncelli, E. P. (2006). Spike-triggered neural characterization. *J Vis*, 6(4):484--507.

Scott, S. (2004). Optimal feedback control and the neural basis of volitional motor control. *Nature Reviews Neuroscience*, 5(7):532--546.

Serruya, M., Hatsopoulos, N., Paninski, L., Fellows, M., and Donoghue, J. (2002). Brain-machine interface: Instant neural control of a movement signal. *Nature*, 416(6877):141--142.

Sharpee, T., Rust, N., and Bialek, W. (2004). Analyzing neural responses to natural signals: maximally informative dimensions. *Neural Computation*, 16(2):223--250.

Sherrington, C. (1910). Flexion-reflex of the limb, crossed extension-reflex, and reflex stepping and standing. *The Journal of physiology*, 40(1-2):28.

Sheth, B., Moore, C., and Sur, M. (1998). Temporal modulation of spatial borders in rat barrel cortex. *Journal of neurophysiology*, 79(1):464.

Shimegi, S., Akasaki, T., Ichikawa, T., and Sato, H. (2000). Physiological and anatomical organization of multiwhisker response interactions in the barrel cortex of rats. *J Neurosci*, 20(16):6241--6248.

Shimegi, S., Ichikawa, T., Akasaki, T., and Sato, H. (1999). Temporal characteristics of response integration evoked by multiple whisker stimulations in the barrel cortex of rats. *J Neurosci*, 19(22):10164--10175.

Simoncelli, E. and Olshausen, B. (2001). Natural image statistics and neural representation. *Annual review of neuroscience*, 24(1):1193--1216.

Simons, D. (1983). Multi-whisker stimulation and its effects on vibrissa units in rat sml barrel cortex. *Brain research*, 276(1):178--182.

Simons, D. and Carvell, G. (1989). Thalamocortical response transformation in the rat vibrissa/barrel system. *Journal of neurophysiology*, 61(2):311.

Simons, D., Carvell, G., Hershey, A., and Bryant, D. (1992). Responses of barrel cortex neurons in awake rats and effects of urethane anesthesia. *Experimental brain research*, 91(2):259--272.

Simons, D. J. (1978). Response properties of vibrissa units in rat si somatosensory neocortex. *J Neurophysiol*, 41(3):798--820.

Simons, D. J. (1985). Temporal and spatial integration in the rat si vibrissa cortex. *J Neurophysiol*, 54(3):615--635.

Simony, E., Bagdasarian, K., Herfst, L., Brecht, M., Ahissar, E., and Golomb, D. (2010). Temporal and spatial characteristics of vibrissa responses to motor commands. *The Journal of Neuroscience*, 30(26):8935.

Slater-Hammel, A. (1960). Reliability, accuracy, and refractoriness of a transit reaction. *Research Quarterly of the American Association for Health, Physical Education, & Recreation*.

Sosnik, R., Haidarliu, S., and Ahissar, E. (2001). Temporal frequency of whisker movement. i. representations in brain stem and thalamus. *Journal of Neurophysiology*, 86(1):339.

Sterbing-D'Angelo, S., Chadha, M., Chiu, C., Falk, B., Xian, W., Barcelo, J., Zook, J., and Moss, C. (2011). Bat wing sensors support flight control. *Proceedings of the National Academy of Sciences*, 108(27):11291.

Stettler, D. and Axel, R. (2009). Representations of odor in the piriform cortex. *Neuron*, 63(6):854--864.

Stinear, C., Coxon, J., and Byblow, W. (2009). Primary motor cortex and movement prevention: where stop meets go. *Neuroscience & Biobehavioral Reviews*, 33(5):662--673.

Stosiek, C., Garaschuk, O., Holthoff, K., and Konnerth, A. (2003). In vivo two-photon calcium imaging of neuronal networks. *Proceedings of the National Academy of Sciences*, 100(12):7319.

Stuttgen, M., Ruter, J., and Schwarz, C. (2006). Two psychophysical channels of whisker deflection in rats align with two neuronal classes of primary afferents. *The Journal of neuroscience*, 26(30):7933.

Stuttgen, M. and Schwarz, C. (2008). Psychophysical and neurometric detection performance under stimulus uncertainty. *Nature neuroscience*, 11(9):1091--1099.

Szwed, M., Bagdasarian, K., and Ahissar, E. (2003). Encoding of vibrissal active touch. *Neuron*, 40(3):621--630.

Szwed, M., Bagdasarian, K., Blumenfeld, B., Barak, O., Derdikman, D., and Ahissar, E. (2006). Responses of trigeminal ganglion neurons to the radial distance of contact during active vibrissal touch. *Journal of neurophysiology*, 95(2):791.

Szwed, M. and Shulz, D. (2007). Pre-neuronal encoding of radial distance by high-frequency whisker vibrations in the rat. In *Society for Neuroscience*.

Talwar, S., Xu, S., Hawley, E., Weiss, S., Moxon, K., and Chapin, J. (2002). Behavioural neuroscience: Rat navigation guided by remote control. *Nature*, 417(6884):37--38.

Taylor, D., Tillery, S., and Schwartz, A. (2002). Direct cortical control of 3d neuroprosthetic devices. *Science*, 296(5574):1829.

Todorov, E. (2000). Direct cortical control of muscle activation in voluntary arm movements: a model. *Nat Neurosci*, 3(4):391--398.

Towal, R. and Hartmann, M. (2006). Right--left asymmetries in the whisking behavior of rats anticipate head movements. *The Journal of neuroscience*, 26(34):8838.

Towal, R. B., Quist, B. W., Gopal, V., Solomon, J. H., and Hartmann, M. J. Z. (2011). The morphology of the rat vibrissal array: a model for quantifying spatiotemporal patterns of whisker-object contact. *PLoS Comput Biol*, 7(4):e1001120.

Tsytsarev, V., Pope, D., Pumbo, E., Yablonskii, A., and Hofmann, M. (2010). Study of the cortical representation of whisker directional deflection using voltage-sensitive dye optical imaging. *NeuroImage*, 53(1):233--238.

Ulanovsky, N., Las, L., and Nelken, I. (2003). Processing of low-probability sounds by cortical neurons. *nature neuroscience*, 6(4):391--398.

Van Der Loos, H. (1976). Barreloids in mouse somatosensory thalamus. *Neurosci Lett*, 2(1):1--6.

Veinante, P. and Deschênes, M. (1999). Single-and multi-whisker channels in the ascending projections from the principal trigeminal nucleus in the rat. *The Journal of neuroscience*, 19(12):5085.

Velliste, M., Perel, S., Spalding, M., Whitford, A., and Schwartz, A. (2008). Cortical control of a prosthetic arm for self-feeding. *Nature*, 453(7198):1098--1101.

Vincent, S. (1912). The function of the vibrissae in the behavior of the white rat. *Behavior Monographs*, 1:1--76.

Vincent, S. (1913). The tactile hair of the white rat. *The Journal of Comparative Neurology*, 23(1):1--34.

Vinje, W. E. and Gallant, J. L. (2000). Sparse coding and decorrelation in primary visual cortex during natural vision. *Science*, 287(5456):1273--1276.

Vinje, W. E. and Gallant, J. L. (2002). Natural stimulation of the nonclassical receptive field increases information transmission efficiency in v1. *J Neurosci*, 22(7):2904--2915.

Von Heimendahl, M., Itskov, P., Arabzadeh, E., and Diamond, M. (2007). Neuronal activity in rat barrel cortex underlying texture discrimination. *PLoS biology*, 5(11):e305.

Voss, M., Ingram, J., Haggard, P., and Wolpert, D. (2006). Sensorimotor attenuation by central motor command signals in the absence of movement. *Nature neuroscience*, 9(1):26.

Walker, J., Monjaraz-Fuentes, F., Pedrow, C., and Rector, D. (2010). Precision rodent whisker stimulator with integrated servo-locked control and displacement measurement. *Journal of neuroscience methods*.

Welker, C. (1971). Microelectrode delineation of fine grain somatiotopic organization of smi cerebral neocortex in abinos rat. *Brain research*, 26:259--275.

Welker, C. and Woosley, T. (1974). Structure of layer iv in the somatosensory neocortex of the rat: Description and comparison with the mouse. *J. COMP. NEUR.*, 58:437--454.

Welker, W. (1964). Analysis of sniffing of the albino rat. *Behaviour*, pages 223--244.

Wessberg, J., Stambaugh, C., Kralik, J., Beck, P., Laubach, M., Chapin, J., Kim, J., Biggs, S., Srinivasan, M., and Nicolelis, M. (2000). Real-time prediction of hand trajectory by ensembles of cortical neurons in primates. *Nature*, 408(6810):361--365.

Wilent, W. B. and Contreras, D. (2005). Dynamics of excitation and inhibition underlying stimulus selectivity in rat somatosensory cortex. *Nat Neurosci*, 8(10):1364--1370.

Wolfe, J., Hill, D. N., Pahlavan, S., Drew, P. J., Kleinfeld, D., and Feldman, D. E. (2008). Texture coding in the rat whisker system: slip-stick versus differential resonance. *PLoS Biol*, 6(8):e215.

Woolsey, T. A. and der Loos, H. V. (1970). The structural organization of layer iv in the somatosensory region (si) of mouse cerebral cortex. the description of a cortical field composed of discrete cytoarchitectonic units. *Brain Res*, 17(2):205--242.

Wright, N. and Fox, K. (2010). Origins of cortical layer v surround receptive fields in the rat barrel cortex. *Journal of neurophysiology*, 103(2):709.

Yu, C., Derdikman, D., Haidarliu, S., and Ahissar, E. (2006). Parallel thalamic pathways for whisking and touch signals in the rat. *PLoS Biology*, 4(5):e124.

Zhu, J. J. and Connors, B. W. (1999). Intrinsic firing patterns and whisker-evoked synaptic responses of neurons in the rat barrel cortex. *J Neurophysiol*, 81(3):1171--1183.